

An assessment of groundwater resources in the Banke district of Nepal

Using groundwater balance approaches on case studies and seasonal groundwater table fluctuation estimates

P.A. van Sabben

An assessment of groundwater resources in the Banke district of Nepal

Using groundwater balance approaches on case
studies and seasonal groundwater table
fluctuation estimates

by

P.A. van Sabben

Student Name	Student Number
van Sabben	4586174

Chair:	Dr. T.A. Bogaard
Committee:	Dr. ir. O.A.C. Hoes Dr. A.V. Urfels Dr. S.R. Sherpa
Project Duration:	February, 2023 - December, 2023
Faculty:	Faculty of Civil Engineering, Delft

Preface

Management of water is a relevant issue everywhere in the world. Every region will have to deal with altering water resources in the future due to the changing climate. I am extremely grateful for the opportunity I got to contribute to the knowledge about groundwater resources in Nepal specifically in the Banke district. Besides researching I also got the chance to visit the country and experience a different culture in contrast to ours.

First of all, I want to extend my gratitude to my thesis committee. Foremost, my chair and 1st supervisor Thom for the endless support and the amazing subject in the first place. You helped me learn more about so many facets of research that surpass what could be described by the credits accompanying a thesis. I would also like to thank Anton for the numerous calls during my time in Nepal, Martine and Olivier for fulfilling the role of second supervisor critically but helpfully and Sonam for the help he offered in Nepal.

I would also like to thank my parents who supported this opportunity along the whole way. Additionally, I would like to thank my friends and family who further helped me complete my thesis in this manner. Lastly, a big thanks to the people in Nepal who helped me feel right at home and aided me in my field-work. Where especially Hemraj was extremely involved in the project and a real sparring partner.

My thesis contributed to my academic knowledge and the development of crucial skills and I am very much looking forward to seeing what challenges will come next.

*Pepijn van Sabben
Delft, December 2023*

Abstract

Groundwater extraction has increased significantly in Nepal. In combination with climate change, this might lead to accelerated groundwater resource depletion. No recent research has been done in the assessment of these resources in the Banke district development area in the Terai. This study aims to assess whether the intensification of extractions has led to a depletion of groundwater in the upper aquifer. We investigated six local case studies during the dry season with a sole focus on the upper aquifer. The hydrological fluxes were quantified at every location. Evaporation and recharge were estimated using remote sensing data and locally obtained meteorological data. Domestic extractions, irrigation return flow and irrigation extractions were approximated by fieldwork. The groundwater storage change over the period was estimated using a recorded groundwater table time series and the Water Table Fluctuation method. The net subsurface flow- and percolation were estimated by closing the water balance for every case study. Subsequently, the fluxes at local case studies were extrapolated using Groundwater Response Units. The groundwater table replenishment was estimated using the relation between effective precipitation and groundwater levels over two years. The net extraction from the groundwater was insignificant compared to the contribution of evaporation. The approximate minimum precipitation needed for the monsoon season to recover the shallow aquifers after the dry season was on average comfortably exceeded over the last ten years. Thus, the groundwater resources are currently not depleting due to the intensification of extractions in the upper aquifer. However, the current extractions from deeper aquifers might decrease the pressure in deeper layers increasing percolation. Eventually, this endangers the groundwater resources in the upper aquifer. The limited number of measurements in deeper wells already indicated potential depletion in deeper layers. Further research is therefore recommended in deeper aquifers.

Contents

1	Introduction	1
1.1	Problem statement	1
1.2	Research objective	1
1.3	Approach	2
1.4	Scope	2
1.5	Report structure	2
2	Physiographic description	4
2.1	Topographic location	4
2.2	Subsurface geology	5
2.3	Land use	6
2.4	Meteorology of the area	7
3	Methodology	8
3.1	Approach strategy	8
3.2	Area definition	9
3.3	Water balance	10
3.4	Recharge	11
3.5	Extraction	12
3.6	Irrigation return flow	13
3.7	Transpiration	13
3.8	Storage change	14
3.9	Sub-surface flow and Percolation	14
3.10	Extrapolation of fluxes in space	15
3.10.1	Characterizing response units	15
3.10.2	Assigning response units	16
3.10.3	Scaling using response units	16
3.11	Groundwater trend	17
3.11.1	Dry season	17
3.11.2	Monsoon season	17
4	Case studies	19
4.1	Field locations	19
4.2	Borders case studies	20
4.3	Case study one	21
4.4	Case study two	24
4.5	Case study three	27
4.6	Case study four	30
4.7	Case study five	34
4.8	Case study six	37
4.9	Conclusions	40
5	Results	41
5.1	Recharge	41
5.1.1	Precipitation data	42
5.1.2	Chloride Mass Balance method	42
5.1.3	Uncertainty recharge	43
5.2	Extractions	44

5.2.1	Domestic extractions	44
5.2.2	Irrigation extractions	44
5.2.3	Total extractions	45
5.3	Irrigation return flow	45
5.4	Transpiration	46
5.5	Storage change	46
5.5.1	Water table fluctuation method	46
5.5.2	Determining storage change	49
5.6	Sub-surface flow and percolation	50
5.7	Net extraction	51
5.8	Contribution fluxes per case study	51
5.9	Extrapolation of fluxes in space	53
5.9.1	Assigning response units	53
5.9.2	Contributions total area	53
5.9.3	Uncertainty extrapolation method	54
5.10	Groundwater trend	55
5.10.1	Dry season	55
5.10.2	Monsoon season	55
5.10.3	Uncertainty groundwater trend	56
6	Discussion	57
6.1	Flux quantification per case study	57
6.2	Extrapolation of case studies to study area using GRU	59
6.3	Groundwater resources depletion	60
6.4	Limitations and recommendations	61
7	Summary and conclusions	63
	References	65
A	Appendix A: Additional information	69
A.1	CIMMYT	69
A.2	Meteorological station data	70
A.3	Pastas Python package	71
A.4	Percentile modelling choice	71
A.5	Case study coordinates	73
A.6	Irrigation times correction	73
A.7	Transpiration results	74
A.8	Net subsurface flow and percolation results	74
A.9	Intermediate calculation flux contributions	74
B	Appendix B: Additional figures	76
B.1	Chapter 2	76
B.2	Chapter 3	77
B.3	Chapter 4	82
B.4	Chapter 5	82
C	Appendix C: Additional documents	93
D	Appendix D: Pictures field locations	98

List of Figures

2.1	Longitudinal soil cross-section of the general subsurface of Terai regions in Nepal [38]. The red line indicates the approximate area of the study area South of the Bhabar zone.	4
2.2	The study area within the Banke district in the Terai region of Nepal	5
2.3	Longitudinal cross-section of the subsurface in the Bardiya district adjacent to the Banke district [38]. The red line indicates the border of the scope of the project	6
2.4	Land use map of Banke district courtesy of the Survey Department of the Ministry of Land Management, Cooperatives and Poverty Alleviation of Nepal [31]. Full size in Appendix C.4	7
3.1	Approach strategy to assess potential groundwater depletion due to intensification of extraction from the subsurface	8
3.2	General conceptual diagram of the groundwater balance in the upper unconfined aquifer at the case studies	10
4.1	Study area with the locations of the pressure devices numbered one through six and the barometer numbered seven. Exact coordinates in Appendix A.5	19
4.2	Two pumping tests performed using the observation well and the pumping domestic well Q_1	20
4.3	The schematic drawing of case study one. The red circle depicts the 50-meter border of the area. The numbered subscripts of Q denote domestic extraction wells and the irrigation well is the regional well used by farmers. The texts agriculture and urban describe land use. Finally, cross-section A-A' captures three additional wells with lettered subscripts of Q to visualize the subsurface.	21
4.4	Recorded time series in Q_1 of the groundwater table at case study one where significant daily fluctuations can be distinguished	22
4.5	Schematic cross-section A-A' of the local subsurface of case study one	23
4.6	Extra hourly time series of the groundwater table above the pressure device in well Q_A of case study one with significantly smaller daily fluctuations	24
4.7	Schematic drawing of case study two where Q_{Supply} denotes a water supplying tap installed by the local drinking water office	24
4.8	Time series of the groundwater table at case study two with small daily fluctuations	25
4.9	Extra time series in Q_A of case study two	26
4.10	Schematic cross-section A-A' of the local subsurface of location two	26
4.11	Schematic drawing of case study three where 'Forest' denotes vegetated land cover	27
4.12	Schematic drawing of the river and fluctuating groundwater level in the observation well of case study three indicating that the Duduwa River is a losing river around case study three at the end of the dry season	28
4.13	Time series of the groundwater table at case study three with large daily fluctuations during nearby irrigation extractions and small fluctuations without irrigation extractions	29
4.14	Schematic cross-section A-A' of the local subsurface of case study three	29
4.15	Extra time series in Q_A of case study three with similar daily fluctuations as the other time series	30
4.16	Schematic drawing of case study four	30
4.17	Water levels at midnight at Kamdi where significant extractions took place in the middle of April	31
4.18	Time series of the groundwater table at case study four with medium daily fluctuations and where the groundwater table notable not redraws quickly after irrigation extraction	32
4.19	Extra time series in Q_A of case study four with similar daily fluctuations	33

4.20	Schematic cross-section A-A' of the local subsurface at location four	33
4.21	Schematic drawing field location five	34
4.22	Schematic drawing of the river and fluctuating groundwater level in the observation well of case study five indicating that the Phalgunj River is an infiltrating river around case study five at the end of the dry season	35
4.23	Time series of the groundwater table at case study five with minimal daily fluctuations	36
4.24	Schematic cross-section A-A' of the local subsurface of case study five	36
4.25	Extra time series in Q_A of case study five with similarly small daily fluctuations	37
4.26	Schematic drawing of case study six	37
4.27	Schematic drawing of the river and fluctuating groundwater level in the observation well of case study six indicating that the Duduwa River is a gaining river around case study six at the end of the dry season	38
4.28	Time series location six with medium daily fluctuations	39
4.29	Schematic cross-section A-A' of the local subsurface of case study six	39
4.30	Extra time series in Q_A of case study six with smaller daily fluctuations	40
5.1	Groundwater table time series simulation at case study one	47
5.2	Groundwater table time series simulation at case study three	47
5.3	Groundwater table time series simulation at case study four	48
5.4	Groundwater table time series simulation at case study five	48
5.5	Groundwater table time series simulation at case study six	49
5.6	Schematic drawing with estimated one-dimensional vertical average fluxes at case study four. Schematic drawings of the other case studies are located in Appendix B.4	52
5.7	Schematic drawing with estimated one-dimensional vertical average fluxes for the whole study area	53
5.8	Dry season groundwater level decrease and groundwater levels at the end of the dry season plotted against precipitation minus actual evaporation for two dry seasons and 22 measurement points	55
5.9	Monsoon groundwater recovery and groundwater levels below the subsurface at the end of the monsoon season plotted against precipitation minus actual evaporation for two monsoon seasons and 22 measurement points	56
6.1	The monsoon groundwater recovery at the end of the monsoon season against the effective precipitation for the five deep wells monitored by CIMMYT	62
A.1	Well depths occurrences by the questionnaire from CIMMYT	69
A.2	Normalized population occurrences in response units	72
A.3	Normalized recharge occurrences in response units	72
A.4	Normalized evaporation occurrences in response units	72
A.5	Uncompensated time series of groundwater levels at case study five	73
B.1	Location of study area within Nepal	76
B.2	Elevation map of Nepal where the red circle marks the approximate location of the study area [43]	77
B.3	Three precipitation stations denoted by green markers. Station one is Nepalgunj Airport, station two is Khajura Khurda and station three is Shyano Chepang	77
B.4	Double mass curve of measurements of one station against the average cumulative measurement of all stations	78
B.5	Double mass curve of measurements of one station against the average cumulative measurement of all other stations	78
B.6	Two stations denoted by purple markers measuring the required parameters to estimate potential evapotranspiration. Station one is Nepalgunj Airport and station two is Khajura Khurda	79
B.7	Precipitation sum of the study area over the relevant time frame using CHIRPS	80
B.8	Average NVDI of the study area over the relevant time frame using Landsat 5, 7, 8 and 9	80
B.9	Actual evaporation sum of the study area over the relevant time frame using Visible Infrared Imaging Radiometer Suite	81

B.10	Locations of 22 relevant monitoring wells of CIMMYT	81
B.11	Photo of pump characteristics of the farmer at case study five	82
B.12	Fitted Pastas time series of case study one with residuals, recharge and transpiration contribution, trend and step response all in meters accompanied by the fitted model parameters. The fitted model parameters A, n and a are used to fit the gamma function, the parameter f is the crop factor, the trend parameters are to fit the trend, alpha and beta represent parameters to fit the noise model and parameter d is the constant base level of the simulation	82
B.13	Observed peaks of recharge contribution to the groundwater table of case study one . .	83
B.14	Fitted Pastas time series of case study three with residuals, recharge and transpiration contribution, trend and step response all in meters	83
B.15	Observed peaks of recharge contribution to the groundwater table of case study three .	84
B.16	Fitted Pastas time series of case study four with residuals, recharge and transpiration contribution, trend and step response all in meters accompanied by the fitted model parameters	84
B.17	Observed peaks of recharge contribution to the groundwater table of case study four . .	85
B.18	Fitted Pastas time series of case study five with residuals, recharge and transpiration contribution, trend and step response all in meters accompanied by the fitted model parameters	85
B.19	Observed peaks of recharge contribution to the groundwater table of case study five . .	86
B.20	Fitted Pastas time series of case study six with residuals, recharge and transpiration contribution, trend and step response all in meters accompanied by the fitted model parameters	86
B.21	Observed peaks of recharge contribution to the groundwater table of case study six . .	87
B.22	Typical specific yield values according to the online books published by The Groundwater Project [52]	87
B.23	Schematic drawing with estimated one-dimensional vertical average fluxes at case study one	88
B.24	Schematic drawing with estimated one-dimensional vertical average fluxes at case study three	88
B.25	Schematic drawing with estimated one-dimensional vertical average fluxes at case study five	89
B.26	Schematic drawing with estimated one-dimensional vertical average fluxes at case study six	89
B.27	Groundwater response units with normalized recharge	90
B.28	Groundwater response units with normalized evaporation	90
B.29	Groundwater response units with normalized population density	91
B.30	Groundwater response units with an assigned location	92
B.31	Average yearly CHIRPS precipitation minus VIIRS actual evaporation in the study area .	92
C.1	Water analysis report 1	94
C.2	Water analysis report 2 page 1	95
C.3	Water analysis report 2 page 2	96
C.4	Full size land use map of the Banke district [31]	97
D.1	Photos taken at case study one	99
D.2	Photos taken at case study two	100
D.3	Photos taken at case study three	101
D.4	Photos taken at case study four	102
D.5	Photos taken at case study five	103
D.6	Photos taken at case study six	104

List of Tables

3.1	Brief description of present fluxes at the case studies	11
3.2	Typical crop factors of different land use types [2]	14
4.1	The hydraulic conductivity, transmissivity and storage coefficient from the pumping tests performed in the observation wells at case studies three and four	21
4.2	Domestic extractions within the borders of case study one	22
4.3	Domestic extractions within the borders of case study two	25
4.4	Domestic extractions within the borders of case study three	28
4.5	Domestic extractions within the borders of case study four	31
4.6	Irrigation activities in case study four	32
4.7	Irrigation activities in case study five	35
4.8	Domestic extractions within the borders of case study six	38
5.1	Recharge flux at relevant case studies	41
5.2	The sum of precipitation measurements via meteorological stations and CHIRPS data	42
5.3	Median chloride in the groundwater at the case studies	42
5.4	Utilization of the chloride Mass Balance method to estimate the range of the one-dimensional recharge flux at the case studies	43
5.5	The consequence of drastically increasing evaporation during precipitation events per case study	43
5.6	The domestic extractions per case study	44
5.7	Irrigation extraction per case study	44
5.8	The sum of extractions for domestic use and irrigation per case study	45
5.9	Total irrigation return flow and average return flow per day per case study	45
5.10	The consequence of drastically increasing evaporation during irrigation events per case study	45
5.11	Transpiration and associated crop factor per case study	46
5.12	Estimated crop factor ranges using visual inspection and the guidelines by the FAO	46
5.13	Estimated specific yields via the Water Table Fluctuation method	49
5.14	Volume storage change over the measurement time frame between the 24 th of March and 4 th of June	49
5.15	Influence of altering specific yield on the storage change	50
5.16	Net sub-surface flow and percolation flux per case study	50
5.17	Uncertainty of the combined net subsurface flow and percolation flux	51
5.18	Net extraction per case study	51
5.19	Volume contribution of fluxes per case study	51
5.20	Average one-dimensional daily water fluxes per case study where $\Delta \bar{H}$ is absolute water instead of groundwater table	52
5.21	Contribution percentage fluxes per case study	52
5.22	Assigned sum of response unit areas per case study	53
5.23	Assigned contribution volumes in m ³ and percentage	54
5.24	Re-assigned sum of response unit areas per case study	54
5.25	Re-assigned contributions for the scenarios in percentage	54
A.1	The coordinates of the six case studies in WGS decimal degrees N and E	73
A.2	Transpiration calculation via the evaporation sum	74
A.3	Net sub-surface flow/percolation calculation via the reversed water balance	74
A.4	Assigned contribution volumes in m ³ and percentage for all relevant case studies	75

Nomenclature

Symbols

Symbol	Definition	Unit
A_{Farm}	Area of the respective farm	m ²
A_{Focus}	Area of the case studies	m ²
A_{Loc-i}	Sum of response unit areas that are assigned to be the same as location i	m ²
C_{GW}	In the field measured median chloride concentration in groundwater	mg/l
C_P	In the field measured median chloride concentration in precipitation	mg/l
E_1	Exponential integral in Theis solution	
ET_0	Potential evapotranspiration	mm
$ET_{T_{Trans}}$	One-dimensional vertical transpiration flux	mm
$ET_{T_{Trans}}$	Average one-dimensional vertical transpiration flux	mm/d
Ev_{GRU}	Average actual evaporation sum in a groundwater response unit using satellite data	mm
Ev_{Loc-i}	Normalized actual evaporation of location i	-
Ev_{Norm}	Normalized actual evaporation using satellite data	-
$Ev_{Res-Unit}$	Normalized actual evaporation of specific response unit	-
$Ev_{2.5-percentile}$	The evaporation value in the GRU at the 2.5 percentile	mm
$Ev_{97.5-percentile}$	The evaporation value in the GRU at the 97.5 percentile	mm
Ex_{Loc-i}	Normalized extraction of location i	-
Ex_{Norm}	Normalized extraction using satellite data	-
$Ex_{Res-Unit}$	Normalized extraction of specific response unit	-
$Ext - Net$	Average one-dimensional vertical net extraction flux	mm/d
$Extr$	Average one-dimensional vertical extraction flux	mm/d
f	Crop factor	-
$\Delta \bar{H}$	Average groundwater table change	mm/d
H_{Rch}	Height of the recharge contribution	mm
$H_{t=0}$	Height of the initial groundwater table of the time series	m
$H_{t=n}$	Height of the last groundwater table of the time series	m
IR	One-dimensional irrigation depth	mm
\bar{IR}	Average one-dimensional irrigation depth	mm/d
i_{GWT}	Slope of the groundwater table	-
i_{max}	Most positive groundwater slope	-
i_{min}	Most negative groundwater slope	-
k	Hydraulic conductivity	m/s
$NVDI_{GRU}$	Average NVDI in a groundwater response unit using satellite data	-
$NVDI_{Norm}$	Normalized NVDI using satellite data	-
$NVDI_{2.5-percentile}$	The NVDI value in the GRU at the 2.5 percentile	-
$NVDI_{97.5-percentile}$	The NVDI value in the GRU at the 97.5 percentile	-
P	One-dimensional precipitation via meteorological stations	mm
P_{An}	Annual precipitation using satellite data	mm
P_{Dry}	Precipitation in the measurement time frame using satellite data	mm
P_{Eff}	Effective precipitation	mm
P_{GRU}	Average precipitation sum in a groundwater response unit using satellite data	mm
P_{Norm}	Normalized precipitation using satellite data	-

Symbol	Definition	Unit
$P_{Remote-Sensing}$	One-dimensional precipitation via CHIRPS	mm
$P_{2.5-percentile}$	The precipitation value in the GRU at the 2.5 percentile	mm
$P_{97.5-percentile}$	The precipitation value in the GRU at the 97.5 percentile	mm
Pop_{GRU}	Total population in a groundwater response unit using satellite data	-
$Pop_{2.5-percentile}$	The population value in the GRU at the 2.5 percentile	-
$Pop_{97.5-percentile}$	The population value in the GRU at the 97.5 percentile	-
p_{Extr}	Contribution percentage of extraction in the whole region	%
$p_{Ext-net}$	Contribution percentage of net extraction in the whole region	%
p_{Perc}	Contribution percentage of groundwater table evaporation in the whole region	%
p_{Rch}	Contribution percentage of recharge in the whole region	%
$p_{Ret-Flw}$	Contribution percentage of return flow in the whole region	%
$p_{SSF-Perc}$	Contribution percentage of net subsurface flow and percolation in the whole region	%
Q	Discharge	m ³ /s
$Q_{1,2,...}$	Domestic extraction well	
$Q_{A,B,...}$	Observation well for local subsurface	
$Q_{Irrigate}$	Closeby irrigation well	
Q_{Obs}	Observation well used for time series	
Q_{Supply}	Drinking water supplying well	
R	One dimensional recharge	mm
\bar{R}	One dimensional average recharge per day	mm/d
RF	One-dimensional irrigation return flow depth	mm
\bar{RF}	Average one-dimensional irrigation return flow	mm/d
$R_{Cl-CHIRPS}$	Interpolated recharge via CMB method with CHIRPS data	mm/d
$R_{Cl-Station}$	Interpolated recharge via CMB method with meteorological station data	mm/d
R_{Rch-An}	Annual recharge using the CMB method	mm
R_{Norm}	Normalized recharge using satellite data	-
R_{Loc-i}	Normalized recharge of location i	-
$R_{Res-Unit}$	Normalized recharge of specific response unit	-
S	Storage coefficient	-
$SSF/Perc$	Two-dimensional lateral subsurface flow flux	mm ² /d
$SSF/Perc$	One-dimensional average lateral subsurface flow and percolation flux	mm/d
$SSF \bar{-} Perc$	One-dimensional average vertical subsurface flow and percolation flux	mm/d
S_{Loc-i}	Similarity score for location i	-
S_y	Specific yield	-
T	Transmissivity	m ² /s
t	Time	s or h
t_0	Initial time	s
u	Parameter in Theis solution	-
V_{Cl-Rch}	Recharge flux via the CMB method	m ³
V_{Cons}	Consumption volumes per case study	m ³
V_{ET_0}	Potential evapotranspiration	m ³
V_{ET_a}	Actual evaporation flux	m ³
$V_{Evap-Rch}$	Evaporation during recharge flux	m ³
$V_{Evap-Irri}$	Evaporation during irrigation flux	m ³
V_{Extr}	Extraction flux	m ³
$V_{Extr-Irri}$	Irrigation extraction flux	m ³
$V_{Extr-Loc-i}$	Extraction flux of location i	m ³
$V_{Extr-Loc-i-Sum}$	Total extraction volume of all locations similar to location i	m ³
$V_{Extr-Net}$	Net extraction contribution flux	m ³

Symbol	Definition	Unit
$V_{Extr-Total}$	Extraction flux in the whole study area	m^3
V_{Prec}	Precipitation flux	m^3
V_{Q_i}	All domestic wells at a location flux	m^3
V_{Rch}	Recharge flux via the effective precipitation method	m^3
$V_{Ret-Flw}$	Return flow flux	m^3
$V_{SSF-Perc}$	Combined subsurface flow and percolation flux	m^3
$V_{Storage}$	Groundwater storage	m^3
V_{Trans}	Transpiration flux	m^3
$V_{Trans-pot}$	Potential transpiration flux	m^3

Abbreviations

Abbreviation	Definition
CHIRPS	Climate Hazards Center InfraRed Precipitation with Station data
CMB	Chloride Mass Balance
DHM	Department of Hydrology and Meteorology from the Ministry of Energy, Water Resources and Irrigation of Nepal
EC	Electrical Conductivity
FAO	Food and Agriculture Organization of the United Nations
GRU	Groundwater Response Units
GWRDB	Groundwater Resources Development Board
GWT	Groundwater Table
Landsat	Land sensing satellite
NVDI	Normalized Vegetation Difference Index
SSEBop	Operational Simplified Surface Energy Balance
VIIRS	Visible Infrared Imaging Radiometer Suite
WTF	Water Table Fluctuations

Glossary

Word	Definition
CIMMYT	CIMMYT is an international organisation that focuses its efforts on aiding developing countries. Their attention centres on farming and mainly on the crops wheat and maize. The primary focus in Nepal is to a great extent on the specified study area. This research is at their request.
Case study	On of the areas which are closely analyzed regarding fluxes. The term is often intertwined with field location.
Dry season	The combination of all seasons outside the monsoon season.
Field location	The same as case study.
Monsoon season	The rain season in Nepal defined by the Ministry of Energy, Water Resources and Irrigation as approximately between June 13 th and September 23 rd [15].
Time frame of interest	The dates between the 24 th of March and 4 th of June.

1

Introduction

1.1. Problem statement

Global groundwater withdrawal increased by around six times over the past century [49] where irrigation currently accounts for roughly 70% of the total water extraction [16, 48]. This increase in groundwater usage can be attributed to the widespread availability of electrical pumps. For instance, the International Energy Agency in Nepal witnessed a twelvefold increase in electricity consumption in the last 30 years in Nepal [39]. This elevated pump usage is beneficial for the everyday availability of groundwater resources for domestic and irrigation purposes. However, if groundwater usage is not appropriately managed, intensification of extraction could accelerate the depletion of groundwater [7]. Climate change puts the groundwater resources even further under pressure [7]. Therefore, it is necessary to be watchful for possible depletion in vulnerable regions.

In the Western Terai of Nepal, a low-lying agricultural region with high temperatures, irrigation is pivotal in protecting agricultural areas against monsoon variability [4]. Compared to irrigated areas, non-irrigated areas show significant yield losses during the dry season [4, 51]. The Ministry of Energy, Water Resources and Irrigation of Nepal sets targets to increase the coverage of year-round irrigation from 18% in 2010 to 80% in the year 2030 nationwide in their 'Irrigation Master Plan 2019' with a particular focus on the Terai region [51]. In combination with the increased population, this led to a heavy increase in domestic irrigation extractions.

Around the city of Nepalgunj, the capital of the Banke district in the Western Terai, the total proportion of area dedicated to agriculture is around 80% [14]. The district ranks among the lowest in terms of socioeconomic indicators and is therefore one of the main regions of interest for development aid nationwide [51]. Groundwater is heavily used by inhabitants to satisfy their domestic and irrigation needs [38]. Therefore, CIMMYT, a research- and development aid organization (Appendix A.1), is concerned about the increased uncontrolled private pumping. The availability of groundwater resources might be altered and lead to depletion [34]. Nonetheless, recent efforts to assess groundwater availability and potential depletion in the Banke district are lacking.

1.2. Research objective

The overarching objective of this research is to aid CIMMYT and local authorities in understanding the development area of the Banke district better. Therefore, an insight into the availability of groundwater resources is crucial in their agricultural research. This study aims to assess whether the availability of groundwater resources is diminishing due to increased extraction in Banke. Furthermore, it aims to contribute to the existing literature on estimating these fluxes and ultimately the groundwater resource

availability with limited data. To do so, the following research question is addressed:

“Are the groundwater resources in the agricultural and urban development areas of the Banke district depleting due to the intensification of extractions from the groundwater?”

In order to answer the research question two parts of the question should be researched.

- “How can the fluxes in the area be quantified and what is the proportional contribution of extractions?”
- “How well are groundwater resources replenished after the monsoon seasons?”

1.3. Approach

Depletion caused by extraction is most pronounced during the dry season due to the relatively minimum levels of the primary fluxes recharge and evaporation. Hence, the research was conducted during the peak of the dry season. An essential tool for assessing depletion is a water balance. A water balance equals the inflows and outflows to the storage change in a system and is required to quantify the individual fluxes influencing the groundwater. According to CIMMYT, there has not been a water balance analysis specific to the Banke district. This signifies no local estimations for the groundwater fluxes have been made so far. Formulating a complete water balance is thus crucial. At the same time, this remains difficult for larger areas with limited data like in the Banke district [24].

In this research, we will start assessing the various water balance components for 6 representative locations in the Banke district's agricultural areas. The key components in these water balances are evaporation, recharge, subsurface flow and groundwater extraction. Subsequently, these water balance components in the case studies will be extrapolated using groundwater response units. The contribution of extraction to potential depletion can then be determined.

Net groundwater resource loss over a longer time signifies depleting groundwater resources [50]. Therefore, the average yearly recharged volume should be more than the yearly lost volume on a longer term to assess groundwater resource depletion. The main seasons are the monsoon and dry season in the Banke district in the Nepal Terai. The monsoon season replenishes groundwater and the dry season decreases the groundwater resources. Effectively, we looked at whether the monsoon seasons recharged more than dissipated during the dry seasons for a longer period.

1.4. Scope

This research specifically targeted the shallow unconfined aquifer of the defined area within the Banke district. Deeper extractions are out of the scope. Furthermore, the Bhabar zone and different districts were outside the scope.

1.5. Report structure

This report is structured as follows.

Chapter two provides a physiographic description of the study area within the Banke district, detailing its topographic location within Nepal, subsurface geology, and land cover.

The third chapter focuses on methodology and begins with a description of the overall approach strategy. It outlines how case studies were defined and utilized to identify present fluxes and quantify them. Subsequently, it was elaborated on how the present fluxes were extrapolated to the whole region of interest using groundwater response units to retrieve the proportion of the extraction flux. Finally, the methodology to estimate potential groundwater depletion using seasonal groundwater table fluctuations was given.

The next chapter describes the individual case studies, delineating their boundaries and offering detailed area descriptions, extraction and irrigation patterns, and subsurface information for each location. The fifth chapter, “Results”, presents the estimated quantification of the individual fluxes per location with corresponding uncertainties. It extrapolates the fluxes spatially and evaluates associated uncer-

ainties. Furthermore, it details seasonal groundwater recovery and decrease.

The discussion analyses the utilized methods, assumptions, parameter choices and findings. It draws conclusions regarding the contribution of extraction, conducts an assessment of groundwater resources, and deliberates on the study's limitations and future recommendations.

Physiographic description

2.1. Topographic location

The study area is situated in southwestern Nepal (Figure B.1), known as the Western Terai region. North of this area lie the impermeable rock formations of the Siwalki hills (Figure 2.1). Adjacent to the Siwalki hills is the Bhabar zone, predominantly comprised of highly permeable materials [38]. The land cover in the Bhabar zone consists of a continuous belt of forested area [19]. It is important to note that lateral recharge via this zone is considered a significant contributor to groundwater recharge in the Terai region [18, 38, 46]. The boundary of the study area coincides with the border of the Bhabar zone.

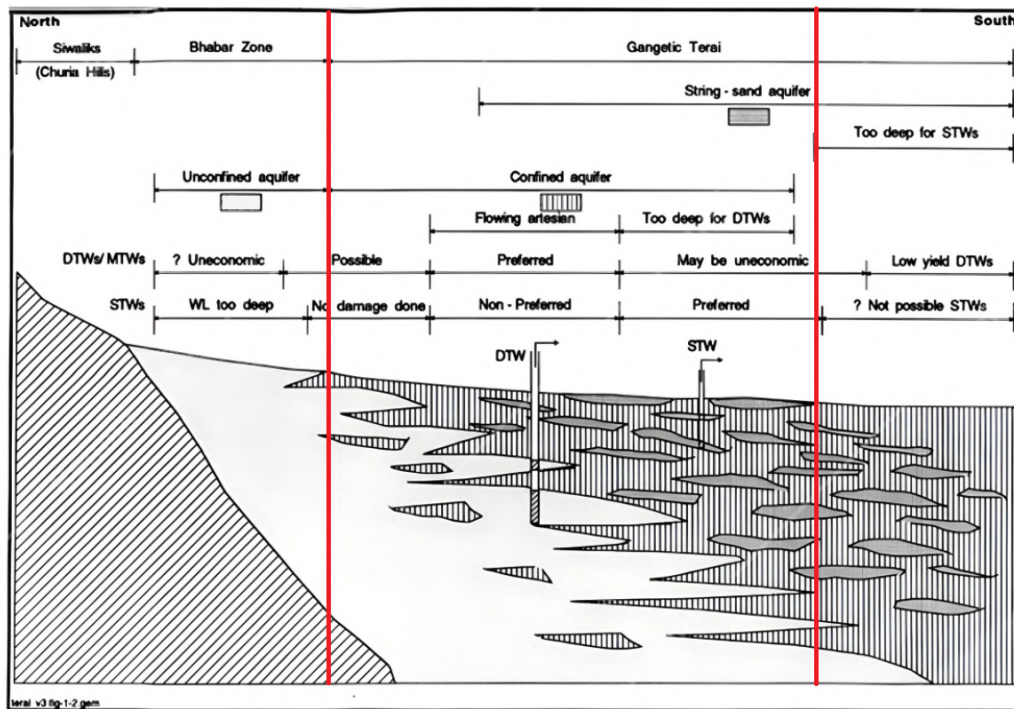


Figure 2.1: Longitudinal soil cross-section of the general subsurface of Terai regions in Nepal [38]. The red line indicates the approximate area of the study area South of the Bhabar zone.

Aside from the forested area delineating the Bhabar zone in the northeast, the study area is additionally demarcated by the Phalgunj River in the northwest, the Rapti River in the southeast, and the Indian border in the southwest (Figure 2.2). Encompassing a total surface area of 480.4 square kilometres, this region stands as a defined geographical space for the study.

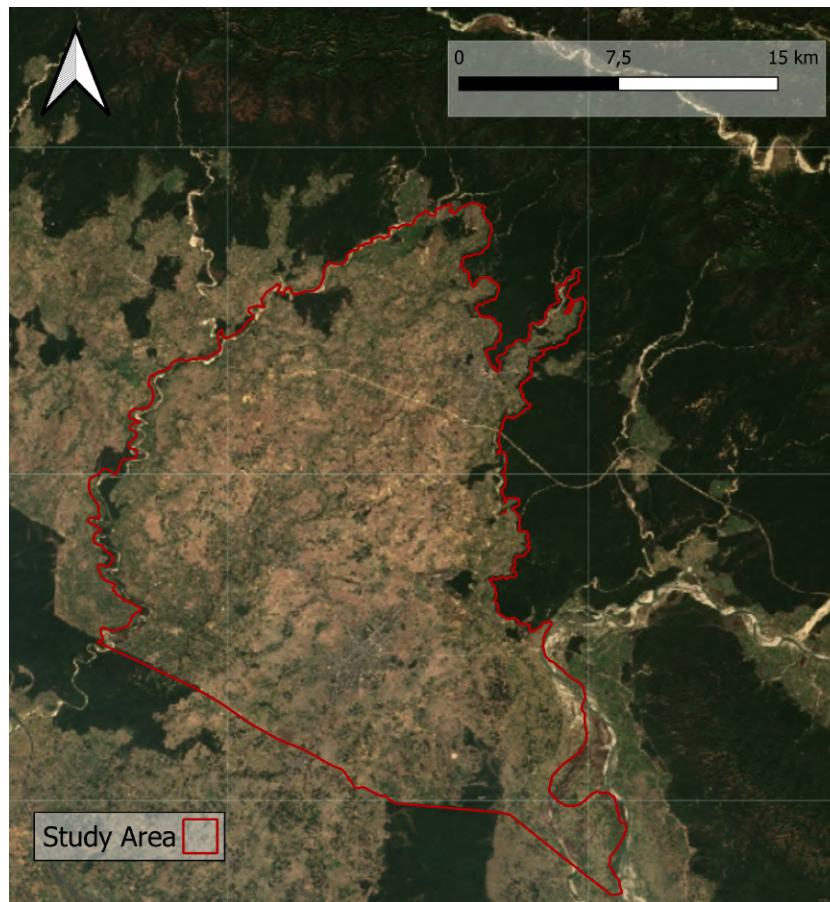


Figure 2.2: The study area within the Banke district in the Terai region of Nepal

2.2. Subsurface geology

A pronounced feature is the position of the alluvium in the subsurface in the Terai. The high variability in seasonal precipitation intensity causes enormous temporal variability in sediment transport. Given that the river systems in the Terai are among the most dynamic in the world [41], the variation in deposited sediment types is considerable [44, 46]. Consequently, this led to significant spatial heterogeneity in the subsurface top layer. Nonetheless, the heterogeneity in the whole Terai plain is of a similar sort. Therefore, the subsurface is homogeneous in its heterogeneity (Figure 2.3).

The subsurface of the plain is generally more comprised of clay, silt, and fine sand than sand and gravel [46]. The shallow aquifers have on average a thickness between 2 and 15 meters [46]. Regrettably, a clear picture of the upper aquifer is not producible due to the limited available information and heterogeneity over space [46]. A clay layer can be found underneath this upper aquifer (Figure 2.3). This clay layer was established as the natural border of the scope of this project because clay is an impermeable texture class. Consequently, the study focused on the upper unconfined aquifer within the region of interest.

The transmissivity in upper aquifers of the region is between 181 m²/d and 1030 m²/d, which is derived from a limited number of pumping tests [46]. However, it remains difficult to spatially quantify exact values for transmissivity and hydraulic conductivity due to the limited pumping tests and lithological logs in the area.

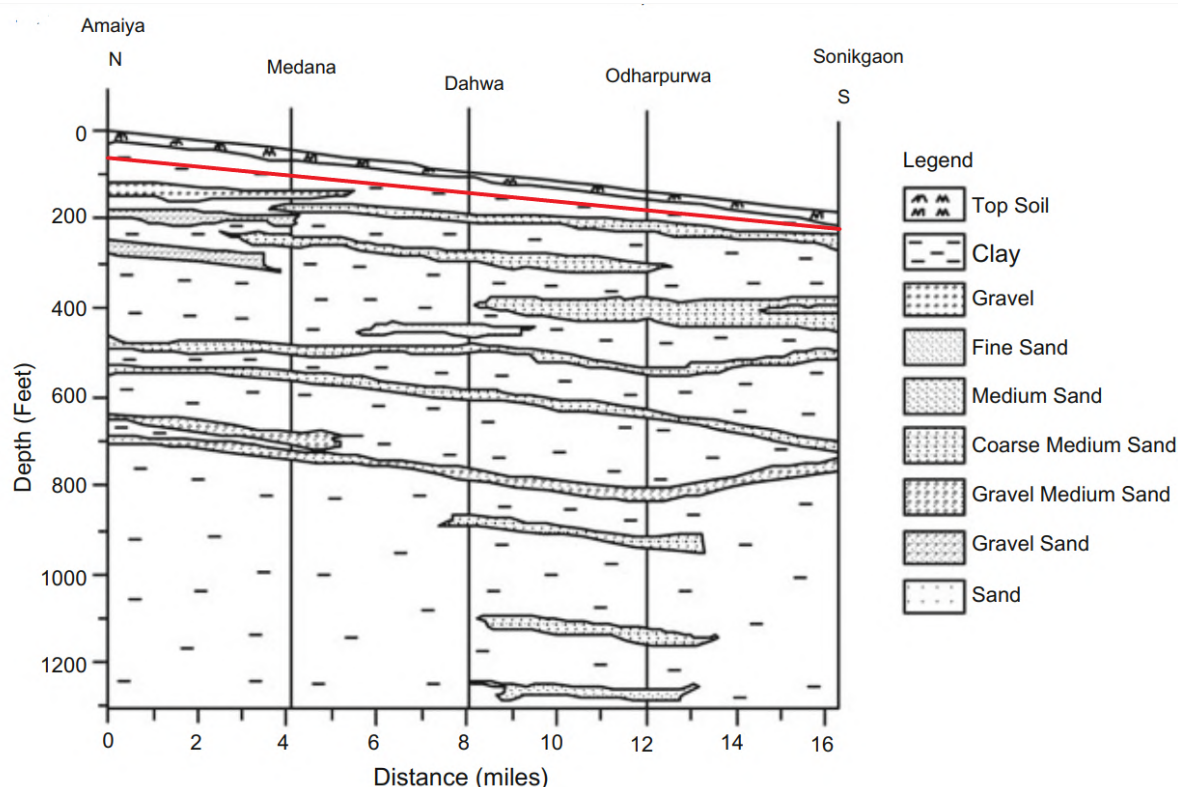


Figure 2.3: Longitudinal cross-section of the subsurface in the Bardiya district adjacent to the Banke district [38]. The red line indicates the border of the scope of the project

2.3. Land use

The West-Terai region is characterized by high temperatures and flat lands with relatively low elevation (Figure B.2). Significant elevation differences in the study area are not present and therefore not featured in this report. However, there is a slight slope towards the South of the area. Within the study area, both agricultural and urban development prevail as the dominant land uses (Figure 2.4). The Nepalgunj sub-metropolitan area contains the highest percentage of agricultural areas of the 12 major cities in Nepal [14]. In substantial rural segments of the region, residents contend with poverty and rely heavily on crop farming for sustenance. Moreover, the urban expanse within the Banke district has experienced significant growth in recent years. For example, in the Nepalgunj district alone, the built-up area expanded tenfold within the past 24 years [42]

CIMMYT conducted 500 questionnaires to understand the local population better. On average, households in the Banke district consist of eight individuals, often due to families residing together for extended periods. These large families were consistently observed during fieldwork. Typically, households own approximately 1.1 hectares of land, which includes domestic farms for personal sustenance and more commercialized farms focused on selling yields. Approximately 64% of the population own shallow wells and the others possess deep wells. These deep wells are often used for irrigation while the smaller wells are mostly used for domestic purposes. The depth of the wells also depends on the permeability of the subsurface. A more permeable material means a shallower well. The median depth of the domestic wells was 20 meters (Figure A.1). Around 39% of the participants used their wells to irrigate their fields with groundwater. Among these farmers, the median irrigation depth during the dry season was around 5 millimetres per day. This number appears to be trustworthy.

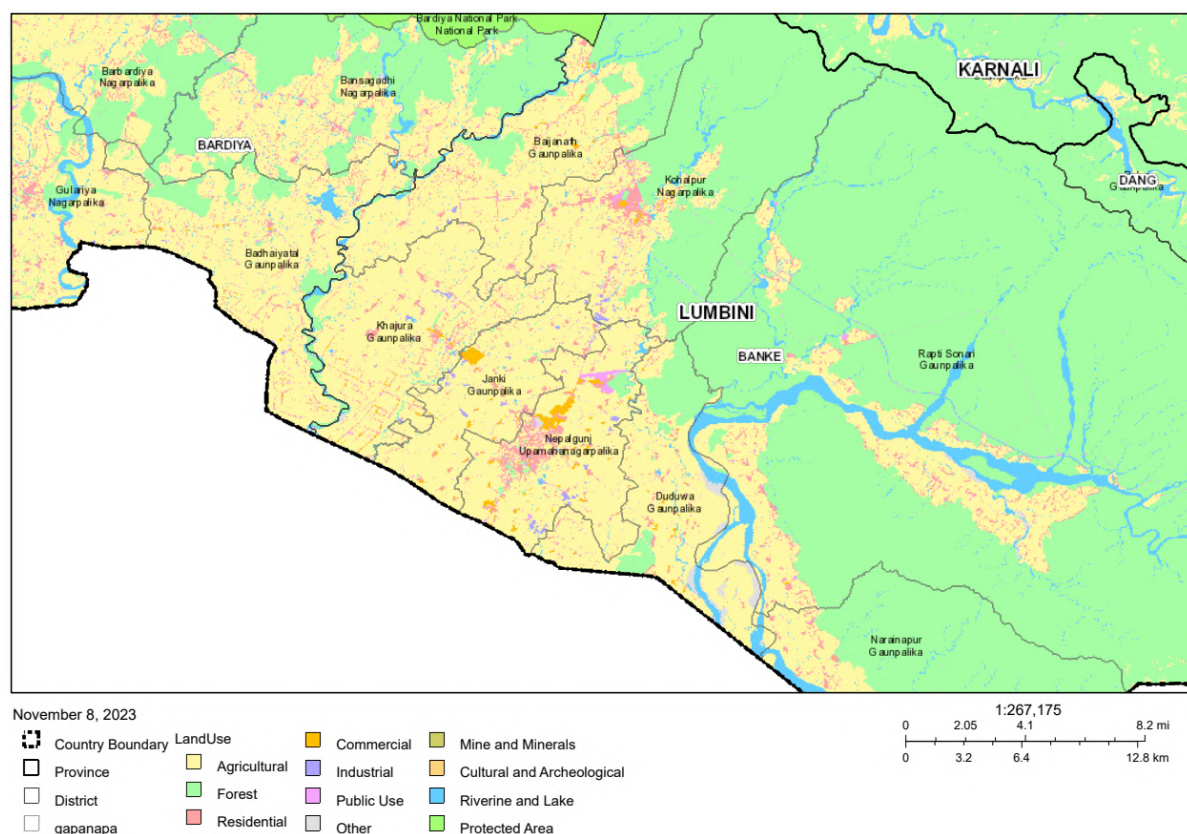


Figure 2.4: Land use map of Banke district courtesy of the Survey Department of the Ministry of Land Management, Cooperatives and Poverty Alleviation of Nepal [31]. Full size in Appendix C.4

2.4. Meteorology of the area

Nepal experiences seasonally great differences in precipitation. Multiple seasons exist but in this study, we only looked at the monsoon season and the dry season, the latter of which is defined as the combination of all the seasons outside the monsoon season. The monsoon season approximately starts June 13th and ends September 23rd according to the Department of Hydrology and Meteorology (DHM) from the Ministry of Energy, Water Resources and Irrigation of Nepal [15]. However, the exact start and end dates vary annually. In the dry season, precipitation hovers around 100 millimetres while this is around ten times larger in the wet season [11]. Actual evaporation in the area is in the dry season around 400 millimetres and during the monsoon season a similar number [11], despite the dry season lasting approximately three times longer. This can be attributed to the increased availability of water during the dry season. It is important to note that the effective precipitation, defined as the precipitation minus actual evaporation, is positive during the wet season but negative during the dry season. The case studies in this research were done during the time frame from March 24th to June 4th. According to the definition by the DHM the time frame was just before the start of the monsoon season. Nonetheless, because the seasons do not change abruptly but rather gradually, the time frame did capture some more precipitation near the end of the measurement time frame.

3

Methodology

3.1. Approach strategy

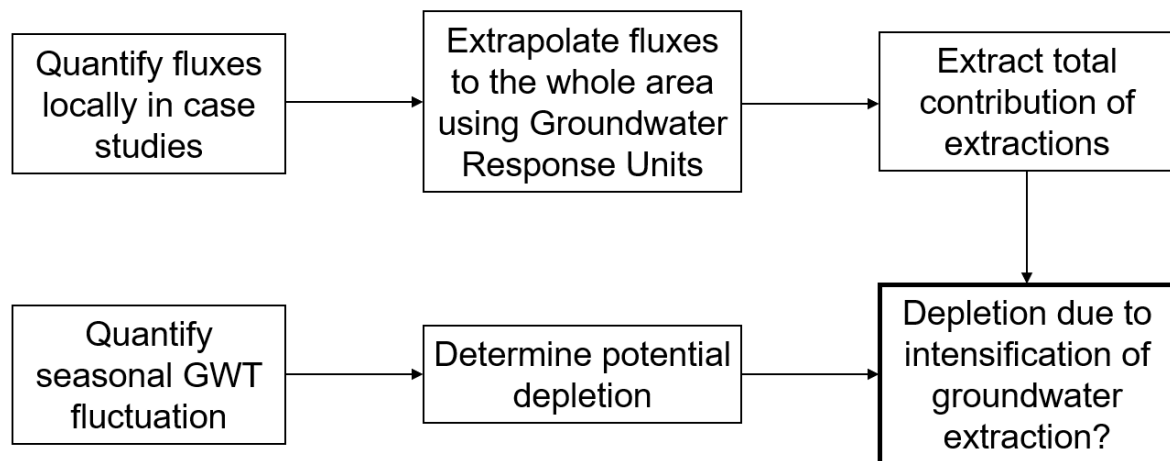


Figure 3.1: Approach strategy to assess potential groundwater depletion due to intensification of extraction from the subsurface

This research adopted a method centred on estimating fluxes through representative case studies. Six representative sites for field measurements were selected, defined within circular areas around local out-of-use observation wells in the upper aquifer. The radius of this circle was determined via the immediate cone of depression caused by representative extractions. Hourly groundwater table fluctuations were measured using pressure devices positioned in observation wells at the centre of these areas. These wells, while out-of-use, were unclogged to ensure the stagnant water level aligned with the groundwater table. Simultaneously, a barometer recorded atmospheric pressure. The devices generated hourly time series from March 24th to June 4th, specifically during the dry season to emphasize the relative extraction flux. These time series were used to calculate the total groundwater table decrease. Analyzing local fluxes during the dry season involved hydrological data, extraction field research, and water balance assessments, inspired by the Water Budget method [25]. Later sections elaborate on how these fluxes were quantified and assumed to represent the broader study area. Subsequently, these local fluxes were extended to the entire study area using groundwater response units to quantify a representative flux for the whole region.

Potential groundwater resource depletion was estimated using an additional method. The seasonal groundwater table changes of the last two years were estimated by data from CIMMYT. By comparing the recoveries between the two years, an estimation could be made for the effective precipitation wherefore groundwater resources are recovered. Using data from the last ten years an assessment can be made as to whether groundwater resources have been depleting.

One other approach, not pursued in this research, involves creating a regional groundwater model structured around regional cross-sections. The model could extrapolate saturated hydraulic conductivity incorporating an uncertainty parameter by using lithological units from the available lithological logs. Local groundwater table time series could be fitted in the model with hydrological information and available extraction pattern information. The potential of this model includes estimating flux contributions to groundwater depletion and predicting seasonal groundwater fluctuations. However, spatially distributed extraction patterns were not available. This means that estimating the extraction flux correctly would be difficult while this flux is the most crucial flux of the research. Additionally, extrapolation using lithological units faced high uncertainty due to substantial spatial heterogeneity in the upper aquifer and limited lithological logs. Hence, the approach based on representative case studies was pursued.

3.2. Area definition

The area surrounding each case study was delineated as a circular zone around the observation wells. This approach aimed to confine the analysis to the immediate vicinity of the wells, minimizing external influences from design choices. To enhance manageability and consistency, a uniform radius was applied across all case studies. The radius was determined using the capture zone of the well, approximated using the influence of the cone of depression as a function of the radius from a pumping test. A homogeneous subsurface was desired to perform pumping tests because homogeneity in the subsurface gives more representative estimates for the hydraulic conductivity and the storage coefficient. Consequently, local subsurface characteristics were estimated based on nearby out-of-use well depths and groundwater table data in every case study. Pumping tests were performed at the locations exhibiting the highest homogeneity in the local subsurface, with an adjacent well to facilitate these tests. Water pressure devices were installed in the observation wells alongside activating a pump in a nearby well. The pressure devices recorded the drawdown during pumping and the groundwater recovery after pumping. An analytic elements method, as detailed in the work by Kruseman and de Ridder [29], was employed to determine suitable hydraulic conductivity (k) and storage coefficient (S). The transmissivity T was determined by multiplying the hydraulic conductivity with the aquifer thickness, assuming the aquifers at the locations were unconfined.

The Theis solution, a widely employed analytical model in groundwater hydrology [45], was utilized to estimate the immediate cone of depression for wells in the most adverse conditions (Formula 3.1). This model was chosen due to its frequent application in groundwater hydrology, ensuring consistency with established methodologies [20].

$$h = -\frac{Q}{4 * \pi * T} * E_1(u) \quad \text{for} \quad t > t_0 \quad (3.1)$$

where E_1 is defined as the exponential integral and parameter u as:

$$u = \frac{S * r^2}{4 * T * (t - t_0)} \quad (3.2)$$

The cone of depression provides a relationship between the drawdown of the groundwater tables and the distance from the well. We established the border of the case studies as the radius where the drawdown reached approximately one-tenth of the drawdown just outside the observation well during the most adverse conditions. This radius, determined by the case studies with relatively homogeneous subsurface, was presumed to be representative of all case studies. The area within the borders of all case studies will be denoted as A_{Focus} .

3.3. Water balance

The fluxes in the general system in the case studies are transpiration, recharge, extraction, subsurface flow, percolation and irrigation return flow (Figure 3.2). Second-order effects like deep extraction or deeper-layer subsurface flow were neglected because they were in a deeper aquifer and thus outside the scope of this study. Actual evaporation during precipitation and irrigation is also a second-order effect but was included because these quantifiable fluxes directly influence the recharge flux and irrigation return flow flux. The subscript at every flux indicates for which case studies the fluxes were relevant. Return flow and actual evaporation from irrigation were only present at locations four and five. These were the sole case studies that contained irrigated areas within their boundaries.

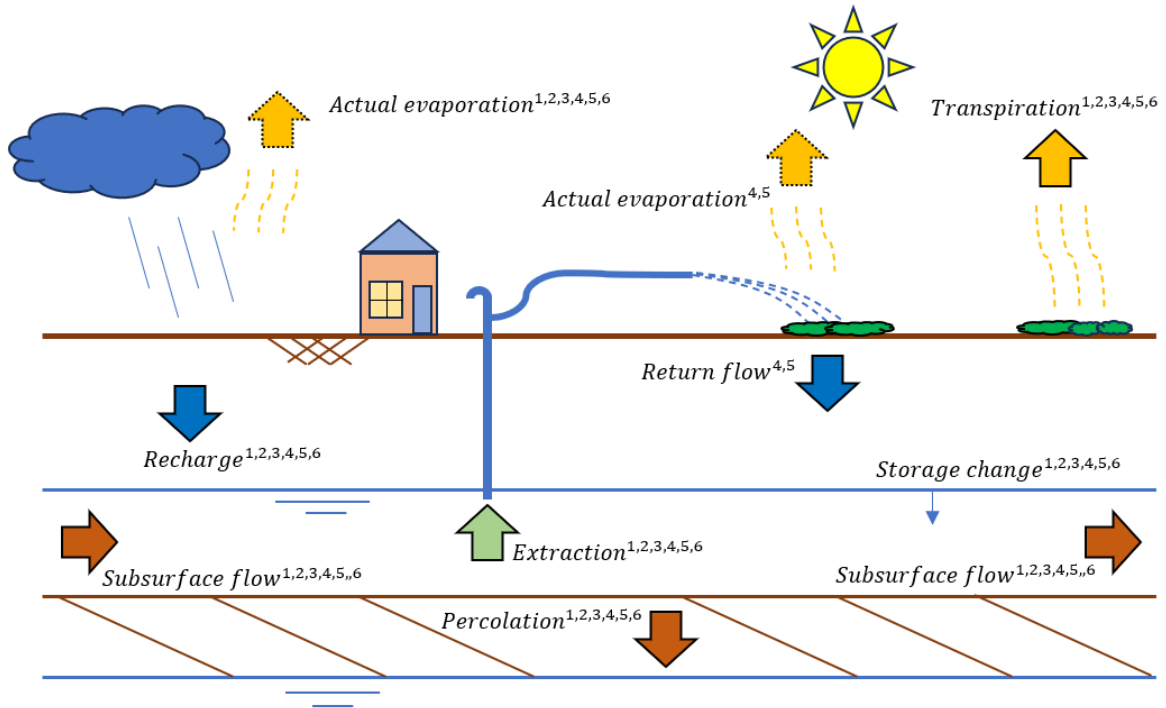


Figure 3.2: General conceptual diagram of the groundwater balance in the upper unconfined aquifer at the case studies

A volume water balance of the system was formulated (Formula 3.3) using the fluxes (Table 3.1) and focus area A_{Focus} . This was done by taking the sum of the volumes entering and leaving the groundwater table.

$$\sum V_{Rch} + \sum V_{Extr} + \sum V_{Ret-Flw} + \sum V_{Trans} + \sum V_{SSF-Perc} = \Delta V_{Storage} \quad (3.3)$$

Flux	How to treat
Recharge	Recharge was estimated by calculating effective precipitation using local station data. The flux was later compared to recharge estimations using the Chloride Mass Balance (CMB) method.
Extraction	The daily domestic extractions and extractions for irrigation were estimated using local research and summed per location.
Irrigation return flow	Irrigation return flow was estimated by using locally collected irrigation patterns and potential evapotranspiration data.

Flux	How to treat
Transpiration	Transpiration was estimated as evaporation that was not due to irrigation or precipitation. Subsequently, a crop factor was estimated per case study to verify the flux using literature.
Net sub-surface flow and percolation	This flux combined percolation and subsurface flow. The net contribution of the flux closed the groundwater balance.

Table 3.1: Brief description of present fluxes at the case studies

Assumptions

Precipitation run-off and river discharge were assumed negligible within the study area during the measurement time. Additionally, throughout all case studies the aquifers were presumed shallow. These assumptions will be verified in Section 4.1. The aquifers were also assumed to be unconfined, an assumption that will be verified in Section 5.5. While the vadose zone was not separately featured within the research, its influence on transpiration and infiltration time lag was factored into the flux assessments.

3.4. Recharge

The recharge flux was deemed equivalent to effective precipitation since the run-off of precipitation was neglected. Hence, the product of effective precipitation P_{Eff} and the focus area A_{Focus} equated to the recharge volume flux (Formula 3.4). Precipitation is denoted by P and the potential evapotranspiration by ET_0 . The actual evaporation was considered equal to potential evapotranspiration data during precipitation events. This assumption implies that water transpires normally once the precipitation events conclude.

$$V_{Rch} = P_{Eff} * A_{Focus} = (P - ET_0) * A_{Focus} \quad (3.4)$$

Precipitation data

Precipitation events varied locally, as observed during fieldwork where rain gauges indicated significantly different fill levels across the case studies. Consequently, hourly precipitation data from three district locations was acquired from the Ministry of Hydrology and Meteorology (Figure B.3). The data spanned from the 4th of February to the 5th of June. This encompasses a period extending more than a month before the water pressure device started measuring and a day after the last measurement of the pressure devices. To refine the dataset, unreliable data was filtered out (Appendix A.2) by examining the double mass curves of the hourly data (Appendix B.4 and B.5). Subsequently, to estimate the most representative combinations of precipitation data, the quadratic inverse distances between case studies and the most relevant stations were utilized (Appendix A.2). This method helped in estimating the most suitable precipitation data sets for each case study.

Evaporation data

Evapotranspiration data encompassing the relevant time frame between the 24th of March and 4th of June was obtained from the Ministry of Hydrology and Meteorology. We acquired minimum/maximum daily air temperature, minimum/maximum daily relative humidity, daily average wind speed at ten meters height, daily solar radiation and daily hours of sunshine from two measuring stations (Appendix B.6). Corrections were applied to rectify missing data, and adjustments were made to align data frequencies (Appendix A.2). Subsequently, the Daily Potential Evapotranspiration (ET₀) calculator developed by the Food and Agriculture Organization (FAO) [32] was used. The psychrometer coefficient was assumed to be 8E-4 which assumes a naturally ventilated area and was the default constant by the calculator. The daily potential evapotranspiration was subsequently converted to hourly data using the hourly solar radiation data. Finally, the data was spatially distributed using the quadratic inverse distance between stations and locations (Appendix A.2).

Chloride Mass Balance method

The chloride mass balance (CMB) method offers an alternative approach to estimate groundwater recharge [6, 9]. This method compares the fraction of infiltrated rainfall to the evaporated water [54]. The re-irrigation of water was assumed to not affect concentrations. Additionally, all chloride within the aquifers was assumed to be derived from atmospheric sources. Both are conditions to use the CMB-method [5, 12, 24]. Effectively, this means there should be negligible runoff and chloride concentration was not gained or lost within the subsurface [1]. The CMB-method estimates yearly recharge (Equation 3.5) [1, 6, 12, 24].

$$R_{Rch-An} = P_{An} * \frac{C_P}{C_{GW}} \quad (3.5)$$

The equation presented defines R as the mean annual recharge, where P_{An} represents the mean annual precipitation, C_P denotes the mean chloride concentration in precipitation, and C_{GW} signifies the mean concentration in the groundwater at a specific case study. Precipitation data utilized for the CMB method was sourced from CHIRPS [11]. The chloride concentrations in the groundwater were measured at least eight times in all case studies. The pore volume, which is the stagnant water in the tube wells, was removed twice, ensuring the accuracy of the samples. The concentration in precipitation was determined by sampling precipitation using rain gauges. The atmospheric sources for chloride were assumed to not vary over space. Therefore no difference between the samples was assumed for the chloride concentration in precipitation. All collected samples were processed at the Environment Research Laboratory in Kathmandu, where chloride concentration and electrical conductivity were measured (Appendix C).

The mean annual recharge was estimated through interpolation using precipitation data to approximate the recharge within the measured time frame (Formula 3.6). This estimation was based on the assumption that the time-proportional recharge equalled the time-proportional precipitation. This assumption is rough because, during the monsoon season, the run-off is not negligible even though this is a requirement for the method. The calculated recharge via the CMB method was then compared to the recharge calculated using effective precipitation. This comparison aimed to assess the consistency or disparity between the estimations derived from the two methodologies.

$$V_{Cl-Rch} = R_{Rch-An} * \frac{P_{Dry}}{P_{An}} * A_{Focus} \quad (3.6)$$

3.5. Extraction

Extractions exist of two main parts, namely domestic extractions and extractions for irrigation. Within the border of every case study, all actively used domestic groundwater taps were identified and mapped. Taps situated beyond these borders were excluded from the scope of the case study. Local field research was performed to quantify the average daily consumption by the owners of these domestic taps. The consumption for residents and cattle was assessed separately, enhancing the estimation accuracy by generating multiple results. The volume of buckets or pots was used if the residents were unable to estimate the volume units themselves. When applicable, irrigation estimates were obtained with input from respective farmers. Only irrigation activities within the border of the case study were in the scope. The total extracted volume was estimated by summing the extractions for consumption and irrigation within the case study areas (Formula 3.7). This method facilitated the comprehensive assessment of total extracted volumes for both domestic use and irrigation within the defined case studies.

$$\sum V_{Extr} = - \sum V_{Qi} - \sum V_{Q_{Extr-Irri}} \quad (3.7)$$

3.6. Irrigation return flow

Irrigation by farmers results in evaporated water and return flow to the subsurface. The amount of water returning to the groundwater table is the so-called field efficiency and replenishes the upper unconfined aquifer with water. Irrigation return flow is zero if all irrigated water evaporates. Otherwise, the return flow is the amount of irrigated water minus the evaporated water (Formula 3.8). The actual evaporation was considered equal to the potential evapotranspiration during the irrigation event for the irrigated area. Additionally, it was presumed that the irrigated water was uniformly distributed across the agricultural lands.

$$V_{Ret-Flw} = \max\left\{0, \frac{Q_{Ext-Irri}}{A_{Farm}} - ET_0\right\} * A_{Farm} * t \quad (3.8)$$

3.7. Transpiration

The flux of transpiration comprises direct evaporation from bare soil due to capillary rise and the process of plants drawing water from the groundwater table, subsequently transpiring it. The rate of this evaporation is contingent on the potential evapotranspiration and land cover characteristics influenced by various factors such as upper aquifer traits, temperature, precipitation and depth of the groundwater table depth. The flux was estimated by reversing the evaporation sum (Formula 3.9).

$$\sum V_{Trans} = -(\sum V_{ET_a} - \sum V_{ET_{Rch}} - \sum V_{ET_{Irri}}) \quad (3.9)$$

Actual evaporation ET_a was estimated utilizing the operational Simplified Surface Energy Balance (SSEBop) model, leveraging data from the Visible Infrared Imaging Radiometer Suite (VIIRS) provided by the U.S. Geological Survey. Furthermore, evaporation during precipitation events was calculated by reversing the volume balance of effective precipitation (Formula 3.10).

$$\sum V_{ET_{Rch}} = \sum V_{Prec} - \sum V_{Rch} \quad (3.10)$$

The evaporation during irrigation was calculated by reversing the volume balance of irrigation. Evaporation during irrigation only occurred at locations four and five and was non-existent in the other case studies within the time frame.

$$\sum V_{ET_{Irri}} = \sum V_{Ext-Irri} - \sum V_{Ret-Flw} \quad (3.11)$$

Crop factor

The crop factor describes the proportional effect of potential transpiration versus actual transpiration from the groundwater table [2]. The factor works well for areas with shallow groundwater and negligibly small runoff [8, 53]. The crop factor was assumed to stay constant over time and thus neglects the influence of land cover changes over time. The crop factor f was calculated by dividing the actual transpiration by the potential transpiration (Formula 3.12).

$$f = \frac{\sum V_{Trans}}{\sum V_{Trans-Pot}} \quad (3.12)$$

The potential transpiration is defined as the potential evapotranspiration outside precipitation and irrigation hours. Because actual precipitation and irrigation evaporation were assumed to be equal to the potential evapotranspiration during irrigation hours, the precipitation and irrigation fluxes can be subtracted without a compensating factor.

$$\sum V_{Trans-Pot} = -(\sum V_{ET_0} - \sum V_{Evap-Rch} - \sum V_{Evap-Irri}) \quad (3.13)$$

Validation using crop factor

The validation of the crop factor involved comparing obtained values against literature-based references. To achieve this, we estimated an anticipated range for the crop factor per case study following FAO guidelines (Table 3.2) [2]. The Terai region has a sub-humid climate and crops were assumed to be in the middle of the growing cycle. Moreover, we assumed all grass represented turf grass and

trees were akin to rubber trees. Areas covered by roofs and pavement were presumed to have a crop factor of zero. Deriving the estimated range of crop factors was based on a visual assessment of land usage per specific location (Appendix D).

Land use	Crop factor f
Roofs and roads	0
Bare soil	0.15 - 0.20
Grass	0.80
Rubber trees	0.90
Sweet corn	1.10

Table 3.2: Typical crop factors of different land use types [2]

3.8. Storage change

Specific yield is necessary to translate groundwater table decrease into a storage change. The water table fluctuation (WTF) method was employed to estimate the specific yield (Formula 3.14) [1, 24]. This method relates the effective precipitation to the actual groundwater table increase using the specific yield. This assumes the rise of the water table results solely from precipitation [26]. This condition was always met by using the derived recharge contribution to the groundwater table. The WTF-method prerequisites an unconfined and shallow aquifer, which were assumed in our study [1, 24].

$$S_y = \frac{P_{Eff}}{\Delta H_{Rch}} \quad (3.14)$$

The specific yield is represented by S_y . The ΔH_{Rch} symbolizes the difference between the lowest point of the extrapolated antecedent recession curve of the recharge contribution at the time of its peak and the recharge contribution at its peak [1, 24]. The contribution of recharge was fitted to the measured groundwater table time series using the Python package Pastas (Appendix A.3) [8]. This Python package fits hydrological data to a groundwater table time series. The required data was potential evapotranspiration, precipitation and a trend representing extractions, subsurface flow and percolation. Through this, we estimated the recharge contribution fitted to the measured groundwater table time series. The groundwater storage change $\Delta V_{Storage}$ was calculated over the time frame of interest using the measured groundwater table H in the time series and the specific yield (Formula 3.15) [24]. The specific yield was assumed to be equal to the effective porosity in the unconfined aquifers.

$$\Delta V_{Storage} = (H_{t=n} - H_{t=0}) * S_y * A_{Focus} \quad (3.15)$$

3.9. Sub-surface flow and Percolation

Subsurface flow

Lateral subsurface flow is caused by a difference in water pressure in the subsurface, where groundwater moves toward areas of lower pressure. This lateral flow is from a shallower groundwater table to a deeper groundwater table (Formula 3.16) [3]. The two-dimensional subsurface flow flux is calculated via the transmissivity denoted by the T and the slope of the groundwater table i . However, obtaining a consistent groundwater slope for the case studies was challenging due to local heterogeneities and limited available information. Therefore, an alternative approach was used to approximate this flux.

$$q_{SSF} = T * i_{GWT} \quad (3.16)$$

Percolation

Percolation represents the vertical subsurface flow, often directed towards a deeper aquifer. This flux occurs due to pressure discrepancies between two aquifers. In certain locations, farmers extracted groundwater from deeper aquifers, reducing the pressure within those deeper layers. Consequently, this increased the pressure contrast between the upper and lower aquifers, facilitating flow through

the leaky layer separating the two aquifers. However, due to limited subsurface information and its heterogeneity, it was cumbersome to specify where and if these aquifers and leaky layers exist, how thick or impermeable the layers in between the aquifers are and how these aquifers develop in space. As a result, estimating this flux required an alternative approach.

Net sub-surface flow and percolation flux

The two unknown fluxes in the groundwater balance were the subsurface flow and percolation. Combined, these two unknown fluxes close the groundwater balance. The fluxes were combined because the fluxes could not be quantified individually and were thought to be of minor importance in answering the research questions. The net subsurface flow and percolation flux ($V_{SSF-Perc}$) combines similar fluxes because both fluxes represent flow due to the pressure differences in the subsurface. Effectively, the lateral and vertical groundwater flow were amalgamated. Note that this flux gives a total volume over the entire time frame. Consequently, temporal-specific information cannot be retrieved, unlike most other fluxes. Therefore, the flux is defined as the net sum of subsurface flow and percolation.

$$\sum V_{SSF-Perc} = \Delta V_{Storage} - \sum V_{Extr} - \sum V_{Rch} - \sum V_{Trans} - \sum V_{Ret-Flw} \quad (3.17)$$

3.10. Extrapolation of fluxes in space

Groundwater Response Units (GRU) were used to extrapolate the six locations to the entire study area. While Hydrologic Response Units have established methodologies for classification [13, 21, 30], GRUs lack a formal delineation framework [40]. Despite this, GRUs often consider key factors such as climate, recharge dynamics, and groundwater utilization in their delineation process [40]. In this study, delineation was based on three pivotal fluxes: evaporation, recharge, and extraction. These fluxes were used as defining parameters to categorize and extend findings across the study area.

3.10.1. Characterizing response units

Using the Polygon Divider (an extension tool within Qgis), the region of interest was divided into polygons, hereafter response units, with approximately the same area as A_{Focus} . This tool divided the area into 69383 response units with a mean area of 7854 m² and a standard deviation of 1.4%. These response units were then each allocated a normalized value ranging from zero to one for recharge, evaporation, and extraction.

Recharge

Initially, recharge was assigned to every response unit. Recharge depends on soil infiltration rate and precipitation [23]. The Normalized Vegetation Difference Index (NVDI) is positively correlated with soil infiltration rate [33]. Therefore characteristic recharge for all units during the relevant time frame was determined using NVDI and the sum of spatial precipitation. The Normalized Vegetation Difference Index quantifies vegetation by calculating the difference in reflection between near-infrared and red light [22]. We used spectral information from Landsat 5, 7, 8 and 9 provided by the U.S. Geological Survey to assess average vegetation cover during the study period (Appendix B.8). The precipitation distribution (Appendix B.7) was determined by the sum of CHIRPS rainfall estimates over the time frame of interest [11]. Eventually, the characteristic precipitation (Formula 3.18) and NVDI values per response unit (Formula 3.19) were normalized between zero and one at the 2.5% distribution tails. This particular normalization process was crucial to avoid skewed distributions (Appendix A.4). Values exceeding the thresholds of 0 and 1 were set to 0 and 1 on the lower and upper boundaries, respectively.

$$P_{Norm} = \frac{P_{GRU} - P_{2.5-percentile}}{P_{97.5-percentile} - P_{2.5-percentile}} \quad (3.18)$$

$$NVDI_{Norm} = \frac{NVDI_{GRU} - NVDI_{2.5-percentile}}{NVDI_{97.5-percentile} - NVDI_{2.5-percentile}} \quad (3.19)$$

Subsequently, the normalized NVDI and precipitation were summed (Formula 3.20) and normalized again (Formula 3.21). This ensured every response unit to be allocated a normalized recharge value between 0 and 1.

$$R_{Norm} = P_{Norm} + NVDI_{Norm} \quad (3.20)$$

$$R_{Norm} = \frac{R_{GRU} - R_{2.5\text{-percentile}}}{R_{97.5\text{-percentile}} - R_{2.5\text{-percentile}}} \quad (3.21)$$

Evaporation

Secondly, evaporation was assigned to every response unit. Spatial evaporation was estimated using the operational Simplified Surface Energy Balance (SSEBop) model (Figure B.9). This model utilized the Visible Infrared Imaging Radiometer Suite (VIIRS), courtesy of the U.S. Geological Survey, to estimate actual decadal evaporation data. No adjustments for land cover were necessary as this data provided an estimation of actual evaporation. All values across response units were normalized to acquire relative values between zero and one for each unit (Formula 3.22). The 2.5% distribution tails on both sides of the distribution were again replaced with zeros and ones (Appendix A.4).

$$Ev_{Norm} = \frac{Ev_{GRU} - Ev_{2.5\text{-percentile}}}{Ev_{97.5\text{-percentile}} - Ev_{2.5\text{-percentile}}} \quad (3.22)$$

Extraction

Thirdly, extractions were assigned to every response unit. The spatial distribution of extractions was approximated based on population densities, assuming a proportional relationship between consumption and the number of people residing in an area. The field locations were considered representative of scaling this assumption. By normalizing the population densities and removing the distribution tails (Appendix A.4) a representative normalization for extraction was found between zero and one (Formula 3.23). The population data was retrieved from 'Dataforgood' which is an initiative from Facebook [17].

$$Ex_{Norm} = \frac{Pop_{GRU} - Pop_{2.5\text{-percentile}}}{Pop_{97.5\text{-percentile}} - Pop_{2.5\text{-percentile}}} \quad (3.23)$$

Ultimately all response units contained normalized characteristic values between zero and one for recharge, evaporation and extraction.

3.10.2. Assigning response units

Normalized values for these fluxes were also calculated for the focus areas of the case studies A_{Focus} . This again required NVDI, precipitation, evaporation and population data. The six locations were normalized using the tails of the distribution of the response units as well. Subsequently, a similarity score was calculated between the response units and every field location (Formula 3.24). Every response unit thus got a similarity score for each case study. Subsequently, every response unit was assigned the case study with its highest resemblance score. Eventually, every unit was treated identically to their assigned field location.

$$S_{Loc-i} = 1 - \sqrt{(R_{Loc-i} - R_{Res-Unit})^2 + (Ev_{Loc,i} - Ev_{Res-Unit})^2 + (Ex_{Loc-i} - Ex_{Res-Unit})^2} \quad (3.24)$$

3.10.3. Scaling using response units

Each response unit was treated identically to its assigned case study, inheriting the characteristic contribution of fluxes from the corresponding case study. This was achieved by aggregating the areas of all response units assigned to each unique case study. Consequently, the aggregated areas each corresponded to one of the case studies. These aggregated areas were then multiplied by the contributions per square meter specific to the corresponding case study. The total extraction volume of all locations

similar to location i was calculated according to Formula 3.25. The summed areas of response units treated the same as location i were denoted with A_{Loc-i} .

$$V_{Extr-Loc-i-Sum} = V_{Extr-Loc-i} * \frac{\sum(A_{Loc-i})}{A_{Focus}} \quad (3.25)$$

The total extraction flux (Formula 3.26) of the whole study area was subsequently calculated by summing the extractions of all six field locations. The other fluxes and volume storage change were calculated using the same described method.

$$V_{Extr-Total} = \sum_{i=1}^{n=6} (V_{Extr-Loc-i-Sum}) \quad (3.26)$$

The extraction contribution percentage was determined by dividing the flux by the total storage volume change in the entire area (Formula 3.27). This calculation method was applied to the other fluxes as well.

$$p_{Extr} = \frac{V_{Extr-Total}}{\Delta V_{Storage}} * 100\% \quad (3.27)$$

3.11. Groundwater trend

Annually, precipitation intensity is more significant in the monsoon season than in the dry season. During the monsoon, the groundwater table tends to recover, while in the dry season, it experiences a decline. For the last two years, CIMMYT has been monitoring groundwater tables at 22 shallow locations with a monthly interval (Appendix B.9). These observations spanned both dry and monsoon seasons twice. The hydrological start and end of the season were determined using precipitation intensity. The start of the monsoon season was defined as the middle day in the first seven consecutive days of the year where it precipitated a minimum of 40 millimetres. The end of the monsoon was defined as the first day of 21 consecutive days without more than 20 millimetres of precipitation. The start and end of the dry season were determined in an identically but reversed manner to the monsoon season. The relation between the seasonal effective precipitation and groundwater level decrease was analyzed for the 22 shallow wells. Additionally, the relation between effective precipitation and groundwater level at the end and start of the seasons was examined. Effective precipitation was defined as CHRIPS precipitation minus remote sensing actual evaporation.

3.11.1. Dry season

Relative between two dry seasons, more effective precipitation should lead to a decreased loss of groundwater resources during the dry season. If this relation was distinguishable the groundwater table decrease in the dry season is dominantly dependent on precipitation and evaporation. If there is no correlation, the groundwater table decrease was significantly caused by other fluxes as well, for instance, annual variable extraction or subsurface flow. The second examination focused on observing potential annual trends in groundwater table levels at the end of each season. This approach aimed to discern patterns or variations in the groundwater table over successive years.

3.11.2. Monsoon season

Analyzing the relationship between effective precipitation and groundwater recovery post-monsoon was aimed at understanding the impact of increased effective precipitation on the strength of groundwater replenishment. Increased effective precipitation was expected to lead to a strengthened groundwater recovery. The recovery occurs until a certain threshold is reached. The excess effective precipitation then runs off to rivers and does not replenish the groundwater resources anymore. When this occurs, groundwater resources are fully replenished. Ultimately, if more effective precipitation does not lead to an increased groundwater recovery between the monsoon seasons, nothing would suggest groundwater resources were depleting. The relation between effective precipitation and groundwater levels

at the end of the monsoon season was analyzed to compare the groundwater levels between the seasons. Whether groundwater tables stay constant through the years or whether groundwater resources are replenished at a lower depth can be distinguished. The latter would effectively still deplete the groundwater resources. If both levels are approximately the same at the end of the seasons, nothing suggests that the saturated groundwater level yearly decreases. Additionally, the precipitation in the last two years was compared to the last 10 years. Groundwater resources did not deplete in the past if the seasonal average effective precipitation remained approximately the same. This analysis was performed to make sure that the last two years were not outliers regarding precipitation.

4

Case studies

4.1. Field locations

The six case studies were numbered one through six and the barometer was numbered seven (Figure 4.1). The coordinates can be found in Appendix A.5. The barometer was strategically positioned in the middle of the other pressure devices to minimize the spatial atmospheric pressure error. The case studies were selected in such a way that the most different types of terrain were included. Three locations in Northern parts close to the Bhabar zone and three more Southern locations were selected.

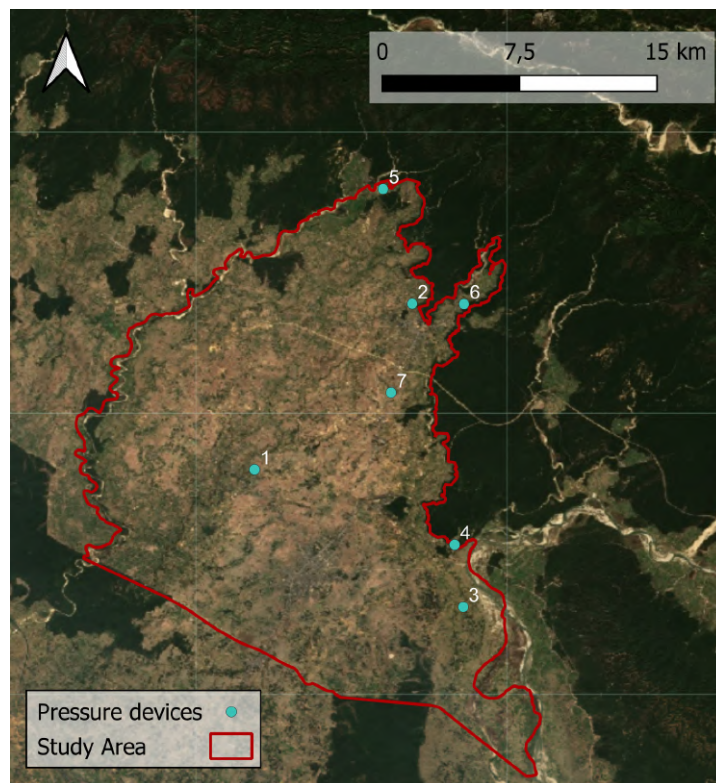


Figure 4.1: Study area with the locations of the pressure devices numbered one through six and the barometer numbered seven. Exact coordinates in Appendix A.5

Location one was selected in a flat region with relatively low vegetation and sparse population. Location three was also opted to be in a flat and urbanized area with low vegetation. Location four was selected to be in a flat, sparsely populated and heavily vegetated area. Locations two, five and six were opted to be close to the Bhabar zone with respectively considerable urbanization, negligible urbanization and moderate urbanisation. The locations were not spatially distributed evenly over the area because of limited resources and accessibility of the Western parts of the Banke District. Ultimately, the case studies represent the present specific land cover types in the study area as best as possible and were therefore assumed representative.

Assumptions

The groundwater table in the observation wells ranged from 3 to 8 meters below the surface. In literature, groundwater depths between zero and nine meters were defined as groundwater in shallow aquifers [24, 35, 36, 47]. Therefore, it is fair to treat the aquifers in the case studies as shallow as well. Ground surface slopes appeared to be negligible and no signs of surface runoff were found in the study area. Furthermore, precipitation events were infrequent during the measurement time. This results in empty pore spaces during the dry season. Empty pore spaces result in more infiltration and thus less run-off [47]. Given these circumstances, runoff was deemed negligible during the time frame from March 24th to June 5th. This conclusion was supported by the absence of noticeable river supply, confirmed through both visual inspection and field expeditions, where river discharge was consistently observed to be minimal.

4.2. Borders case studies

Two pumping tests were performed at locations three and four because these locations were judged to be the most suitable for pumping tests (Figure 4.2). The case studies were most suitable because an adjacent pumping well was present close to the observation wells and the subsurface appeared to have a relatively homogeneous subsurface at these locations. Further details regarding their selection and assessment will be provided in this chapter.

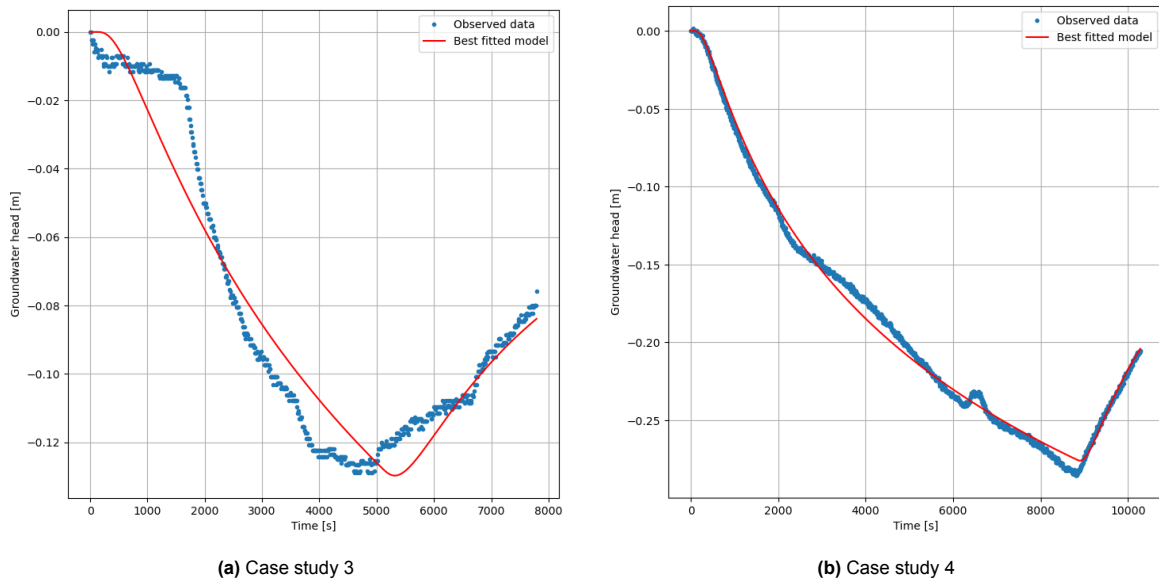


Figure 4.2: Two pumping tests performed using the observation well and the pumping domestic well Q_1

The pump at location three pumped for 83 minutes and the pump at location four for 146 minutes with discharge Q . The drawdown and recovery in the observation well were recorded and the saturated hydraulic conductivity and specific storage were determined using an analytic elements method (Ta-

ble 4.1) [29]. Although there were potential background extractions during the test at location three, their impact on determining hydraulic conductivity and transmissivity seemed minimal, leading to their neglect for simplicity without compromising representativeness. The radius of both observation wells was 0.02 meters. A maximum of 13 consecutive hours per day were used for pumping which is an estimate based on the irrigation patterns. The cone of depression, calculated using the Theis solution, gave a function for the drawdown of the groundwater table as a function of the radius from the well. A comparison between the drawdown at a radius of 50 meters and at 0.05 meters from the well indicated a tenfold difference at location three and an 8.5-fold difference at location four. Considering these differences under the most critical extraction conditions, the 50-meter range was deemed appropriate for analysis across all locations, defined as A_{Focus} , with an area equivalent to 7854 m² due to the circular shape of the area.

Location	Hydraulic conductivity [m/s]	Transmissivity [m ² /s]	Storage coefficient [-]
3	$3.8 * 10^{-5}$	$2.9 * 10^{-4}$	$3.3 * 10^{-3}$
4	$1.3 * 10^{-5}$	$1.5 * 10^{-4}$	$1.2 * 10^{-3}$

Table 4.1: The hydraulic conductivity, transmissivity and storage coefficient from the pumping tests performed in the observation wells at case studies three and four

4.3. Case study one

Area description

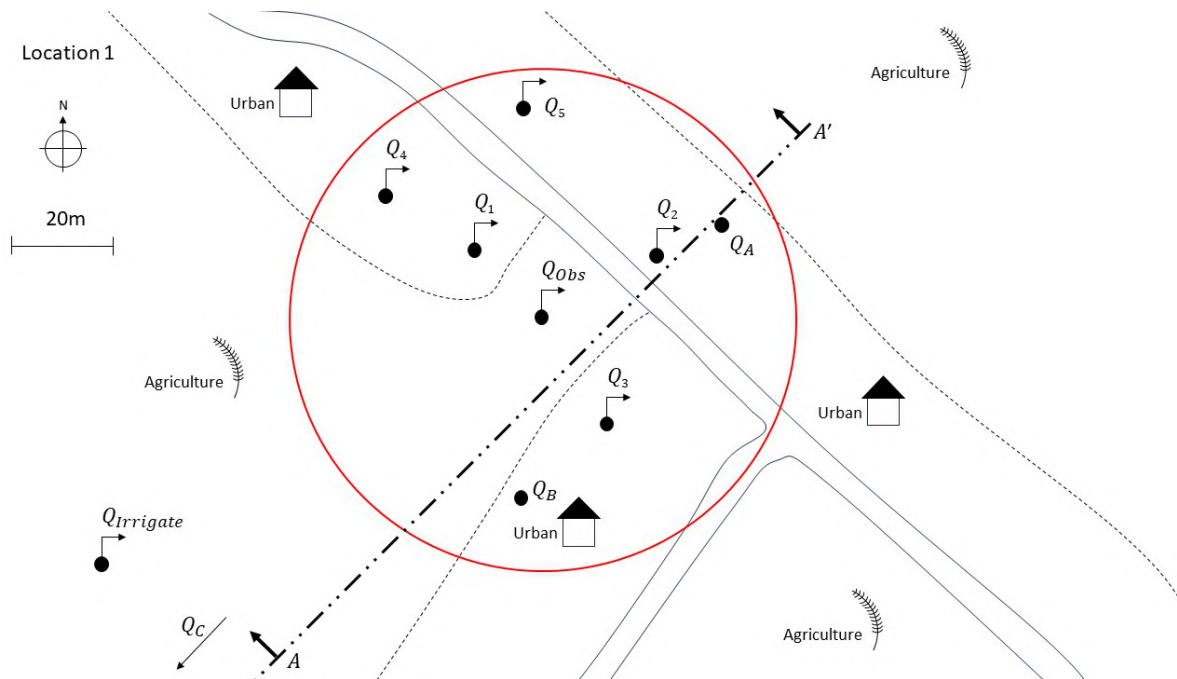


Figure 4.3: The schematic drawing of case study one. The red circle depicts the 50-meter border of the area. The numbered subscripts of Q denote domestic extraction wells and the irrigation well is the regional well used by farmers. The texts agriculture and urban describe land use. Finally, cross-section A-A' captures three additional wells with lettered subscripts of Q to visualize the subsurface.

Location one was selected in the middle of the study area in the agglomeration Khajura Khurda (Figure

4.3). No major year-round rivers flow near this area. The terrain consists of bare agricultural lands with small houses, a road through the town, some grass and thinly scattered trees (Appendix D.1). Considering the land cover, the estimated crop factor fell within the range of 0.25 to 0.50. The roads were depicted in the sketch and the symbols of urban and agriculture refer to the land cover. The label 'Urban' was given if areas of land were paved or urbanized. Bare lands that were normally dedicated to agriculture were labelled 'Agriculture'. The symbols for Q_1 , Q_2 , and so on denote domestic extractions and Q_A , Q_B , and similar labels pertain to abandoned wells, details of which will be discussed later. The cross-section A-A' was used to sketch the subsurface.

Domestic extractions

The observation well Q_{Obs} of 18.72 meters deep belongs to a family that occasionally uses the well to irrigate. However, during the measurement time frame, no crops were farmed and the well was thus out of use. All in-use groundwater taps within a range of 50 meters were mapped in the sketches with the symbol Q . Wells Q_2 and Q_4 belong to the same household. The extractions were evenly distributed over these two wells because the household estimated that both wells were utilized equally frequently (Table 4.2).

Well	Distance Q_{Obs} [m]	People	Consumption [L/d]	Cattle	Consumption [L/d]	Consumption total [L/d]
Q_1	19	6	320	2 buffaloes	180	500
Q_2	25	5	300	6 goats	120	420
Q_3	25	4	400	-	-	400
Q_4	39	-	300	-	-	300
Q_5	42	6	400	3 goats	75	475
<i>Total</i>	-	21	1720	-	375	2095

Table 4.2: Domestic extractions within the borders of case study one

Irrigation

Farmers within the border regularly irrigate their fields with groundwater. However, during the measured time frame, no crops were farmed. The fields of farmers that farmed crops in the time frame were outside the borders of the case study. $Q_{Irrigate}$ denotes the local well that is used for irrigation. The well is approximately 50 meters deep and at a distance of 100 meters from the observation well. The well was therefore outside the scope of this project because it is not in the upper aquifer and outside the border.

Groundwater table time series

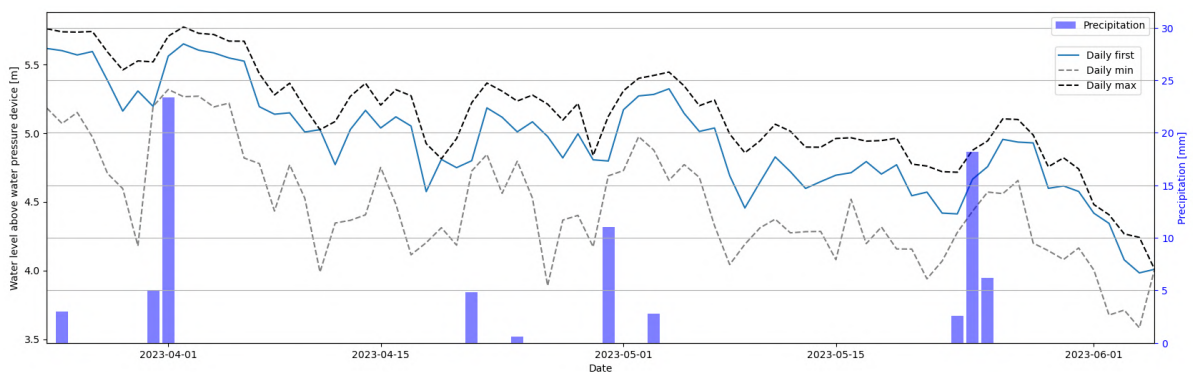


Figure 4.4: Recorded time series in Q_1 of the groundwater table at case study one where significant daily fluctuations can be distinguished

The pressure device at location one measured significant fluctuations during a median day (Figure 4.4). The daily measurements at midnight (daily firsts) were mostly between the daily minimum and maximum. Median daily differences were significant with more than half a meter. Therefore, a low local specific yield was expected around the observation well in this case study. Following precipitation events, the groundwater consistently increased as expected. The groundwater table also occasionally increased when no precipitation events were present. This was most likely subsurface flow from outside the case study border caused by irrigation events. Possibly a deep irrigation well like $Q_{Irrigate}$ was used because no extraction drops in the time series can be distinguished.

Local subsurface

The Groundwater Resources Development Board (GWRDB) shed light on the process of digging domestic wells, explaining that they are typically dug until an impermeable texture class is reached and enough permeable material surrounds the well. Consequently, permeability alters in space when shallow wells with different depths are found near the observation well. This spatial diversity in well depth, combined with the distribution of groundwater tables across the area, strongly suggests soil heterogeneity. Besides the observation well, three additional abandoned wells were observed along the cross-section A-A' in the case study denoted as Q_A , Q_B and Q_C . The groundwater tables of the wells were measured twice and the average groundwater depth was assumed to be representative of the subsurface (Figure 4.5).

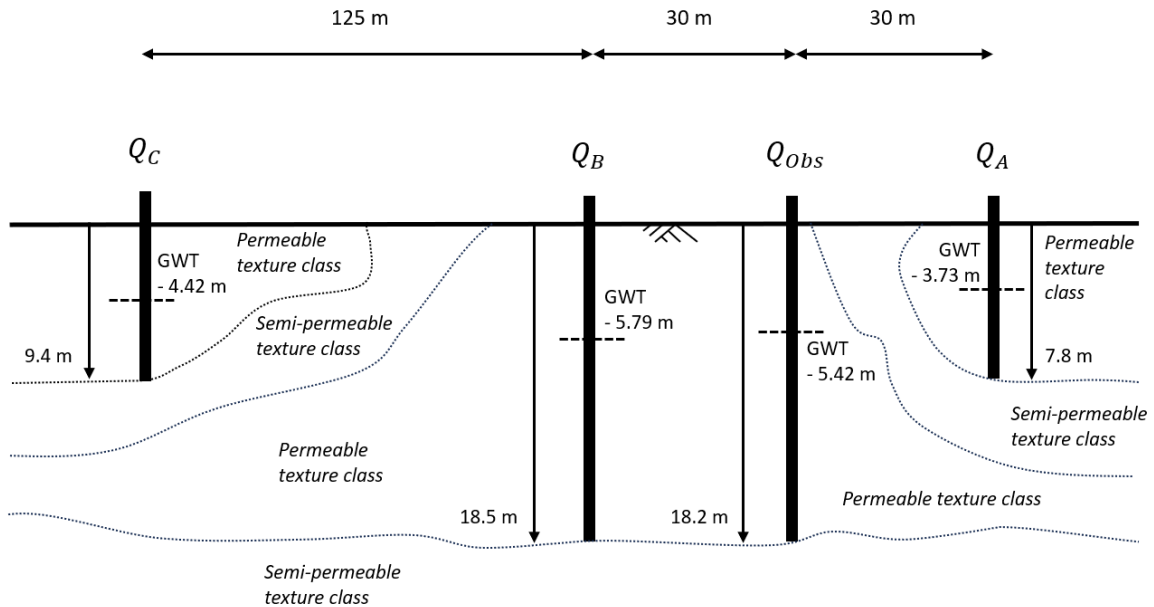


Figure 4.5: Schematic cross-section A-A' of the local subsurface of case study one

The groundwater table and well depth difference between well Q_A and Q_C and the observation well suggest the wells are likely separated by a layer of a semi-permeable texture class. This was verified for well Q_A with an extra time series (Figure 4.6). In this time series, hourly fluctuations were maximally 0.1 meters unlike in the time series of Q_{Obs} where fluctuations were daily around 0.5 meters. This means that the groundwater table in Q_A was always more than a meter higher than in Q_{Obs} which suggests that the wells are separated by a semi-permeable layer. The specific yield in the soil surrounding Q_A is likely significantly higher due to the lower amplitude of the fluctuations. This justifies the lower well depth because enough permeable material surrounds the well Q_A at a shallower depth. The well Q_B is likely directly connected to the observation well because the well is nearby and the groundwater table and well depth were similar. Well Q_C was shallower, at a further distance and the groundwater table was significantly higher than well Q_B . The well was therefore assumed to be in another aquifer.

Ultimately, the additionally observed wells suggested some sort of spatial heterogeneity. Location one was therefore not selected to perform the pumping test (Section 4.2).

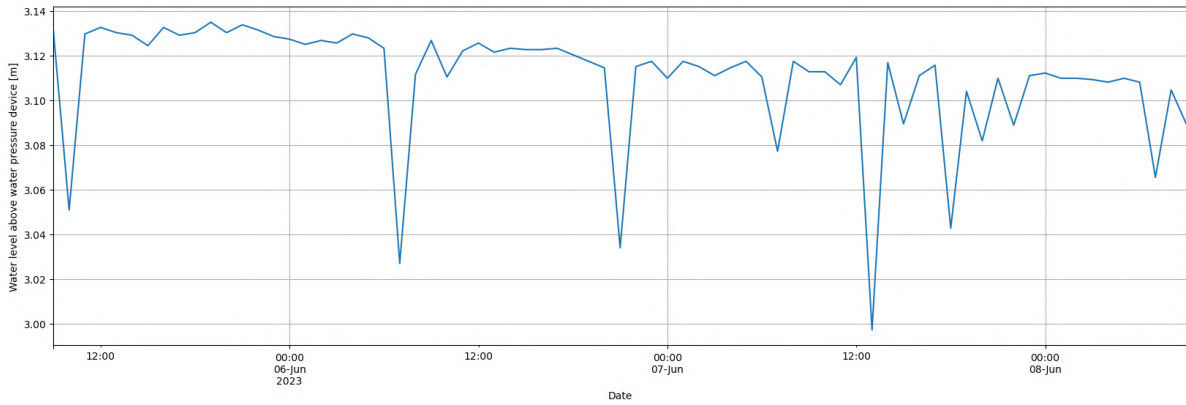


Figure 4.6: Extra hourly time series of the groundwater table above the pressure device in well Q_A of case study one with significantly smaller daily fluctuations

Chloride measurements

The precipitation needed for the chloride measurements was captured by a rain gauge on the roof of the owner of Q_1 . The well was used to sample the groundwater with a chloride concentration of 7 mg/L.

4.4. Case study two

Area description

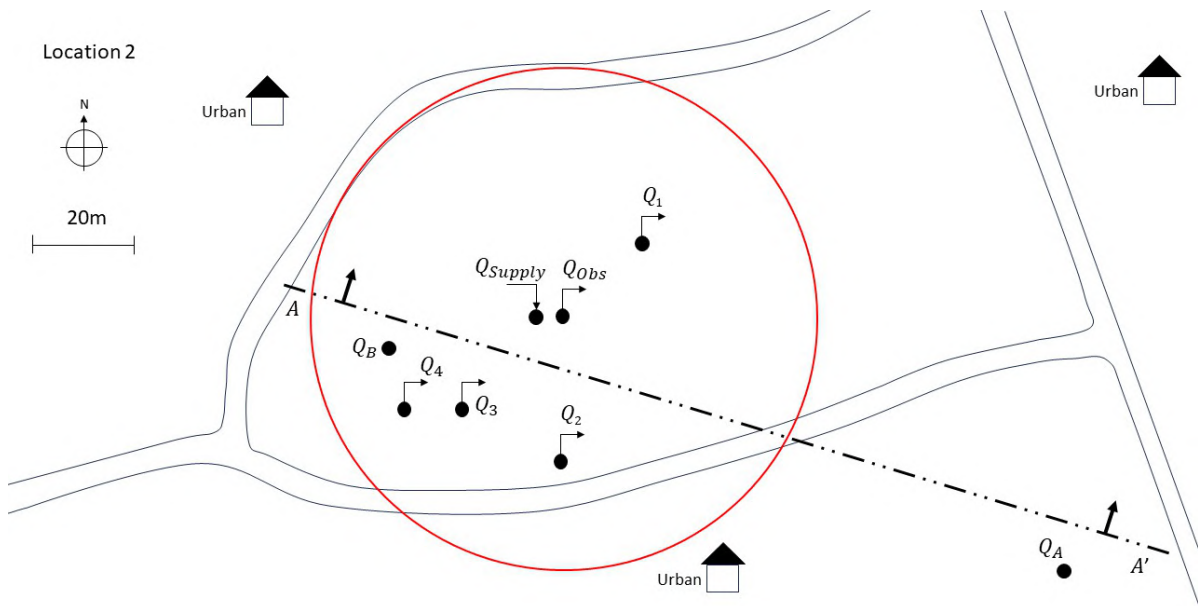


Figure 4.7: Schematic drawing of case study two where Q_{Supply} denotes a water supplying tap installed by the local drinking water office

Field location two was located in the middle of Rajhena (Figure 4.7). An urbanized area located in the North, next to the border of the study area. The Duduwa River flows at around a one-kilometre distance from the east side of Rajhena. The area surrounding the location is mostly made up of urbanization with patches of vegetation (Appendix D.2). Small farmlands are present a little outside Rajhena.

Domestic extractions

The observation well belongs to the water research office of the local government. The well with a depth of 21.74 meters is out of use because a heavy object got stuck in the well. There are not many households in direct proximity of 50 meters. This is because of the space-occupying water research office which was visualized as Q_1 . A tap was installed by the drinking water office of Rajhena five meters from the observation well (Appendix D.2). This tap was indicated as Q_{Supply} and constantly provides water at a rate of 0.59 litres per second in the dry season. All nearby residencies use that tap for domestic purposes. The inhabitants still have domestic pumps as well. However, these are almost exclusively used during the monsoon season. Extractions from the groundwater table during the dry season are therefore minimal (Table 4.3). The supplying tap even makes the total extractions supplying instead of extracting.

Well	Distance Q_{Obs} [m]	People	Consumption [L/d]	Cattle	Consumption [L/d]	Consumption total [L/d]
Q_1	21	-	15	-	-	15
Q_2	26	4	200	-	-	200
Q_3	27	2	-	-	-	-
Q_4	35	3	-	-	-	-
Q_{Supply}	-	-	-50,980	-	-	-50,980
<i>Total</i>	-	11	-50,765	-	-	-50,765

Table 4.3: Domestic extractions within the borders of case study two

Groundwater table time series

The groundwater time series at location two displayed average daily fluctuations of around 0.2 meters (Figure 4.8). The specific yield of the subsurface is therefore expected to be moderate at this location. The groundwater table increased only significantly after precipitation events. Therefore, likely no irrigation activities were within the borders of the case study. A significant drop in the groundwater table is visible at the end of the time series. This was probably caused by big extractions for irrigation outside the border of the case study. Despite this observation, the drinking water office of Rajhena was not aware of any major extractions in the region at that time.

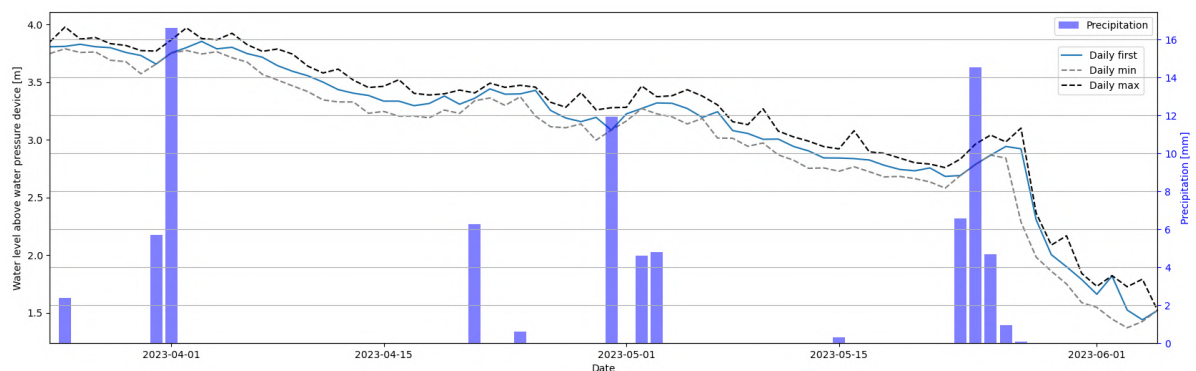


Figure 4.8: Time series of the groundwater table at case study two with small daily fluctuations

Local subsurface

Two additional wells, Q_A and Q_B , were measured around the cross section A-A'. A pressure device recorded a time series for 3 days in well Q_A (Figure 4.9). Daily fluctuations between the time series in Q_A and Q_{Obs} were substantially different. The time series in the observation well fluctuated daily minimally by around 0.1 meters (Figure 4.8) while the additional time series maximally fluctuated by 0.02 meters (Figure 4.9). This indicates the subsurface at well Q_A is likely characterized by a bigger specific yield number. The well was presumably dug shallower because enough impermeable material surrounds the well at a shallower depth. The observation well was dug deeper because the material is less permeable.

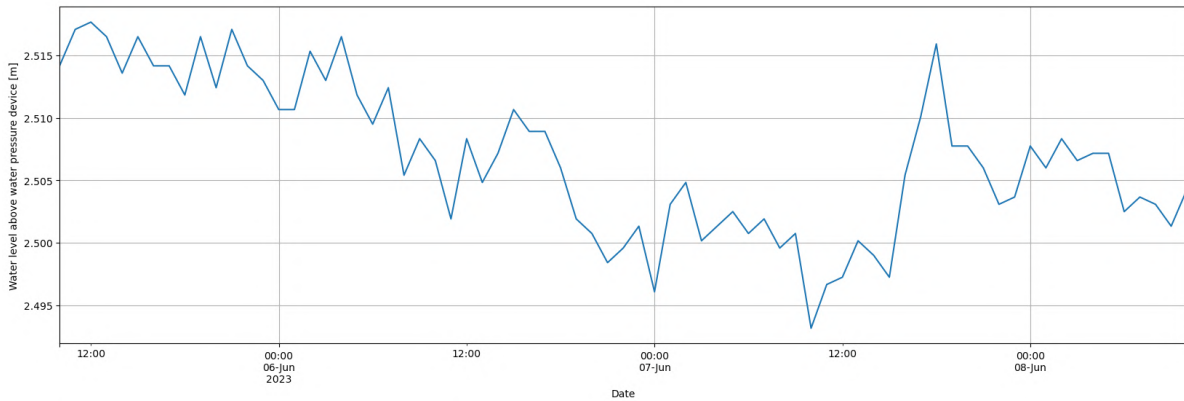


Figure 4.9: Extra time series in Q_A of case study two

The groundwater tables were measured twice and the average was assumed representative. The groundwater tables and well depths significantly varied over space. Therefore it was assumed that the wells are separated by a semi-permeable layer (Figure 4.10). Conclusively, the subsurface at location two is heterogeneous.

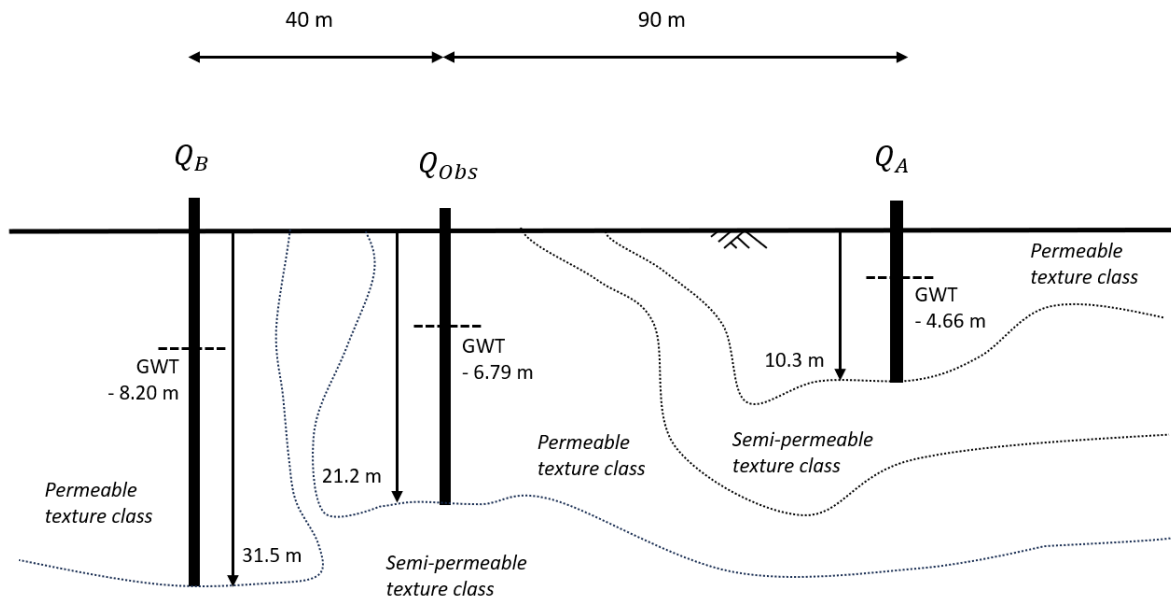


Figure 4.10: Schematic cross-section A-A' of the local subsurface of location two

Chloride measurements

The rain gauge captured precipitation from the roof of the water research office. The groundwater was sampled using the domestic well Q_2 . The median chloride concentration in the groundwater was 45 mg/L. This is a too high number and probably contaminated by wastewater discharge.

Case study conclusion

Location two has a substantial drinking water supply by the drinking water company. This supply is significantly larger than extraction in other case studies. Furthermore, the chloride concentration in the groundwater is disproportionate. Ultimately, the tap compromises the representativeness of the second case study and the case study was therefore neglected.

4.5. Case study three

Area description

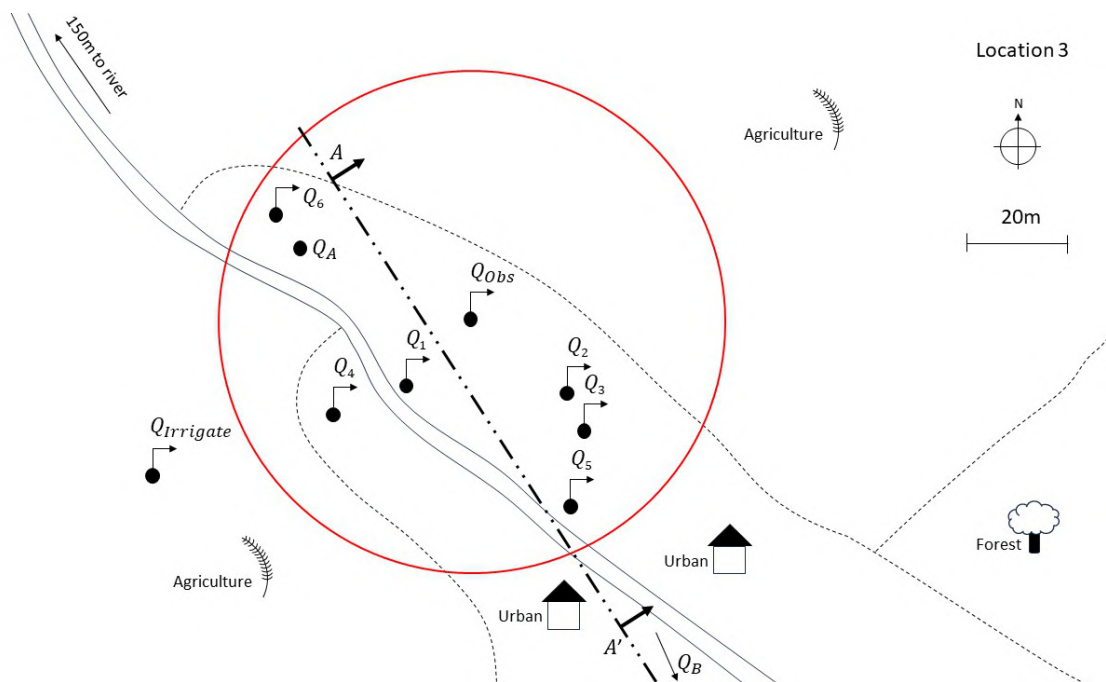


Figure 4.11: Schematic drawing of case study three where 'Forest' denotes vegetated land cover

The third field location (Figure 4.11) was located at the edge of Banakatti, a town located in the south-east corner of the study area. The little patch of forested area around the case study was given the label 'Forest'. The observation well is on the edge between bare agricultural fields and urban areas (Appendix D.3). The case study dominantly contains bare lands, much urbanization and little vegetation. The crop factor was therefore estimated between 0.15 and 0.35. Banakatti is in between two rivers. The Rapti River flows one kilometre to the East and the Duduwa River passes location three 250 metres to the West.

Rivers

The Duduwa River was levelled to the observation well using a levelling device (Figure 4.12). The water table of the Duduwa River was measured on the 29th of May and 2nd of June. Both times the water table in the river was the same and only 0.24 meters above the bottom of the deepest part of the river. The river level was therefore assumed as constant during the end of the measurement period. The groundwater table in the well was measured on the 29th of May at 4 PM and 0.28 meters below

the river level. The maximum groundwater table that day was 0.08 meters higher and thus 0.20 meters below the river level. This was used to calculate the minimum groundwater slope between the river and the observation well. The minimum groundwater table that day was 0.07 lower which was used to calculate the steepest groundwater slope. In the last two weeks of the measurements, the groundwater level was at its high point 0.08 meters higher than the earlier measured maximum. This was still significantly lower than the river. This means that the river was constantly draining at the end of the dry season. This decreases the discharge in the river and ultimately increases the risk of water scarcity [37]. The river banks were 4.38 meters higher than the groundwater table. This suggests the river might also be draining during the monsoon season when discharge is maximum. However, a draining river does not increase the risk of water scarcity during the monsoon season.

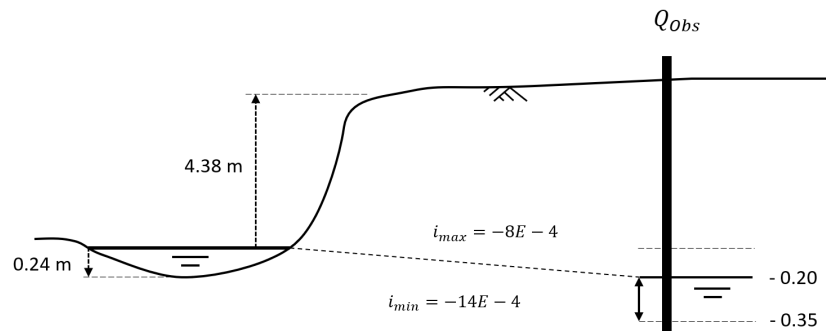


Figure 4.12: Schematic drawing of the river and fluctuating groundwater level in the observation well of case study three indicating that the Duduwa River is a losing river around case study three at the end of the dry season

Domestic extractions

The observation well of 12.26 metres deep belongs to a family with recently a new well installed. The observation well is out of use because the pump is broken and a new well with pump was subsidised by the local authorities. A significant number of domestic wells were found within the border of the case study (Table 4.4).

Well	Distance Q_{Obs} [m]	People	Consumption [L/d]	Cattle	Consumption [L/d]	Consumption total [L/d]
Q_1	19	9	700	9 goats	180	880
Q_2	24	11	460	2 goats	40	500
Q_3	32	10	500	2 buffaloes 3 goats	125	625
Q_4	34	6	400	9 goats	180	580
Q_5	42	4	250	-	-	250
Q_6	47	9	400	10 goats	200	600
<i>Total</i>	-	49	2710	-	725	3435

Table 4.4: Domestic extractions within the borders of case study three

Irrigation

An irrigation bore is present in the agricultural fields. This bore is used by people who own a farm but need a bigger pump than their domestic one to extract groundwater. The irrigation bore is outside the border of the case study and therefore outside the scope.

Groundwater table time series

The daily fluctuations recorded in the observation well at location three were less than 0.1 meters on a

median day (Figure 4.13). This suggests a high specific yield number. Starting in April, the daily minimum got significantly lower than the daily first while the daily maximum remained relatively the same in contrast to the daily first. Only around precipitation events, the daily minimum was approximately equal to the daily first. The groundwater reached lower levels but replenished quickly again. This suggests farmers extract water from the subsurface in a connected aquifer which they subsequently irrigate, quickly replenishing the groundwater again. One well that could have been used for this was the irrigation well $Q_{Irrigate}$ which is 12.9 meters deep and thus approximately as deep as the observation well. The subsurface at location three thus appears to be relatively homogeneous because all extractions were distinguishable in the time series but subsequently immediately replenished by irrigation return flow.

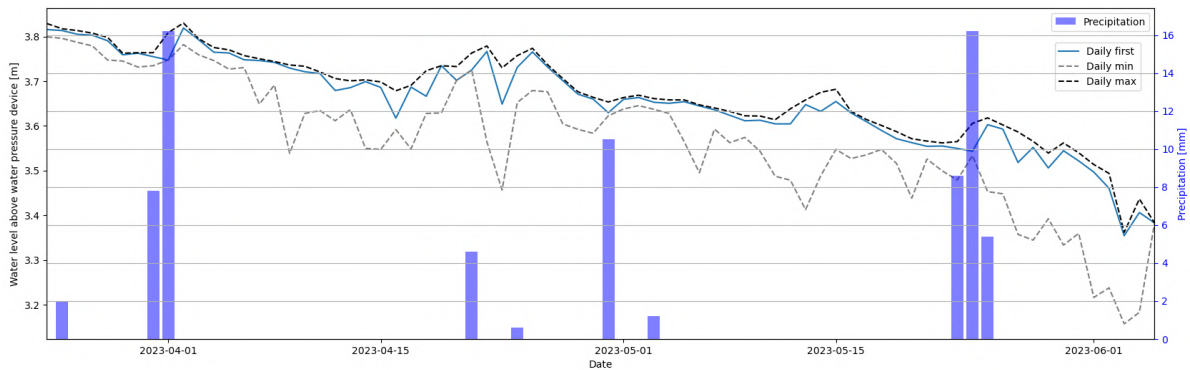


Figure 4.13: Time series of the groundwater table at case study three with large daily fluctuations during nearby irrigation extractions and small fluctuations without irrigation extractions

Local subsurface

Two additional wells were measured in the area along the cross-section A-A'. The wells were all approximately the same depth and the groundwater tables were similar as well (Figure 4.14). Both suggest a relatively homogeneous local subsurface.

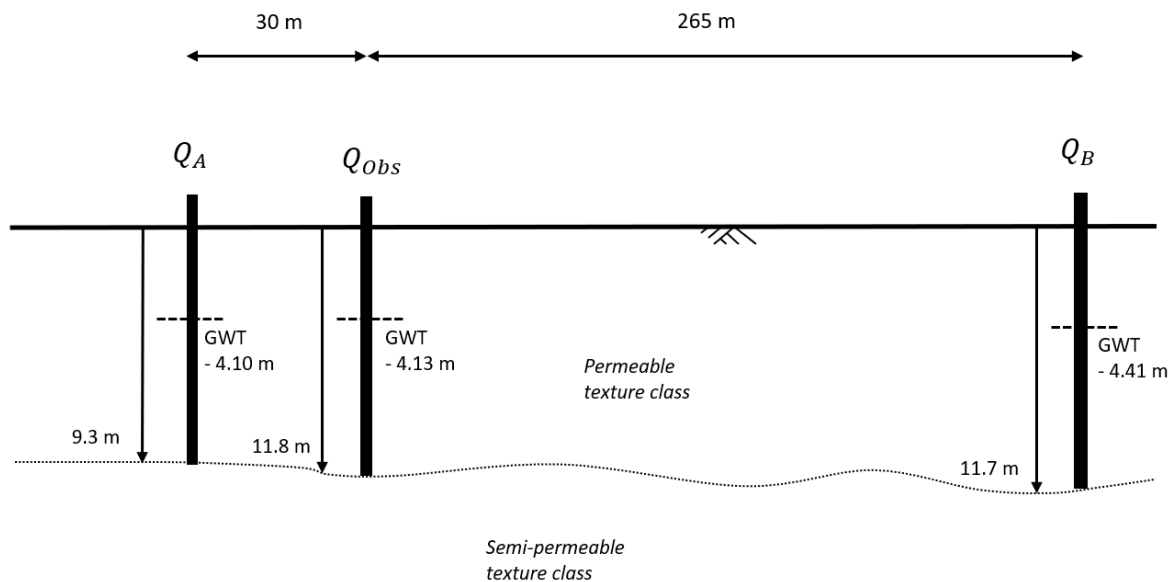


Figure 4.14: Schematic cross-section A-A' of the local subsurface of case study three

A water pressure device recorded hourly fluctuations in well Q_A (Figure 4.15). Fluctuations in the well were similar to the measured fluctuations in the observation well. This suggests that the texture class in the shallow subsurface is locally relatively homogeneous over space. Ultimately, location three was used for the pumping test because the local subsurface at location three appeared to be homogeneous (Section 4.2).

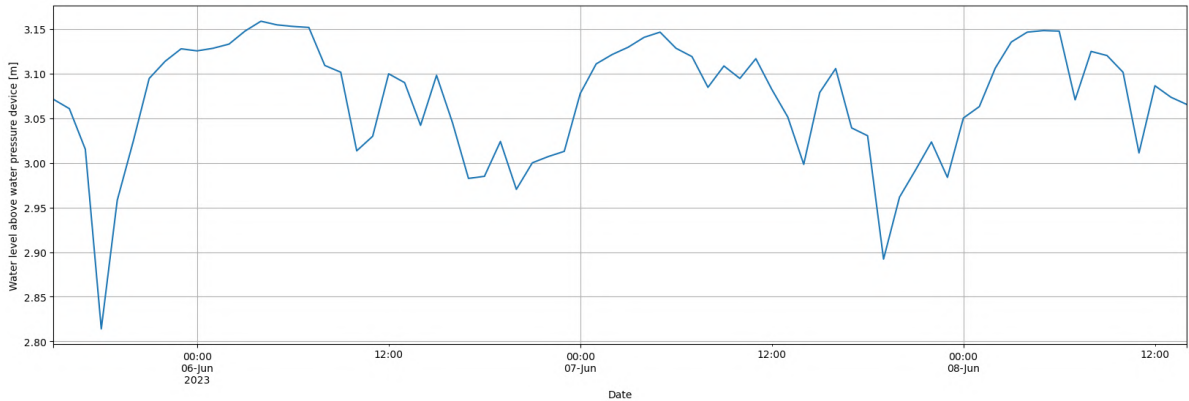


Figure 4.15: Extra time series in Q_A of case study three with similar daily fluctuations as the other time series

Chloride measurements

The rain gauge was located on the roof of the owner of the observation well. The groundwater was sampled using their extraction well Q_1 . The concentration of the groundwater was 14 mg/L.

4.6. Case study four

Area description

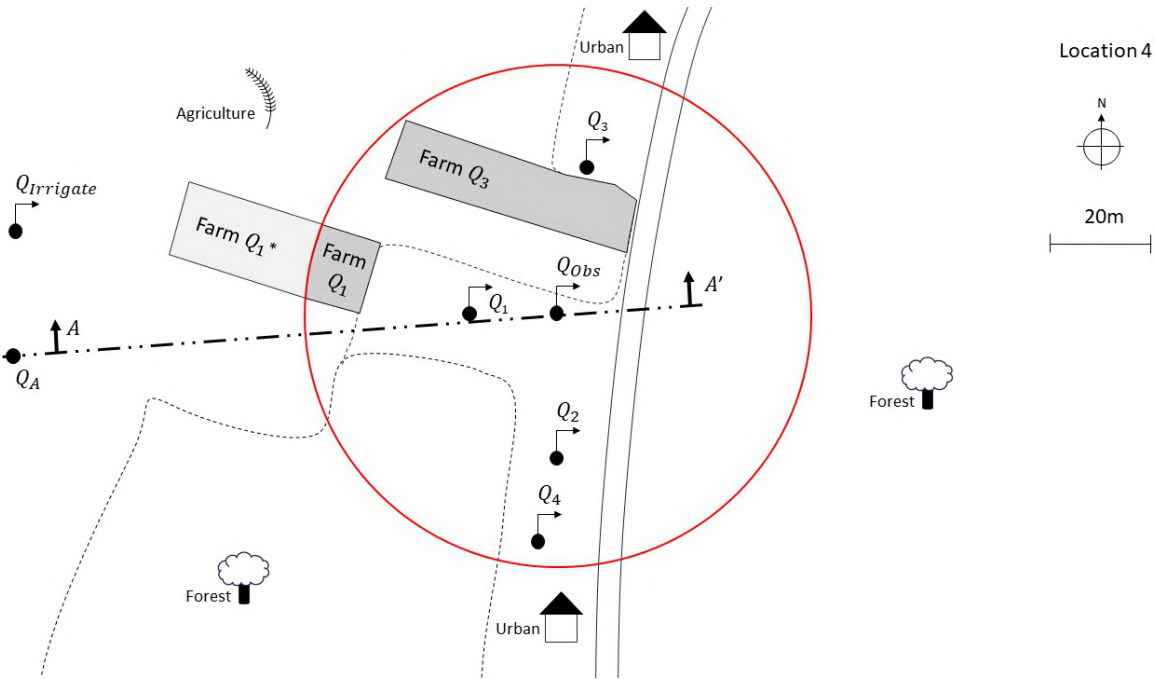


Figure 4.16: Schematic drawing of case study four

The fourth case study (Figure 4.16) was done in Kamdi, a town on the edge of the study area. The Rapti River is located around one kilometre to the East. The area of the case study is vegetated and a big forest is located to the east (Appendix D.4). Relevant farms within the 50-meter border were marked grey and maize was farmed there. Dark grey for areas within the borders and lighter grey outside the case study's border. The crop factor was estimated between 0.45 and 0.75 because of the heavy vegetation in the area.

Domestic extractions

The observation well is 17.74 meters deep and abandoned because of the dusty road passing the well at a short distance. Inhabitants around the observation well own many cattle which greatly influence total consumption (Table 4.5).

Well	Distance Q_{Obs} [m]	People	Consumption [L/d]	Cattle	Consumption [L/d]	Consumption total [L/d]
Q_1	18	6	320	58 goats	1200	1520
Q_2	28	4	250	3 buffaloes 35 goats	450	700
Q_3	30	4	240	6 chickens	10	250
Q_4	45	5	300	7 goats	150	450
<i>Total</i>	-	19	1110	-	1810	2920

Table 4.5: Domestic extractions within the borders of case study four

Irrigation

Two fields within 50 meters were being farmed with maize during the measurement time. The farm fields belong to the house owning the observation well, Q_1 , and the neighbouring house to the north, Q_3 . $Q_{Irrigate}$ is used by the farmers to irrigate the fields. The irrigation well is located at a distance of 115 meters from the observation well. The owner of Q_1 uses the pump once every necessary dry week for 2 hours. Q_3 uses the bore each month for 2 hours if required. The actual timing of the irrigation activities was unknown. Therefore using the time series and mentioned approximate frequencies by the farmers the irrigation patterns were estimated.

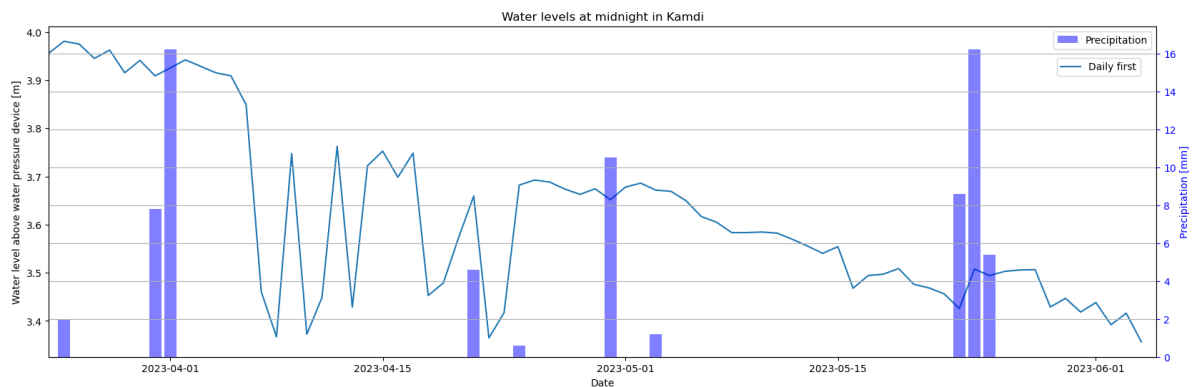


Figure 4.17: Water levels at midnight at Kamdi where significant extractions took place in the middle of April

There were extractions from the bore in April which are visible in the groundwater table time series in the observation well (Figure 4.17). In the week between the 5th of April and the 13th of April there were many extractions and it was therefore assumed that both farmers Q_1 and Q_3 extracted for irrigation. Between the 17th of March and the 23rd of April only farmer Q_1 was assumed to have extracted. There

were multiple extractions in that time frame but only 10 days passed since the last extraction and because farmer Q_3 only extracts once per month it was assumed Q_3 did not irrigate. The rest of the time series did not seem to contain significant drops, it was therefore assumed no more extractions took place. In summary, this estimation indicated one extraction by farmer Q_3 and two extractions by farmer Q_1 within the relevant time frame.

The farmers both indicated that they usually irrigate for two hours in the morning starting at 8 AM. The exact irrigation dates were assumed to be in the middle of the week between 8 AM and 10 AM (Table 4.6). Farmers were assumed to distribute the water evenly over all their fields. The relevant irrigation volume of farmer Q_1 was therefore limited because parts of his farm were outside the focus area borders. The farmers share the same 2-horsepower submersible pump which pumps approximately at a rate of $18 \text{ m}^3/\text{h}$. The average irrigation volume and irrigation depth were calculated using this discharge (Table 4.6).

Farmer	Irrigation date	Pumping times	Relevant farm area [m^2/m^2]	Irrigation volume [m^3]	Irrigation depth [m]
Q_1	8 th of April	8 AM till 10 AM	190/680	10	0.05
Q_3	9 th of April	8 AM till 10 AM	660/660	36	0.05
Q_1	20 th of April	8 AM till 10 AM	190/680	10	0.05
<i>Total</i>	-	6h	-	56	0.9

Table 4.6: Irrigation activities in case study four

Groundwater table time series

The time series of location four displayed median daily fluctuations of around 0.15 meters (Figure 4.18). This suggests a relatively mediocre specific yield value. Significant extractions occurred in April which were likely from the irrigation well $Q_{irrigate}$ (Figure 4.11). However, recovery was often slow unlike at location three as can be seen via the daily first value. This was caused by irrigation at a significant distance from the observation well or irrigation where the subsurface is separated by a semi-permeable layer. Both would argue for slow irrigation return flow to the observation well.

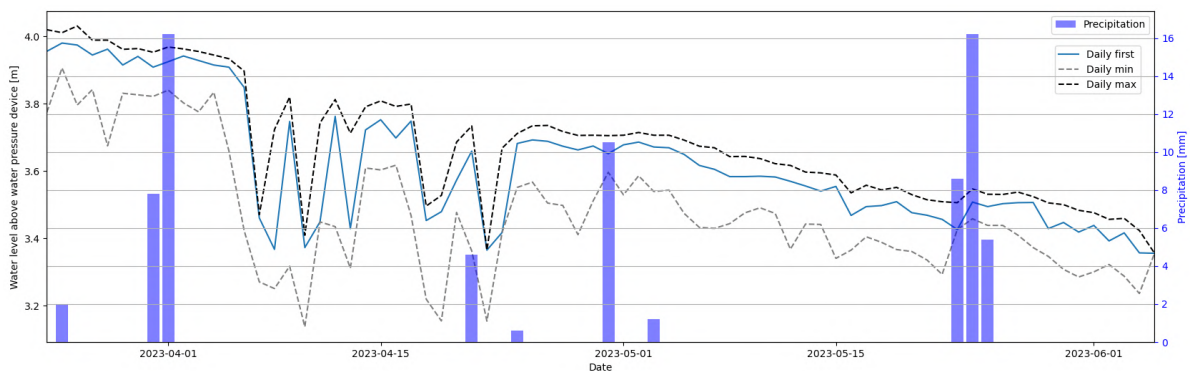


Figure 4.18: Time series of the groundwater table at case study four with medium daily fluctuations and where the groundwater table notable not redraws quickly after irrigation extraction

Local subsurface

A time series of another abandoned well Q_A was measured (Figure 4.19). In this time series, the fluctuations were approximately the same as in the observation well during the day. This suggests the specific yield and thus texture classes are locally similar.

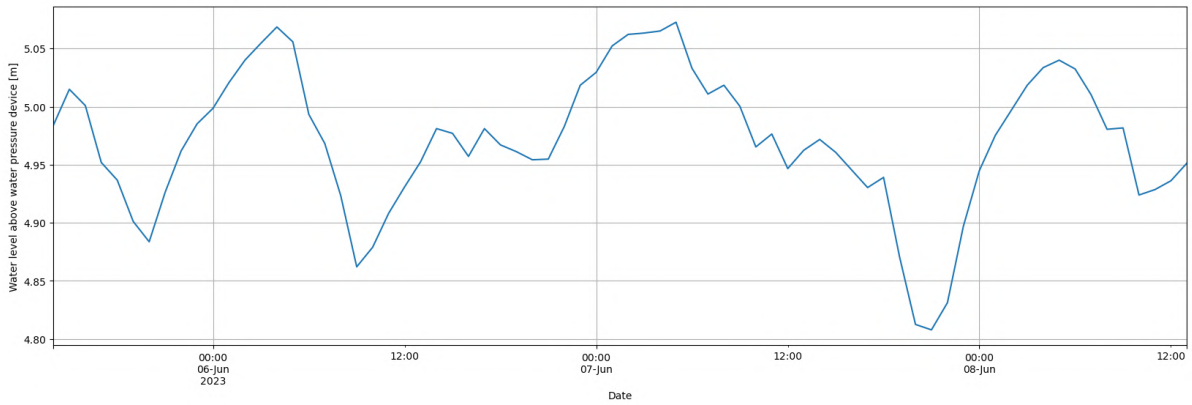


Figure 4.19: Extra time series in Q_A of case study four with similar daily fluctuations

Additionally, the depths of wells Q_1 and Q_A along the cross-section A-A' were measured and the groundwater tables were recorded in Q_{Obs} and Q_A (Figure 4.20). The groundwater table in Q_1 was not measured because the well had just been used both measurement times. This would make the potentially observed groundwater tables unreliable. The wells Q_{Obs} and Q_A were approximately as deep and the groundwater tables were similar as well. Conclusively, location four was selected for a pumping test because the texture class and subsurface were locally relatively homogeneous (Section 4.2).

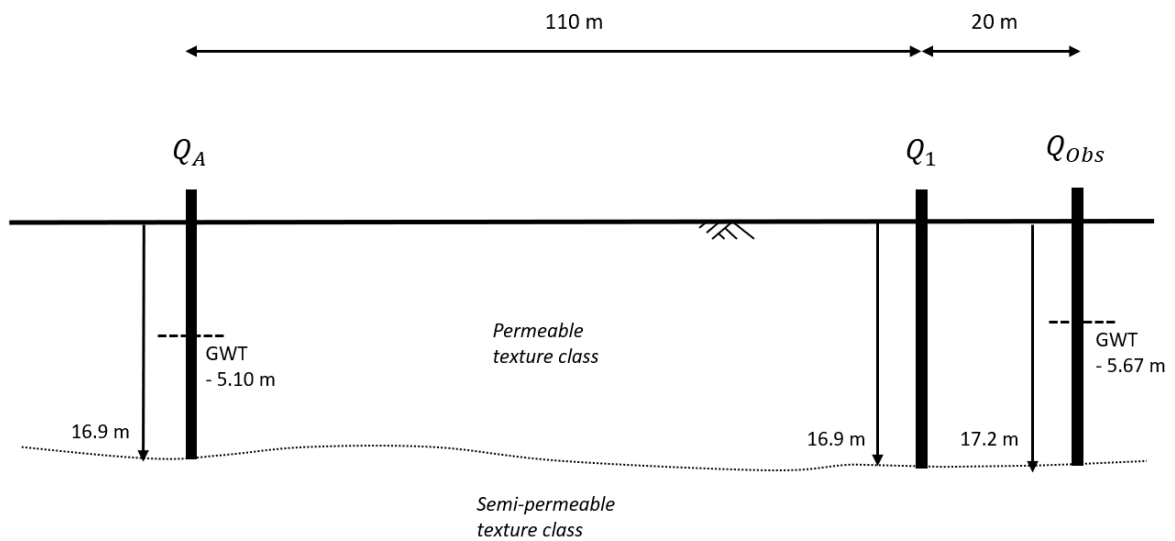


Figure 4.20: Schematic cross-section A-A' of the local subsurface at location four

Chloride measurements

The rain gauge was placed on the roof of the house that owned the observation well. The groundwater samples were taken from well Q_1 . The concentration of chloride in the groundwater was 7 mg/L.

4.7. Case study five

Area description

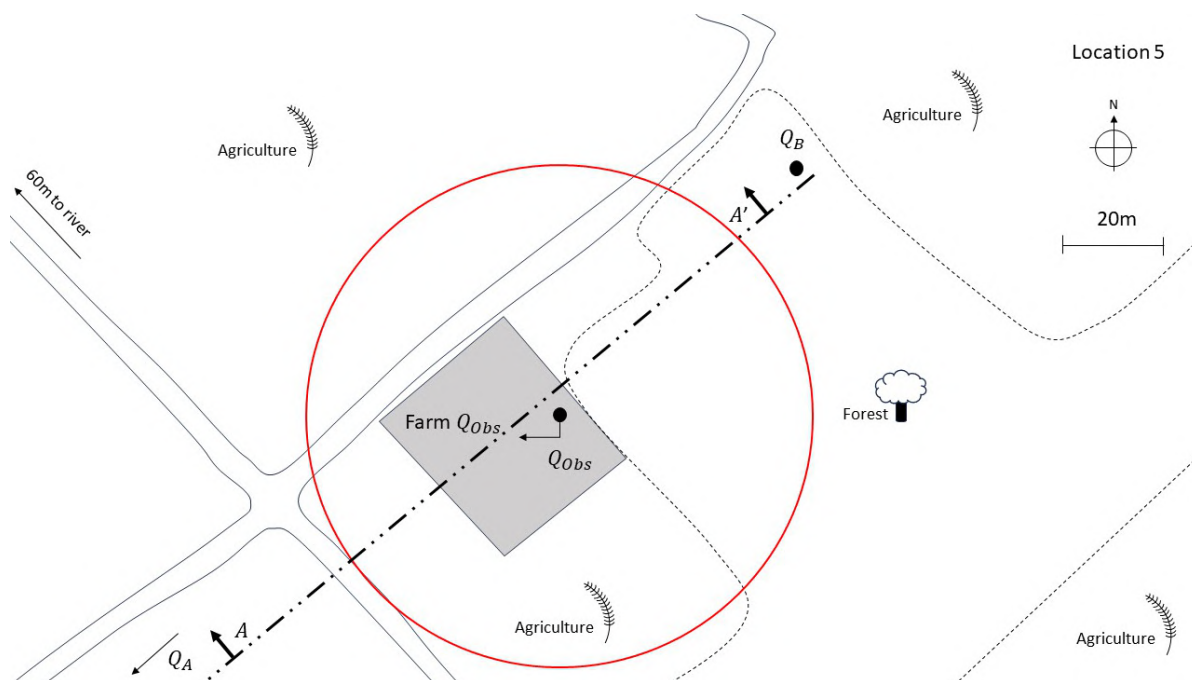


Figure 4.21: Schematic drawing field location five

Location five (Figure 4.21) was in the area called Baijanath which is located in the far north of the area of interest. The area is remote and filled with bare agricultural fields (Appendix D.5). Maize was farmed at the observation well and a little forest is located close to the well. Considering the vegetation present, the estimated crop factor ranged between 0.35 and 0.65 (Appendix D).

Rivers

The Phalgunj river flows approximately 165 meters to the North of the observation well. The river was levelled in contrast to the observation well and was measured twice, both times 0.40 meters above the bottom of the deepest part of the river. The river was therefore assumed constant during the end of the dry season. On the 30th of May, the groundwater level in the observation well was 0.41 meters higher than the level in the river. The maximum value that day was 0.02 meters higher and the minimum was 0.05 meters lower (Figure 4.22). This suggests the Phalgunj River at location five is an infiltrating river at the end of the dry season. The height of the river banks is 3.13 meters. A draining river might thus be likely with significant river discharge. However, during monsoon season this does not increase the risk of water scarcity.

Domestic extractions

The observation well is 7.94 meters deep and the property of a farmer who lived elsewhere. The remote area does not have any domestic extractions within a range of 50 meters.

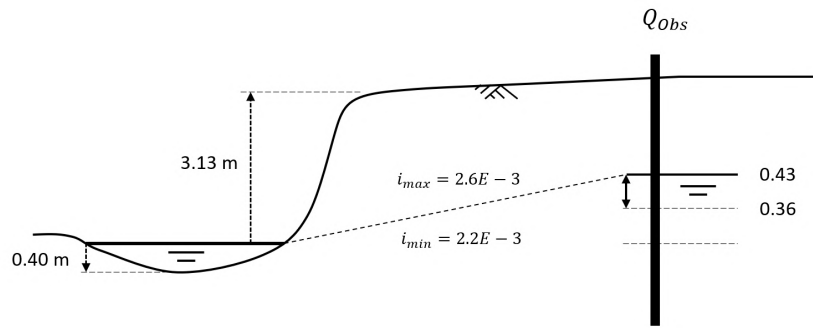


Figure 4.22: Schematic drawing of the river and fluctuating groundwater level in the observation well of case study five indicating that the Phalgunj River is an infiltrating river around case study five at the end of the dry season

Irrigation

The observation well is occasionally used by the farmer to irrigate. The farmer extracts whenever he feels it is necessary to irrigate due to too much drought. When he irrigates he turns on his pump in the evening and turns it off in the morning. During the measurement time, he extracted water five times in total where he recorded the date and pump duration. We altered his record to make it correspond to the observed time series (Appendix A.6). The discharge of the pump he uses is $36 \text{ m}^3/\text{h}$ (Appendix B.11) [27]. The irrigation volume was calculated using the discharge and the extraction pattern (Table 4.7).

Irrigation date	Pumping times	Farm area [m^2]	Irrigated volume [m^3]	Irrigation depth [m]
19/20th of April	20:15 PM till 12:35 AM	1000	588	0.588
20/21st of April	20:10 PM till 10:35 AM	1000	519	0.519
11/12th of May	19:00 PM till 05:00 AM	1000	360	0.360
17/18th of May	20:15 PM till 11:00 AM	1000	531	0.531
18/19th of May	20:40 PM till 10:40 AM	1000	540	0.540
<i>Total</i>	70h 30min	-	2538	2.538

Table 4.7: Irrigation activities in case study five

An irrigation depth of around 0.5 meters is a substantial irrigation depth. Therefore the discharge of the pump was verified twice. The farmer irrigated during the night and because he lives elsewhere he likely did not turn off his pump in the night. The diver still measured atmospheric pressures during the nights of irrigation. The farm is also around 0.3 meters below the grass edges of the farm (Appendix D) which keeps the irrigated water from leaking. All in all, an irrigation depth of 0.5 meters is substantial but it appears that the farmer did irrigate that significant amount of water. Therefore, the irrigated volumes were still assumed reliable in this research. Someone should however inform the farmer to be more careful with the amount of water he irrigates because irrigating this amount of water does not help crops grow better and is not beneficial for his financial or the groundwater resource availability in the region either.

Groundwater table time series

The daily median groundwater fluctuations at location five were negligible (Figure 4.23). This suggests few extractions, a relatively high specific yield value or both. This time series underwent some error adjustments (Appendix A.6).

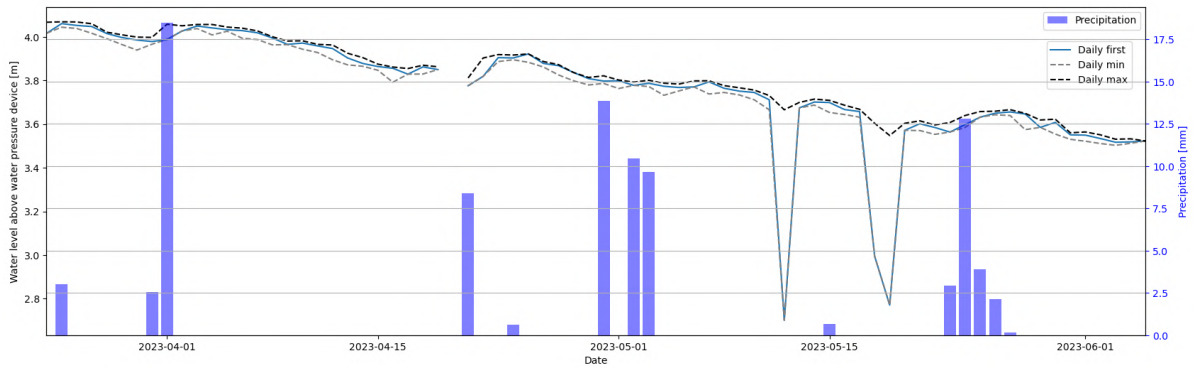


Figure 4.23: Time series of the groundwater table at case study five with minimal daily fluctuations

Local subsurface

Along cross-section A-A' two extra shallow wells were measured (Figure 4.24). The observed wells are all approximately as deep. The groundwater table in well Q_A was significantly lower than in the observation well. However, they are likely in the same aquifer because of the substantial distance to the observation well. Additionally, there are significantly more domestic extractions around well Q_A leading to relatively more drawdown.

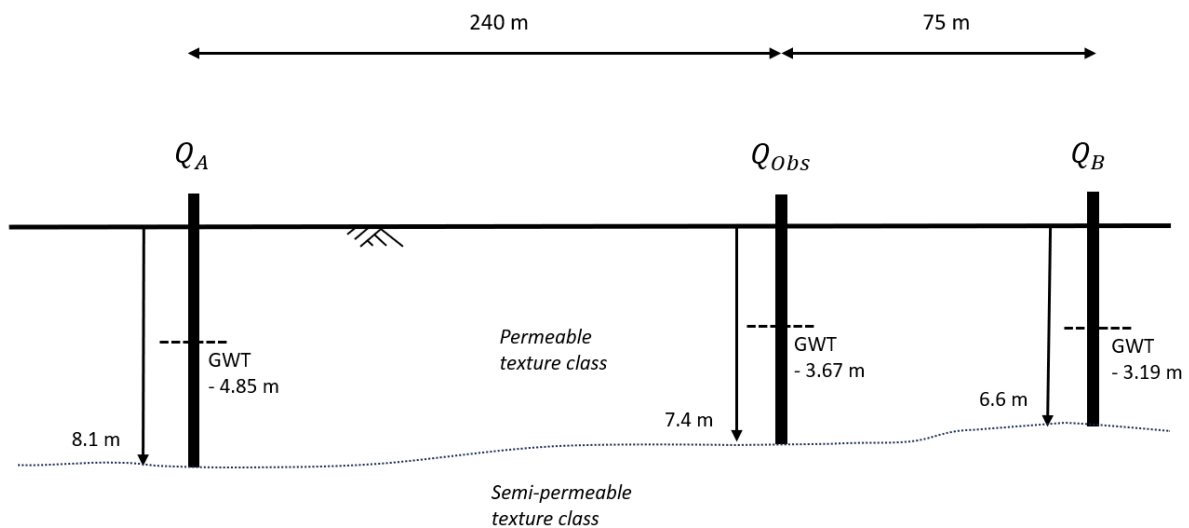


Figure 4.24: Schematic cross-section A-A' of the local subsurface of case study five

In both wells, the fluctuations during the day were negligibly small (Figure 4.25). This suggests a local homogeneous subsurface. However, no other wells are located near the observation well which made it difficult to perform a representative pumping test. Therefore no pumping test was performed at this location (Section 4.2).

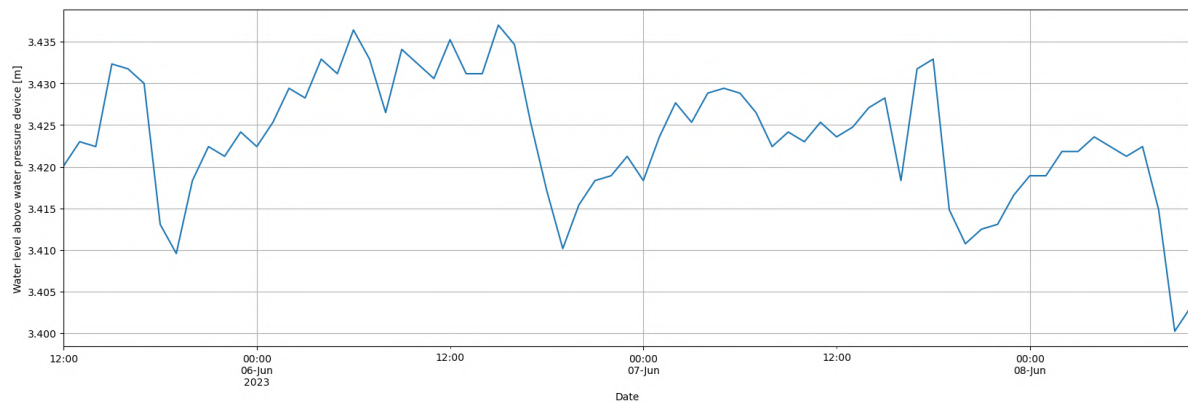


Figure 4.25: Extra time series in Q_A of case study five with similarly small daily fluctuations

Chloride measurements

The rain gauge was placed on the roof of a house in the northwest of the observation well location at a distance of 180 meters from the observation well. The groundwater samples were taken from a groundwater well next to this house. The measured concentration of chloride in the groundwater was 10 mg/L.

4.8. Case study six

Area description

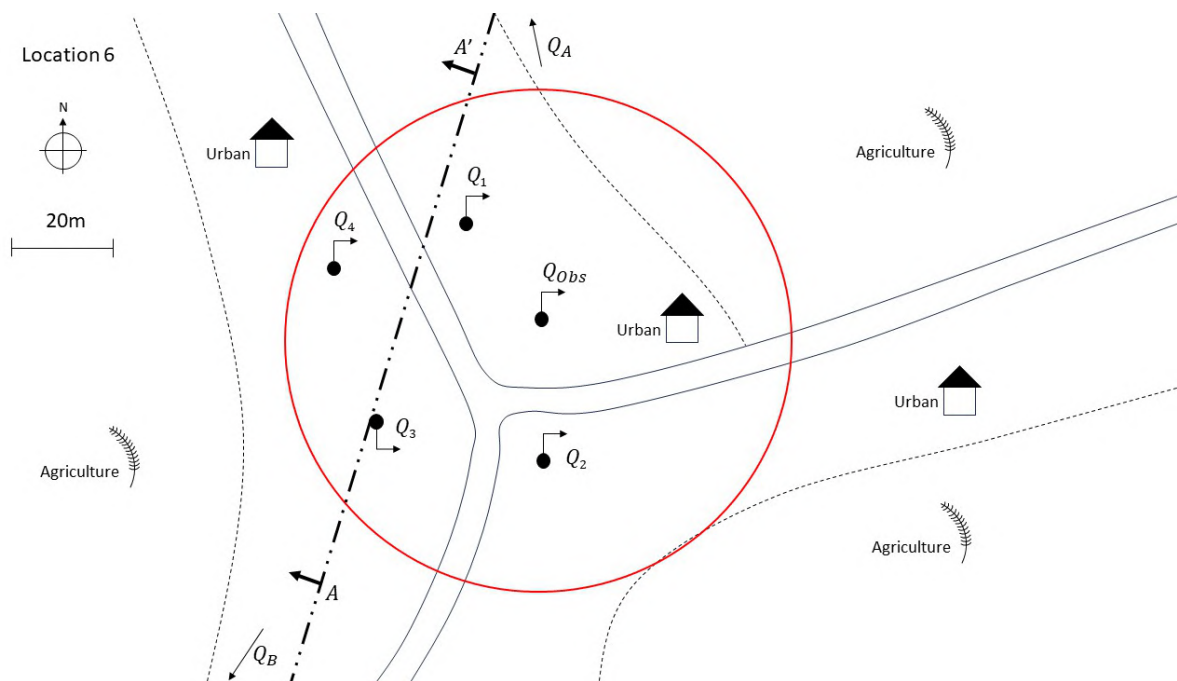


Figure 4.26: Schematic drawing of case study six

The last case study (Figure 4.26) was done in the town called Kohalpur which is in the far North-Eastern corner of the study area. The location is surrounded by houses, bare agricultural fields, some vegetation and thinly scattered trees (Appendix D.6). The range of the crop factor was therefore estimated to be between 0.30 and 0.60.

Rivers

The Duduwa River is located around 360 meters to the West of the observation well. This is the same river that downstream flows past locations two and three. The river level was 0.21 meters above the deepest part of the river bottom and was measured twice. On the 30th of May, the groundwater in the observation well was 2.10 meters higher than the river level. The daily maximum measurement was 0.07 meters higher and the measured value was at the daily minimum (Figure 4.27). The river is thus relatively heavily infiltrating groundwater. The highest river level before the river banks flood was measured to be 2.70 meters above the river level. The river at location six is therefore likely always infiltrating because groundwater levels would also increase if the river level is at a maximum.

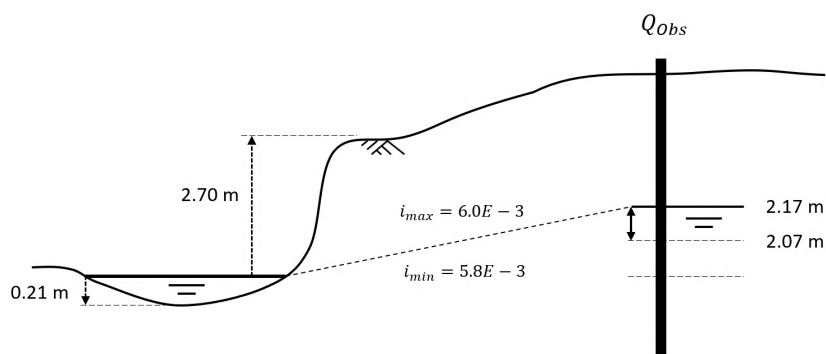


Figure 4.27: Schematic drawing of the river and fluctuating groundwater level in the observation well of case study six indicating that the Duduwa River is a gaining river around case study six at the end of the dry season

Domestic extractions

The observation well has a depth of 21.30 meters and belongs to a family with 6 members. The family owns two wells and stopped using the observation well because the pump of that well is broken. Four domestic pumps were observed in the area (Table 4.6).

Well	Distance Q_{Obs} [m]	People	Consumption [L/d]	Cattle	Consumption [L/d]	Consumption total [L/d]
Q_1	25	6	430	-	-	430
Q_2	27	4	300	2 goats	40	340
Q_3	39	5	350	2 buffaloes 9 goats	480	830
Q_4	41	7	400	-	-	400
<i>Total</i>	-	22	1480	-	520	2000

Table 4.8: Domestic extractions within the borders of case study six

Groundwater table time series

The median daily fluctuations of the groundwater table were less than 0.1 meters (Figure 4.28). The subsurface around the observation well therefore likely has a high specific yield number. Small and frequent irrigation activities occurred during the time series. However, the irrigation return flow was quick because the daily first values at 00:00 were recovered daily. This suggests farmers irrigate nearby in spatially connected aquifers.

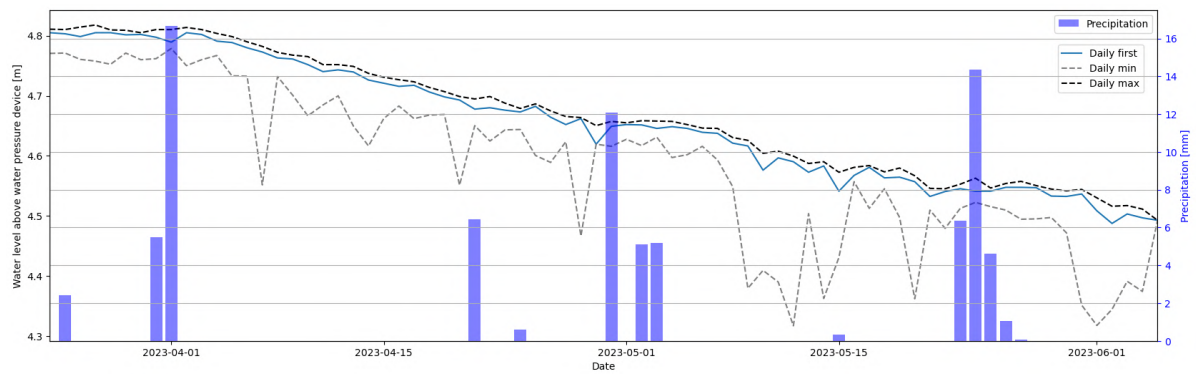


Figure 4.28: Time series location six with medium daily fluctuations

Local subsurface

Two extra out-of-use wells were measured along the cross-section A-A' (Figure 4.29). The well depths are spatially different but groundwater tables in the wells were similar. Therefore, it was estimated that the permeable texture classes were connected even though the well depths are different.

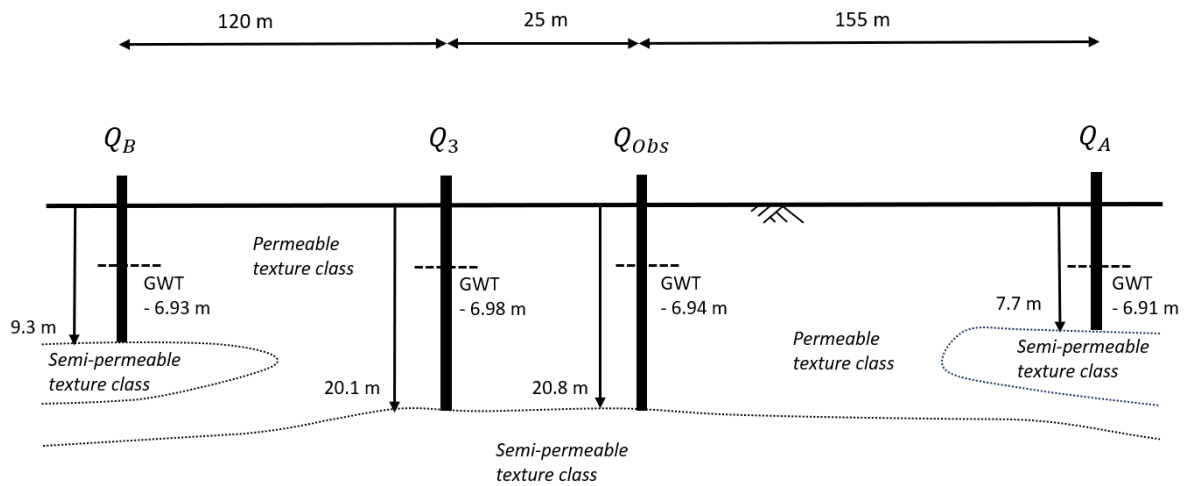


Figure 4.29: Schematic cross-section A-A' of the local subsurface of case study six

Groundwater table fluctuations in well Q_A were around 0.01 meters (Figure 4.30). The fluctuations in the observation well varied on a median day around 0.05 meters. The lower fluctuations of the additional well suggest a permeable texture class with a higher specific yield around well Q_A which is also likely the reason the well was dug shallower.

Chloride measurements

The rain gauge captured precipitation from the roof of a nearby house outside the sketch to the South-East of the observation well. The groundwater sample was taken from Q_1 and the median chloride concentration of the groundwater was 9 mg/L.

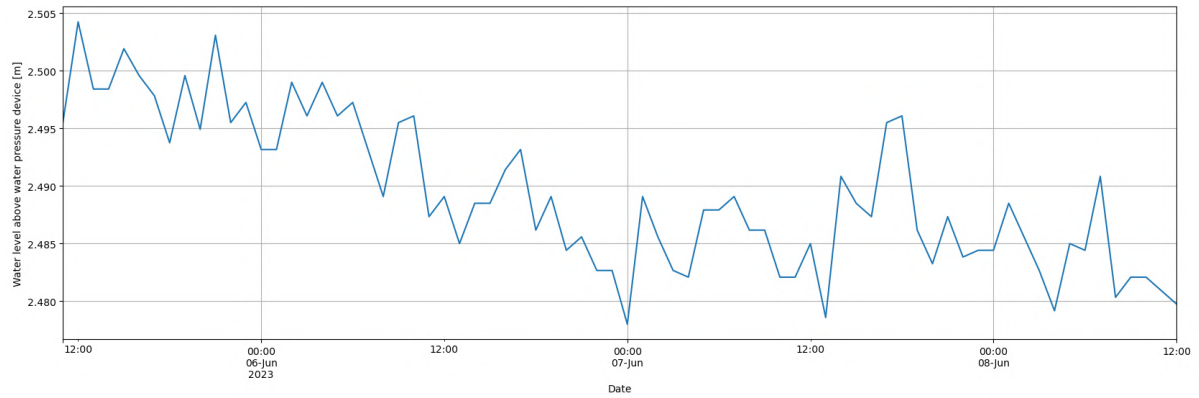


Figure 4.30: Extra time series in Q_A of case study six with smaller daily fluctuations

4.9. Conclusions

Crop factors were estimated to be lower in case studies one and three. These locations are also furthest from the Bhabar zone. This is logical because of moisture recycling, there is likely more vegetation close to the Bhabar zone. The rivers at the locations were infiltrating water upstream and losing water downstream. This is likely due to the position from the Bhabar zone where the rivers originated. Downstream the groundwater is recharged less easily by the Bhabar zone and therefore recharges via river water. No relation between specific yield and spatial location was observed. The subsurface in case study one has a low specific yield number but the specific yield in the extra well Q_A is likely significantly higher. Higher specific yields were expected closer to the Bhabar zone due to the nearby largely permeable Bhabar zone. However, with the limited number of case studies, this pattern was not recognized. The local sub-surfaces in the cross sections are also different between the locations and no real spatial pattern can be distinguished there either.

5

Results

This chapter presents the findings derived from the methodology chapter. It will initially list the volume of fluxes and total storage change for the case studies, including their associated uncertainties. Following that, it will outline the results for the whole area obtained from extrapolating via groundwater response units, accompanied by an uncertainty analysis. Finally, it will showcase the results of a distinct analysis of groundwater trends using historical data to assess potential depletion, once more considering associated uncertainties.

5.1. Recharge

The volume contributions for every location were estimated using the A_{Focus} of 7854 m² and the time interval of interest of 73 days between the 24th of March and the 4th of June. Recharge ($\sum V_{Rch}$) was calculated to a one-dimensional unit to verify the credibility of the results (Table 5.1).

Case study	$\sum V_{Rch}$ [m ³]	$\sum R$ [mm]	\bar{R} [mm/d]
1	584	74	1.0
3	549	70	1.0
4	549	70	1.0
5	664	85	1.2
6	597	76	1.0

Table 5.1: Recharge flux at relevant case studies

5.1.1. Precipitation data

Precipitation using remote sensing was significantly higher than precipitation via the measurement stations (Table 5.2).

Case study	$\sum P$ [mm]	$\sum P_{Remote-Sensing}$ [mm]
1	78	119
3	73	133
4	73	116
5	90	141
6	81	141

Table 5.2: The sum of precipitation measurements via meteorological stations and CHIRPS data

Reliability precipitation data

The measurement stations independently recorded 73.1, 77.6 and 92.3 millimetres of total precipitation during the measurement time frame. The last measurement, obtained in the Bhabar zone where higher precipitation was anticipated, aligns with those expectations. Because measurements are done independently these measurements are reliable. However, spatially distributing the data to the locations using the inverse proportional distance makes the exact precipitation per case study slightly uncertain. Remote sensing estimated average precipitation of 129.9 millimetres, notably higher than the 78.8 millimetres estimated by the weather stations. This discrepancy might arise from the calibration limitation. CHIRPS data is calibrated using local weather stations. However, likely no local meteorological stations were included in the calibration around the study area because the differences in precipitation measurements between the two observation methods are significant. The exact magnitude of the CHIRPS data is thus inaccurate in the study area.

5.1.2. Chloride Mass Balance method

Considering the Electrical Conductivity measurements the water is not brackish, the chloride measurements in the groundwater of the case studies are therefore plausible (table 5.3) [10].

Case study	Chloride [mg/L]	Chloride [meq/L]
1	7	0.20
3	14	0.40
4	7	0.20
5	10	0.28
6	9	0.24

Table 5.3: Median chloride in the groundwater at the case studies

The median chloride in precipitation of all samples combined was measured to be 6 mg/L. However, a number between 0 and 2 mg/L was expected for the West-Terai region. The values of 0 and 2 mg/L were therefore used as a normative range estimate. The CMB-method (V_{Cl-Rch}) was used with CHIRPS data and meteorological station data (Table 5.4). The data set from the meteorological stations does not cover the entire year. Therefore the same precipitation proportion as the CHIRPS data was used to estimate yearly precipitation by the meteorological stations.

Case study	$R_{Cl-CHIRPS}$ [mm/d]	$R_{Cl-Station}$ [mm/d]
1	0; 0.46	0; 0.30
3	0; 0.26	0; 0.14
4	0; 0.45	0; 0.28
5	0; 0.39	0; 0.25
6	0; 0.45	0; 0.26

Table 5.4: Utilization of the chloride Mass Balance method to estimate the range of the one-dimensional recharge flux at the case studies

Uncertainty CMB method

The recharge calculated through effective precipitation (Table 5.1) significantly differed in magnitude from the estimates obtained via the CMB method (Table 5.4). Several underlying assumptions in the CMB method could account for this disparity. For instance, the CMB-method was assumed to give representative results when interpolated using yearly precipitation data, overlooking the considerable difference in precipitation between the monsoon and dry seasons. Additionally, all chloride within the aquifers was assumed to be derived from atmospheric sources. This means run-off should always be negligible which is not true during the monsoon season. Furthermore, this assumed a minimal effect of subsurface flow on chloride concentration in the aquifers even though there is significant subsurface flow [18, 38, 46]. Additionally, this assumed precipitation did not pick up chloride increasing salts or other pollution from the surface before infiltrating. Likely, there was some sort of pollution on the streets because in all case studies inhabitants lived within 100 meters of distance. Lastly, the effect of re-irrigation of water was assumed to not affect concentration even though there were signs of irrigation at all locations. Ultimately, the CMB method was not reliable in this research.

5.1.3. Uncertainty recharge

The evaporation during precipitation was quadrupled to test the uncertainty of the recharge (Table 5.5). Surprisingly, even with this drastic increase in evaporation, the recharge decreased by only about 20%. Such a modest reduction following an extreme evaporation change indicates the stability of effective precipitation as a reliable method for recharge estimation. Another point reinforcing reliability is the consistency between independently recorded hourly values from the measurement stations, indicating their likely reliability. Lastly, an average recharge of around 1 millimetre per day seems like a plausible number.

Case study	Increase of evaporation [%]	Decrease in recharge [%]
1	400	16
3	400	17
4	400	17
5	400	23
6	400	23

Table 5.5: The consequence of drastically increasing evaporation during precipitation events per case study

5.2. Extractions

5.2.1. Domestic extractions

The total domestic extraction was calculated by summing the daily domestic consumption over 73 days (Table 5.6). Inhabitants of the study area without cattle used on average 63 litres per day per person. This is a little more than average usage in the Kathmandu valley [28]. The domestic consumption is a fairly certain number because it was estimated by 18 people for 122 inhabitants, no estimate stood out and below 100 litres per person is what might be expected for the region.

Case study	$\sum V_{Cons} [m^3]$	Cons. [l/p/d]
1	153	82
3	251	55
4	213	58
5	-	-
6	146	67

Table 5.6: The domestic extractions per case study

5.2.2. Irrigation extractions

Irrigation in the case studies stood out because of their dissimilarity in average irrigation depth (Table 5.7). Case study four produced low numbers while five produced high. The estimated median irrigation depth of around 5 millimetres per day (Section 2.3) was in between the two estimates.

Case study	$\sum V_{Irri} [m^3]$	$\sum IR [mm]$	$\bar{IR} [mm/d]$
4	56	66	0.9
5	2538	2538	34.8

Table 5.7: Irrigation extraction per case study

Uncertainty case study 4

The irrigation depth at location four was low. This was likely because of the local climate and the awareness of the farmers in the case study about the amounts they pumped. The farmers lived next to their farm and irrigated likely more responsibly and thus effectively. Furthermore, the subsurface was largely homogeneous at location four. This means that they might notice the pressure head in their domestic tube well decreasing whenever they pump. The number of trees and other vegetation in the nearby area was also significantly larger at location four than in median irrigation areas in the Banke district. Vegetation tends to lower temperatures and enhance moisture recycling, thereby reducing the required irrigation depth. This also partly explains why the irrigation depth is lower than the found value using questionnaires (Section 2.3). While the exact pumping times were unknown, the known pumping frequency helped establish a relatively accurate irrigation depth at location four.

Uncertainty case study 5

The farmer of observation well 5 lived elsewhere and no inhabitants lived close to the well either. He was less likely to be conservative with groundwater consumption because he does not live at the location and even pumps during the night. He made grass edges to prevent the water from leaking from his farm. The farmer also noted down the pumping times and the pump. Despite discrepancies in the observed irrigation depth, the values obtained for the case studies are not uncertain.

5.2.3. Total extractions

The total extraction flux was estimated by summing the irrigation extraction and domestic extraction (Table 5.8).

Case study	$\sum V_{Extr}$ [m ³]
1	-153
3	-251
4	-269
5	-2538
6	-146

Table 5.8: The sum of extractions for domestic use and irrigation per case study

5.3. Irrigation return flow

The return flow volume was calculated via the irrigated volume (Table 5.7) and actual evaporation during irrigation (Table 5.9). The total and daily return flow was calculated as an average value for both locations because at location four there were two farms. The total evaporation during the summed irrigation events was only 0.7 millimetres for location 4 and 5.2 millimetres for location 5. This meager figure was influenced in part by the timing of irrigation, which took place in the morning when solar radiation was negligible.

Case study	$\sum V_{Ret-Flw}$ [m ³]	\bar{RF} [mm]	\bar{RF} [mm/d]
4	56	65	0.9
5	2533	2533	34.7

Table 5.9: Total irrigation return flow and average return flow per day per case study

Uncertainty irrigation return flow

Evaporation during irrigation was quadrupled to check the uncertainty of the return flow (Table 5.10). The irrigation return flow would still be 96 percent and 99 percent of the current value even when the evaporation during irrigation would be quadrupled. Therefore, because irrigation extraction is a certain number, the return flow is a reliable number as well.

Case study	Increase of evaporation [%]	Decrease in RF [%]
4	400	4
5	400	1

Table 5.10: The consequence of drastically increasing evaporation during irrigation events per case study

5.4. Transpiration

The transpiration results via the evaporation sum (Appendix A.7) were rewritten to total and daily-average one-dimensional transpiration (Table 5.11).

Case study	$ \sum V_{Trans} $ [m ³]	ET_{Trans} [mm]	ET_{Trans}^- [mm/d]	Crop factor f
1	1048	133	1.8	0.38
3	925	118	1.6	0.27
4	1850	236	3.2	0.54
5	1331	169	2.3	0.43
6	1757	224	3.1	0.56

Table 5.11: Transpiration and associated crop factor per case study

Uncertainty transpiration using the crop factor

The calculated crop factors were in the expected range of the case studies (Table 5.12). Location six was barely within the described data limit, which was likely caused by the coarse resolution of the actual evaporation data by the satellite. Given the proximity to the Bhabar zone, the pixel area within location six likely encompassed more forest than representative of the actual case study. Consequently, this increased observed evaporation, elevating the estimated transpiration and consequently, the crop factor within this area. The other estimated crop factors via remote sensing were in the middle of the expected range. However, the crop factor range widths were significant due to the difficulty of estimating crop factors of a larger area. While the SSEBop method offers reliable estimates based on energy balance, the coarse resolution of data per case study introduces a moderate level of uncertainty in the estimated transpiration fluxes.

Case study	Present vegetation	f_{Min}	f_{Max}
1	Dominantly bare lands, average grass, some trees, some urbanization	0.25	0.50
3	Dominantly bare lands, little grass, little trees, much urbanization	0.15	0.35
4	Some bare lands, average grass, many trees, little urbanization, much maize	0.45	0.75
5	Many bare lands, average grass, some trees, much maize	0.35	0.65
6	Many bare lands, average grass, some trees, some urbanization	0.30	0.60

Table 5.12: Estimated crop factor ranges using visual inspection and the guidelines by the FAO

5.5. Storage change

5.5.1. Water table fluctuation method

To determine storage change the specific yield was necessary. This was determined by applying the Water Table Fluctuation method to the recharge contributions. These recharge contributions were determined by fitting a model to the time series (Appendix B.4).

Specific yield case study one

The model was simulated with a crop factor of 0.38 at location one (Figure 5.1). The simulation captured the magnitude of the first and last peaks satisfactorily. This is difficult to observe however due to the enormous hourly groundwater table fluctuations. The peak around the 1st of May was not correctly modelled which can be attributed to the missing data from the weather station (Appendix A.2). The WTF method was applied to the recharge contribution on three peaks (Figure B.13) as described in Formula 3.14. Chronically, the estimated specific yields were 0.047, 0.044 and 0.048. The average of 0.047 was adopted as the true value.

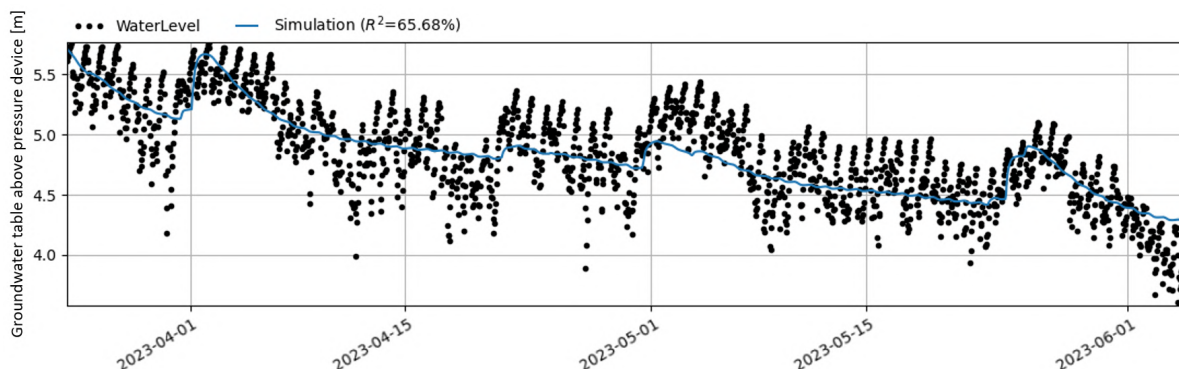


Figure 5.1: Groundwater table time series simulation at case study one

Specific yield case study three

Heavy extractions took place at the end of the simulation of time series three but no record was available of these extractions (Figure 5.2). Subsequently, the last 14 days of the time series were removed because these days complicated the least squares fit. Removal of this data was possible because only recharge events should fit properly for the determination of the specific yield using the water table fluctuation method. The first peak and the peak around the 1st of May fitted satisfactorily. There were many extractions in the case study which complicated the simulation. Nonetheless, the visualized simulation was the best fit for the peaks. Two peaks were used in the WTF method to calculate the specific yields (Figure B.15). Chronically, the estimated specific yields were 0.42 and 0.38. The specific yield was therefore estimated to be the mean which is 0.40.

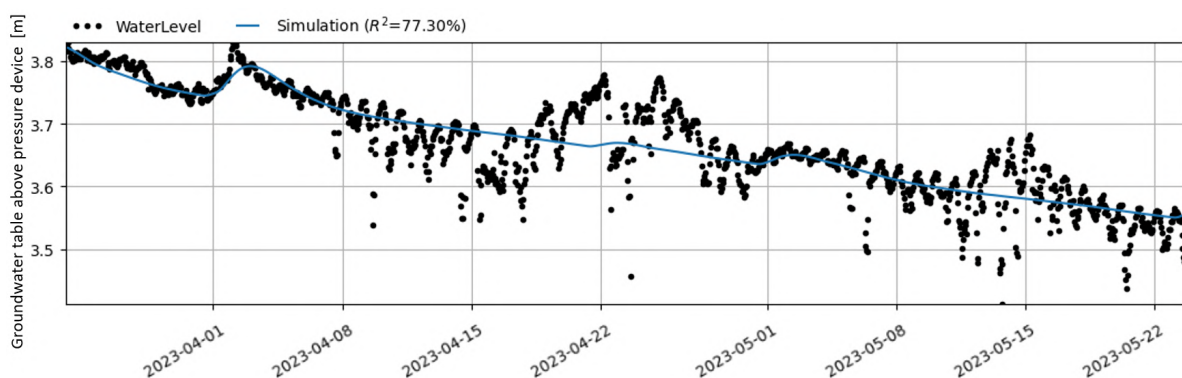


Figure 5.2: Groundwater table time series simulation at case study three

Specific yield case study four

The simulation (Figure 5.3) was fitted with a crop factor of 0.54. The simulated fit constantly underestimated the measurements slightly which was due to the heavy extractions in the region. Nonetheless, the magnitude of the simulated peaks fitted the time series satisfactorily. The two estimated specific

yields were estimated to be 0.18 and 0.18 using the WTF method (Figure B.17). Conclusively, the specific yield was estimated to be 0.18 in case study four.

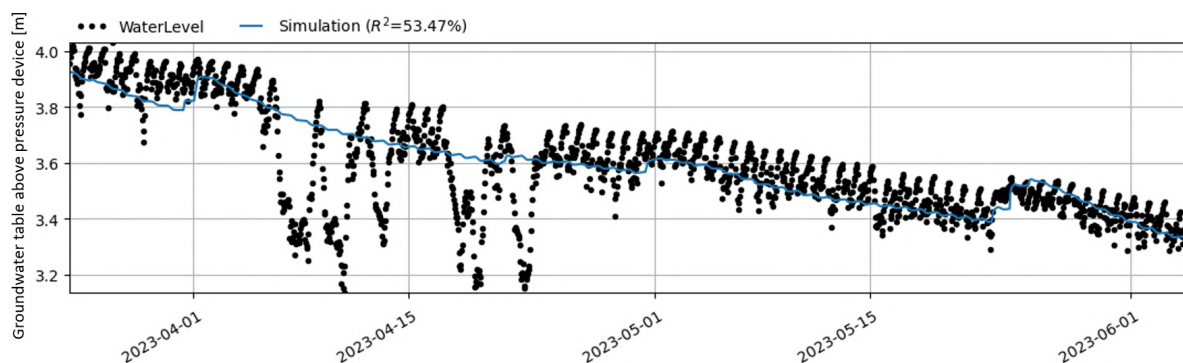


Figure 5.3: Groundwater table time series simulation at case study four

Specific yield case study five

Most of the extraction and recovery parts of the fifth time series were removed. This was done to make the least squares fit as properly as possible. The model was fitted using a crop factor of 0.43 (Figure 5.4). Peaks were difficult to fit because presumably there were local extractions at those moments as well. The estimated precipitation at the 1st of May was likely overestimated at location five. However, the first peak fitted perfectly and the magnitude of the last peak was correct. Therefore the fit was satisfactory. The two peaks used for the water table fluctuation method chronically estimated specific yields of 0.17 and 0.19 (Figure B.19). The average specific yield was therefore 0.18 at location five.

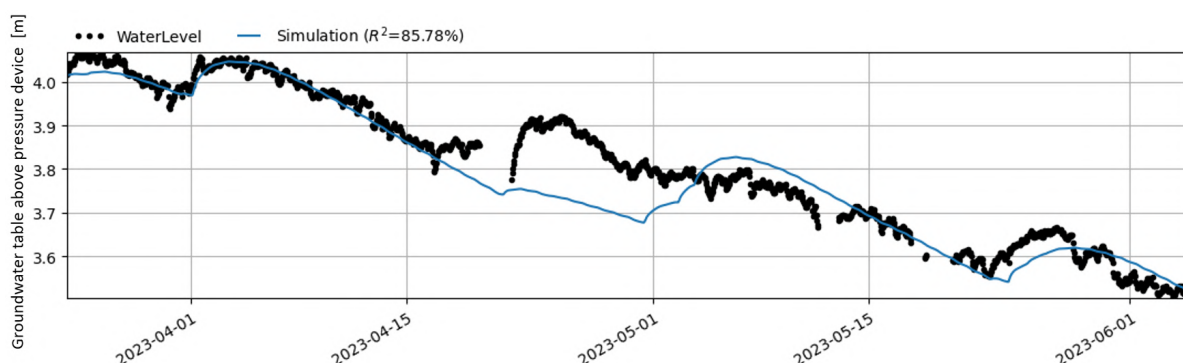


Figure 5.4: Groundwater table time series simulation at case study five

Specific yield case study six

The sixth simulation was fitted with a crop factor of 0.56 (Figure 5.5). The simulation captured the peaks after precipitation in the water level measurements satisfactorily and model parameters were not out of reasonable bounds (Figure B.20). The specific yield was estimated using the WTF method (Figure B.21) and was respectively 0.48, 0.37 and 0.41. The average specific yield was assumed to be the mean of 0.42 at location six.

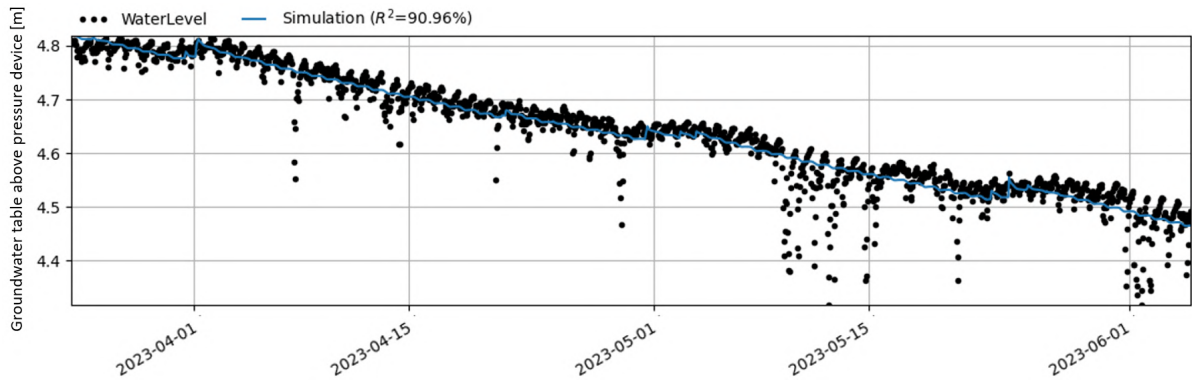


Figure 5.5: Groundwater table time series simulation at case study six

Conclusion

Specific yields varied heavily between the case studies (Table 5.13). The specific yield at location one was relatively low, at locations four and five mediocre and at locations three and six high. Locations three and six experience specific yields of around 0.40 which is an exceptionally high number but still just within the boundaries of the expected range of subsurface material (Figure B.22) [52]. It was still assumed these values were correct because we already predicted high specific yield values using the time series in case studies three and six (Chapter 4). Additionally, the fitted groundwater reaction to precipitation was modelled by Pastas to be instant in all case studies. This means that precipitated or infiltrated water quickly reaches the groundwater table. The pressure devices in the case studies were thus measuring groundwater tables in upper aquifers as was assumed in Section 3.3.

Case study	S_y
1	0.05
3	0.40
4	0.18
5	0.18
6	0.42

Table 5.13: Estimated specific yields via the Water Table Fluctuation method

5.5.2. Determining storage change

Storage change was calculated using the total decrease in the water table and specific yield (Table 5.14). The storage change was calculated via specific yield which was derived using precipitation data. Because the precipitation was a relatively uncertain parameter, storage change was as well. Nonetheless, all storage changes are in the same order of magnitude even though the specific yields are not.

Case study	$H_{t=n} - H_{t=0}$ [m]	$\Delta V_{Storage}$ [m ³]
1	1.60	-593
3	0.43	-1360
4	0.60	-849
5	0.49	-698
6	0.31	-1038

Table 5.14: Volume storage change over the measurement time frame between the 24th of March and 4th of June

Uncertainty storage change

The specific yields were increased by 20% and subsequently decreased by 20% (Table 5.15). The uncertainty in storage change is solely influenced by altered specific yield when the pressure device was assumed to record without errors. The storage change alters accordingly to the change in specific yield because they are linearly dependent. These altered specific yields will be used later in Section 5.6.

Case study	$\Delta V_{Storage}$ [m ³] in- crease by 20%	$\Delta V_{Storage}$ [m ³] de- crease by 20%
1	-712	-494
3	-1632	-1133
4	-1019	-708
5	-838	-582
6	-1246	-865

Table 5.15: Influence of altering specific yield on the storage change

5.6. Sub-surface flow and percolation

The net sub-surface flow/percolation flux was calculated by reversing the water balance (Appendix A.3) and rewritten to an average horizontal net flux (Table 5.16). The fluxes were calculated in the horizontal direction using the circumference of the case studies and the aquifer thickness approximated by the depth of the observation well. Note, that this value was only to check the order of magnitude because it assumed the flux was solely subsurface flow. The values found for two-dimensional average net flow were well below the expected possible transmissivity range of between 181 m²/d and 1030 m²/d (Section 2.2).

Case study	$\sum V_{SSF-Perc}$ [m ³]	$SSF/Perc$ [mm ² /d]	$SSF/Perc$ [mm/d]
1	23	2.0	0.1
3	-733	-32.0	-2.7
4	666	29.0	1.7
5	-26	-1.1	-0.2
6	268	11.7	0.6

Table 5.16: Net sub-surface flow and percolation flux per case study

Uncertainty net subsurface flow and percolation

Net subsurface flow and percolation values vary greatly between case studies. Because the flux was estimated as the missing component in the water balance, uncertainty can only be assessed by changing other arguments in the balance. The increased and decreased specific yields from the previous paragraph were applied for the net subsurface flow and percolation as well (Table 5.17). The specific yield was estimated using visually fitting a model using the Pastas package in Python. The specific yield was therefore not a certain number and could easily be 20% different. The net subsurface flow and percolation flux changed significantly with varying specific yields. The flux could switch between infiltrating or losing water in the case studies. The net subsurface flow and percolation is therefore not a certain flux. Furthermore, because the flux is a combined flux, interpretation of the individual fluxes is difficult.

Case study	$\sum V_{SSF-Perc} [m^3]$ with S_y increase by 20%	$\sum V_{SSF-Perc} [m^3]$ with S_y decrease by 20%	Range $SSF/Perc$ [mm/d]
1	-96	122	-0.2; 0.3
3	-1005	-506	-3.7; -1.9
4	496	807	1.3; 2.0
5	-166	90	-0.1; 0.5
6	60	441	0.1; 0.9

Table 5.17: Uncertainty of the combined net subsurface flow and percolation flux

5.7. Net extraction

An extra result parameter was introduced which is the difference between extraction and irrigation return flow. Extraction of water that later returns to the groundwater table as return flow does not deplete the groundwater resources. Therefore, the net contribution ($\sum V_{Ext-Net}$) is a proper parameter to estimate depletion due to extraction. Because extraction and evaporation were reliable numbers, the net extraction is also a certain parameter.

Case study	$\sum V_{Extr} [m^3]$	$\sum V_{Ret-Flw} [m^3]$	$\sum V_{Ext-Net} [m^3]$
1	-153	-	-153
3	-251	-	-251
4	-269	56	-214
5	-2538	2533	-5
6	-146	-	-146

Table 5.18: Net extraction per case study

5.8. Contribution fluxes per case study

The volume contributions of all fluxes in previous paragraphs were summarized (Table 5.19).

Case study	$\sum V_{Rch} [m^3]$	$\sum V_{Extr} [m^3]$	$\sum V_{Ret-Flw} [m^3]$	$\sum V_{Ext-Net} [m^3]$	$\sum V_{Trans} [m^3]$	$\sum V_{SSF-Perc} [m^3]$	$\Delta V_{Storage} [m^3]$
1	584	-153	-	-153	-1048	23	-593
3	549	-251	-	-251	-925	-733	-1360
4	549	-269	56	-214	-1850	666	-849
5	664	-2538	2533	-5	-1331	-26	-698
6	597	-146	-	-146	-1757	268	-1038

Table 5.19: Volume contribution of fluxes per case study

Water Balances

The fluxes were calculated to one-dimensional average vertical units (Table 5.20). The estimates of case study four were displayed in the respective schematic drawing of the water balance (Figure 5.6). The water balances of the other case studies can be found in Appendix B.4.

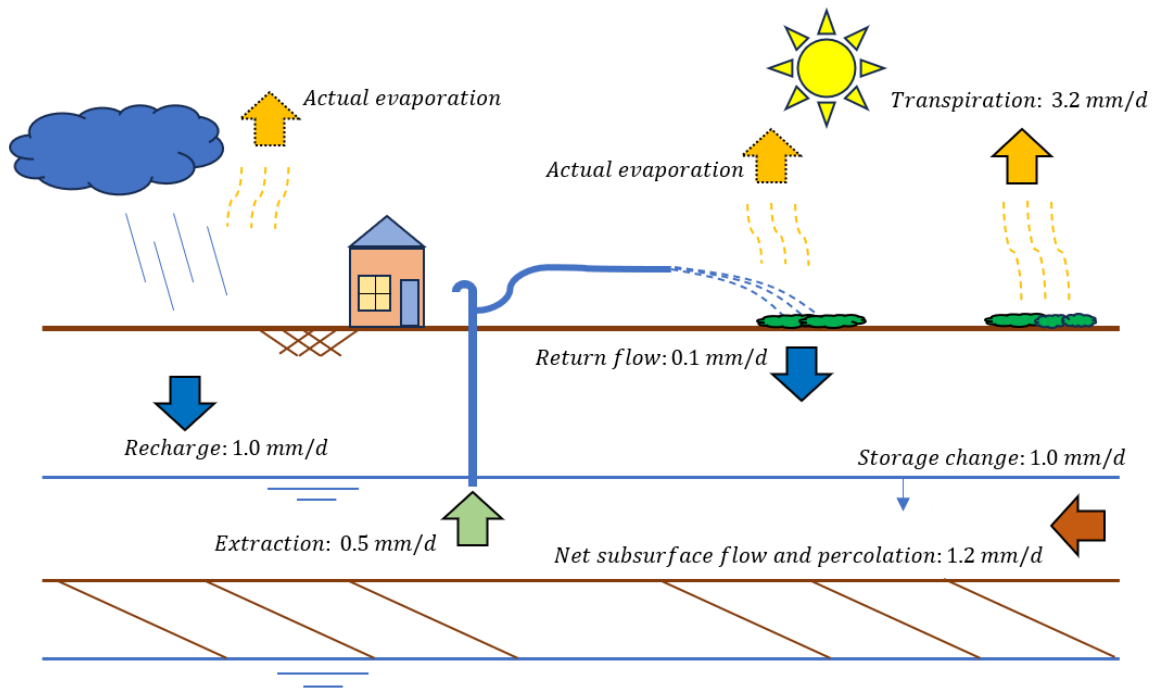


Figure 5.6: Schematic drawing with estimated one-dimensional vertical average fluxes at case study four. Schematic drawings of the other case studies are located in Appendix B.4

Case study	\bar{R} [mm/d]	\bar{E}_{extr} [mm/d]	\bar{RF} [mm/d]	$\bar{Ext} - \bar{Net}$ [mm/d]	\bar{ET}_{Trans} [mm/d]	$\bar{SSF} - \bar{Perc}$ [mm/d]	$\Delta \bar{H}$ [mm/d]
1	1.0	-0.3	-	-0.3	-1.8	0.0	-1.0
3	1.0	-0.4	-	-0.4	-1.6	-1.3	-2.4
4	1.0	-0.5	0.1	-0.4	-3.2	1.2	-1.5
5	1.2	-4.4	4.4	-0.0	-2.3	-0.0	-1.2
6	1.0	-0.3	-	-0.3	-3.1	0.5	-1.8

Table 5.20: Average one-dimensional daily water fluxes per case study where $\Delta \bar{H}$ is absolute water instead of groundwater table

Proportional contributions

Subsequently, the fluxes were calculated to proportional contributions (Table 5.21) in contrast to the storage change (Formula 3.27). Mostly net extraction was in the same order of magnitude for all case studies. The other fluxes varied significantly between locations.

Case study	p_{Rch}	$p_{E_{extr}}$	$p_{Ret-Flw}$	$p_{Ext-Net}$	p_{Trans}	$p_{SSF-Perc}$
1	99%	-26%	-	-26%	-177%	4%
3	40%	-18%	-	-18%	-68%	-54%
4	65%	-32%	7%	-25%	-218%	78%
5	95%	-364%	363%	-1%	-191%	-4%
6	58%	-14%	-	-14%	-169%	26%

Table 5.21: Contribution percentage fluxes per case study

5.9. Extrapolation of fluxes in space

5.9.1. Assigning response units

The study area was divided into response units of approximately the same size as A_{Focus} (Section 3.10). Subsequently, every response unit was assigned a representative value for recharge (Figure B.27), evaporation (Figure B.28) and population (Figure B.29). A resemblance score (Formula 3.24) was then calculated per response unit and every response unit was assigned the location with the highest score (Figure B.30). The total assigned area A_{Loc-i} per location was calculated by summing the areas of the polygons that were assigned to the concerned case study (Table 5.22). Approximately 79% of the polygons were most similar to location one. Therefore location one is the most representative location.

Case study	Number of assigned response units	Assigned area A_{Loc-i} [m ²]
1	53912	37.30E7
3	4176	2.89E7
4	1013	0.70E7
5	7406	5.12E7
6	2876	1.99E7
Total	69383	4.80E8

Table 5.22: Assigned sum of response unit areas per case study

5.9.2. Contributions total area

The contributions of fluxes in the total area (Table 5.23) were generated using the contribution of the fluxes (Section 5.8) and assigned areas (Table 5.22). The average one-dimensional vertical flux was calculated as well (Figure 5.7). The total proportion of net extraction in the total region was equal to -21%. Intermediate calculation can be found in Appendix A.9

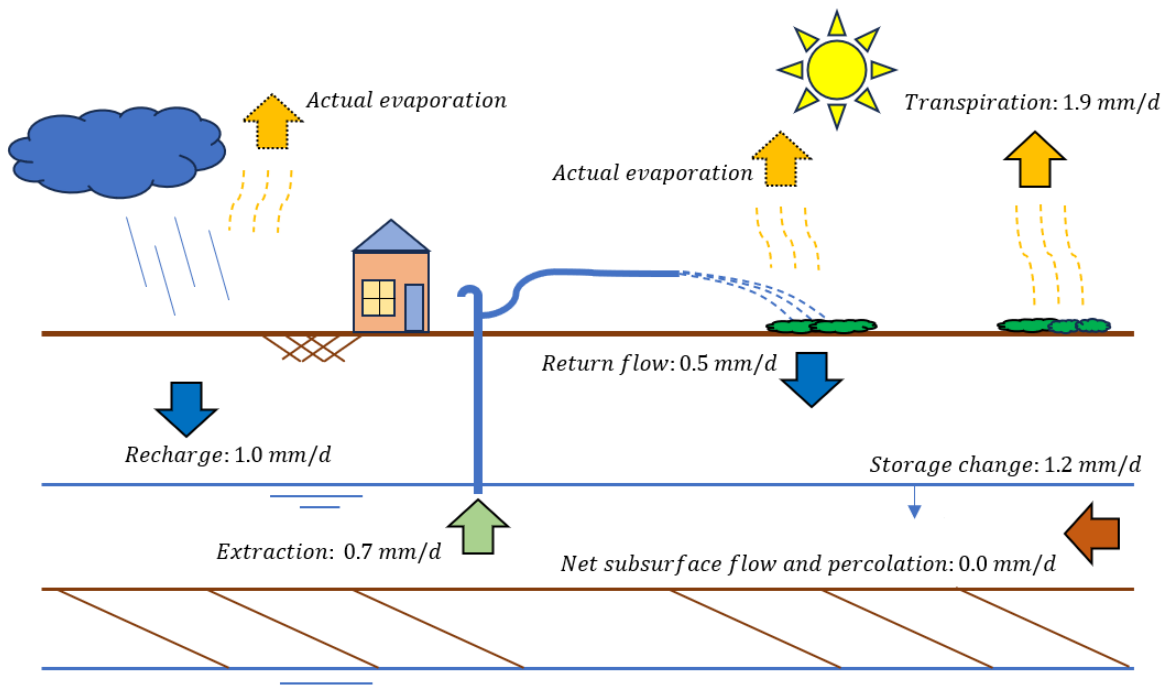


Figure 5.7: Schematic drawing with estimated one-dimensional vertical average fluxes for the whole study area

Flux	$\sum V_{Rch}$	$\sum V_{Extr}$	$\sum V_{Ret-Flw}$	$\sum V_{Ext-Net}$	$\sum V_{Trans}$	$\sum V_{SSF-Perc}$	$\Delta V_{Storage}$
Total [m ³]	3.62E7	-2.54E7	1.66E7	-8.8E6	-6.81E7	-5E5	-4.12E7
Total [mm/d]	1.03	-0.72	0.47	-0.25	-1.94	0.01	-1.17
Total [%]	88	-62	40	-21	-165	-1	-

Table 5.23: Assigned contribution volumes in m³ and percentage

5.9.3. Uncertainty extrapolation method

The uncertainty of the extrapolation using groundwater response units on the final result was evaluated using scenarios. Each case study was left out of the computation once in every scenario to check the effect of dominant types of locations.

Re-assigned areas

The newly hypothetical assigned areas were calculated per scenario (Table 5.24). The scenario where case study one was left out was most relevant because in the standard condition case study one was assigned the most response units. Most response units were similar to case study five when location one was left out.

Case study	Without location one [m ²]	Without location three [m ²]	Without location four [m ²]	Without location five [m ²]	Without location six [m ²]
1	-	39.71E7	37.32E7	39.90E7	37.34E7
3	3.85E7	-	2.93E7	2.91E7	2.89E7
4	0.84E7	1.05E7	-	1.21E7	2.48E7
5	40.55E7	5.26E7	5.33E7	-	5.29E7
6	2.76E7	1.99E7	2.42E7	3.99E7	-

Table 5.24: Re-assigned sum of response unit areas per case study

Re-calculating flux contributions

The assigned areas resulted in the following contributions for the different scenarios (Table 5.25). The results were similar regardless of the scenario which is caused by the similarity between the case studies. The net extraction decreased when the first location was left out. In the other scenarios, the net extraction remained relatively the same around 21%.

Left out case study	$\sum V_{Rch}$	$\sum V_{Extr}$	$\sum V_{Ret-Flw}$	$\sum V_{Ext-Net}$	$\sum V_{Trans}$	$\Delta V_{Storage}$	$\sum V_{SSF-Perc}$
1	84%	-282%	277%	-5%	-172%	-	-7%
3	94%	-66%	44%	-22%	-179%	-	6%
4	88%	-63%	42%	-21%	-164%	-	-2%
5	85%	-24%	0%	-23%	-164%	-	2%
6	89%	-64%	42%	-22%	-168%	-	1%

Table 5.25: Re-assigned contributions for the scenarios in percentage

5.10. Groundwater trend

Groundwater trends were determined using the 22 shallow wells monitored by CIMMYT over two years. The groundwater trends were analysed by subdividing the measurements in the monsoon and dry seasons (Section 3.11). The start and end of the hydrological seasons were estimated using precipitation data (Section 3.11). The hydrological monsoon season in 2021 was estimated to start on the 4th or 5th of May and end on the 21st or 22nd of October depending on the location. The hydrological dry season subsequently began and lasted until the 18th or 26th of May or between the 20th and 26th of June. Subsequently, the monsoon started again and ended on the 12th of October 2022 for all locations. Finally, the second dry season began and lasted till the 20th of May. Notably, the dry seasons started and ended when the monsoon seasons ended and started respectively.

5.10.1. Dry season

No correlation was found between groundwater level decrease and the effective precipitation in the dry season (Figure 5.8a). This same applies to the relation between effective precipitation and the groundwater table (Figure 5.8b). Additionally, the effective precipitation and influence on the groundwater table were similar in both dry seasons for the 22 measurement points.

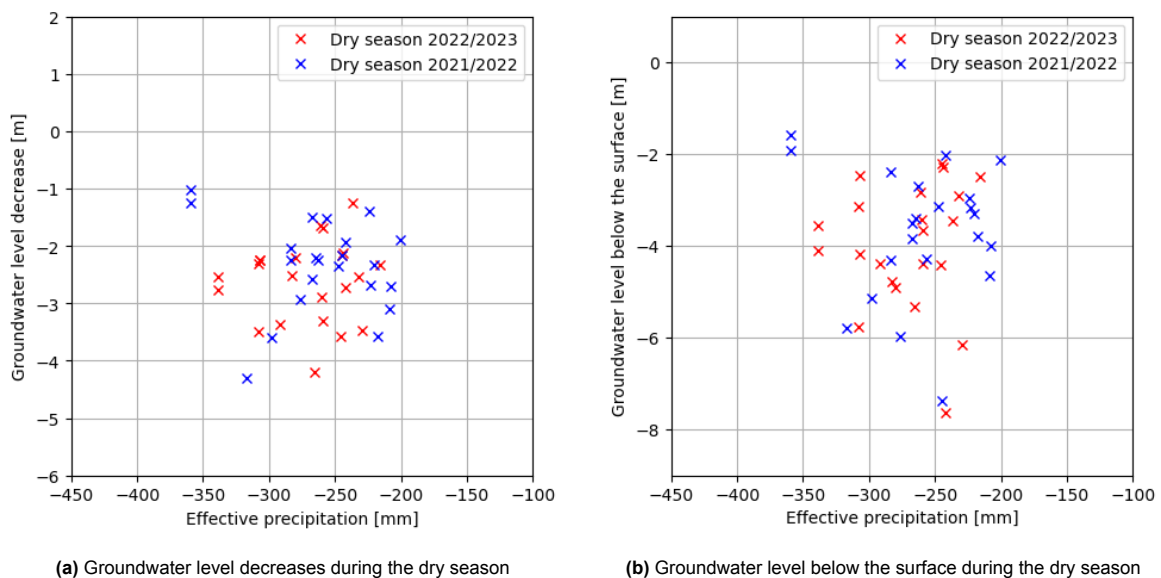


Figure 5.8: Dry season groundwater level decrease and groundwater levels at the end of the dry season plotted against precipitation minus actual evaporation for two dry seasons and 22 measurement points

5.10.2. Monsoon season

We discovered a relationship between groundwater level increase during monsoon and the effective precipitation (Figure 5.9a). The monsoon season in 2021 received more effective precipitation compared to the monsoon season in 2022. However, the groundwater level increase was approximately the same in both years when it precipitated more than approximately 600 millimetres of effective precipitation at the measurement point. The groundwater tables at the end of the monsoon season against the effective precipitation showed similar results between the years (Figure 5.9b). There is no clear difference in groundwater level between the two years. Ultimately, the groundwater recovery and groundwater levels below the subsurface were similar between the years even though the effective precipitation was significantly different. The average effective precipitation in the monsoon seasons between 2013 and 2022 was 799 millimetres in the study area (Appendix B.31) [11]. The effective precipitation sums of the monsoon seasons of 2021 and 2022 were 907 and 675 millimetres respectively [11].

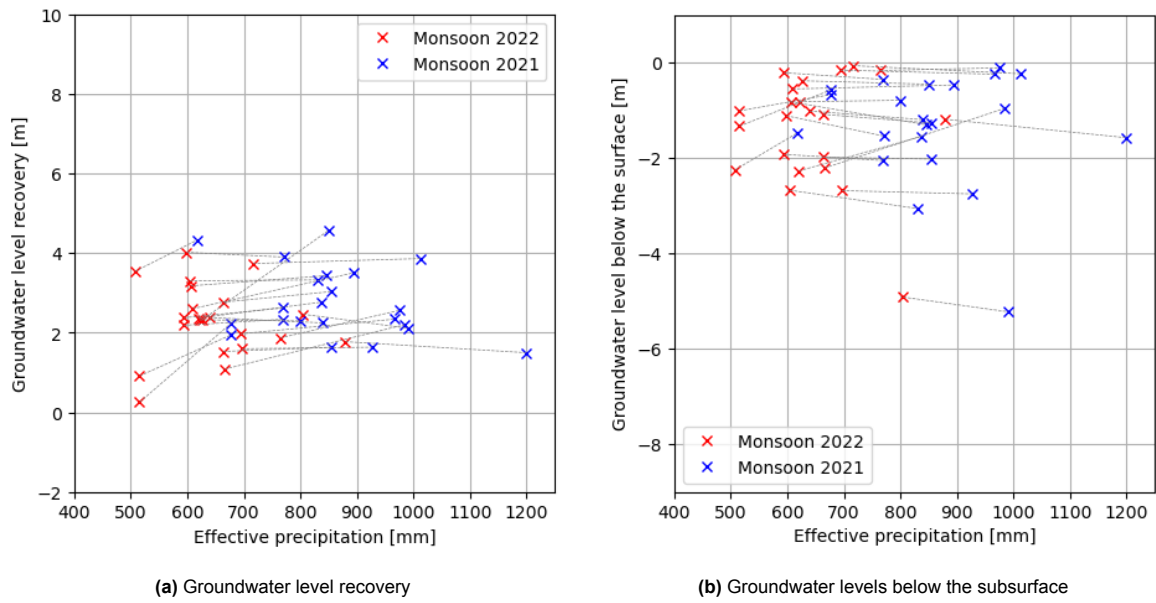


Figure 5.9: Monsoon groundwater recovery and groundwater levels below the subsurface at the end of the monsoon season plotted against precipitation minus actual evaporation for two monsoon seasons and 22 measurement points

5.10.3. Uncertainty groundwater trend

Actual evaporation data by SSEBop using VIIRS was reliable because it involves a closed energy balance. Despite that, the precipitation data was data by CHIRPS which was unreliable because it was not calibrated (section 5.1.1). The exact value of the seasonal effective precipitation might thus be different for both seasons. However, internal differences in precipitation sums are likely still reliable and these are only required to draw conclusions.

CIMMYT measured the groundwater tables approximately once every month. Due to the determination of seasons using precipitation, the season could be over at an unfortunate time between groundwater measurements. The general trend in the analysis was reliable but therefore possibly contained outliers. This could be observed in the monsoon with one outlier with more than 600 millimetres of effective precipitation (Figure 5.9a).

6

Discussion

This research aims to assess whether groundwater resources are depleting due to the intensification of groundwater extraction. In order to evaluate this, the size of flux contributions was analyzed and seasonal groundwater recoveries were researched. This chapter discusses the findings, the process itself, the assumptions, parameter influence, interpretation, limitations and recommendations.

6.1. Flux quantification per case study

We estimated the contributions of fluxes using case studies. Representative sites were selected within the study area and a conceptualization was made for every location. Using the conceptualized water balance, local fluxes were quantified within the border of each case study.

Reflection on methodology

Six representative case studies were selected in the area. These locations represented all different possible types of land cover as best as possible. A standard border for all case studies was determined via the immediate effect of the cone of depression of pumping. Subsequently, in every case study a conceptualization of the fluxes was made. The recharge flux was estimated by neglecting runoff and assuming effective precipitation was equal to recharge. The precipitation and evaporation data was obtained from the Ministry of Hydrology and Meteorology and subsequently assigned to the case studies via the inverse quadratic proportion of the distance. The Chloride Mass Balance method was also performed to compare the recharge estimates. Extractions were estimated by separately visiting the six case studies and inquiring about extractions for irrigation purposes and daily domestic extractions. Location two was neglected because the extractions in the case study were not representative. Extraction for irrigation was only present at locations four and five. Subsequently, irrigation return flow, defined as the non-evaporated irrigation water, was only present at these locations as well. Transpiration was present at all locations and estimated by remote sensing. The actual evaporation minus evaporation during precipitation and irrigation was defined as transpiration. Transpiration was verified using a derived crop factor. Storage change was determined via the specific yield and the total water table decrease between the beginning and the end of the measurement time frame. The specific yield was determined via the water table fluctuation method which required shallow and unconfined aquifers. Subsurface flow and percolation were combined into one flux because individual quantification was not possible. The combined net flux was estimated to close the groundwater balance.

Assumptions and parameter choice influence in methodology

The field locations were assumed to be representative of all types of terrain even though they were not spatially distributed. All types of terrain were included with different populations, vegetation, land uses and positions with regard to the Bhabar zone and were therefore still assumed representative.

The border of the case studies was determined by pumping tests at two case studies. This assumed that the subsurface at the other locations was similar. The resulting border of the two locations was similar even though specific yield was different between the two locations. Specific yield also differed between the other locations but this thus appears to be no issue. The border is therefore likely appropriate for all locations. Besides, representative pumping tests were not possible due to the heterogeneity of the subsurface or the absence of nearby wells.

Precipitation runoff was neglected because ground surface slopes appeared to be negligible, no sign of surface runoff was found and precipitation events were infrequent. As a result, discharge in the river was minimal which was also observed in the field.

The Chloride Mass Balance method to determine recharge did not result in reliable results. The interpolation of the method likely caused biased results due to the precipitation distribution between seasons. Furthermore, the source of chloride was assumed to be solely precipitation even though this was most certainly untrue. Conclusively, the CMB-method does not give reliable results when measurements only take place over a limited time frame. Perhaps the method does work when multiple years of measurements are done. However, this is not a certainty due to the precipitation intensity diversity between seasons and the likely pollution of the groundwater.

The inverse quadratic proportion of the distance was used to estimate the spatial distribution of evaporation and precipitation data. This design choice was judged to be the most effective method. Other methods are Thiessen Polygons, Kriging and inverse linear proportion of the distance.

The effective porosity was assumed equal to the specific yield. The specific yield and effective porosity are similar but not entirely equal. However, the difference between the values is minimal and what this difference exactly is, was not determinable. Therefore the best guess was adopting specific yield as the effective porosity.

Discussion on findings

The recharge flux via effective precipitation was on average between 1.0 and 1.2 mm per day at the locations. This sounds like a reasonable estimate. Even when evaporation during precipitation was drastically increased, the recharge did not significantly change. At every location, the flux was approximately as big. However, at location three the flux was proportionally less significant because of the larger storage loss.

Domestic extractions in the study area were per person approximately equal in all case studies. The contribution of these domestic extractions was small compared to the other present fluxes. However, if irrigation was present in the case study, the extractions increased drastically. The flux altered again when irrigation return flow was included to estimate net extraction. Most irrigated water returned to the subsurface. This was due to the timing of irrigation and the quick infiltration rates of the water. The farmers irrigated in the early morning and during the night. Likely, most farmers irrigate during these times because of the temperatures during the day. This is beneficial for groundwater resources because most water returns to the subsurface.

Transpiration was the largest flux in every case study during the measurement time frame (Table 5.19). The flux was the dominant driver for groundwater table decrease during the dry season. Future climate change will strengthen evaporation which increases potential transpiration and evaporation during irrigation and precipitation, ultimately causing accelerated groundwater depletion.

The subsurface flow- and percolation fluxes were directed inward and outward depending on the field location. The net subsurface flow and percolation flux was slightly directed outwards at location five even though a substantial amount of groundwater was extracted for irrigation at location five during the measurement time. This would generally lead to subsurface flow towards location five. However, the subsurface flow was outwards. Basically, the subsurface flow- and percolation flux outwards of location five suggests that the net extraction was significantly lower than the total extraction. Thus confirming actual evaporation during irrigation was not significant. The flux was uncertain because the determination of specific yield was an uncertain process. The flux consists of percolation and subsurface flow however, the flux was mostly gaining water at the locations. This is remarkable because percolation loses water to deeper layers. The general trend at the five locations was thus that the subsurface flow

has on average a replenishing effect on the groundwater resources. This is in line with the expected lateral recharge replenishment from the Bhabar zone (Section 2.1).

6.2. Extrapolation of case studies to study area using GRU

Local fluxes in the case studies were extrapolated using groundwater response units. This resulted in a contribution per flux in the total study area.

Reflection on methodology

The entire study area was divided into multiple groundwater response units with all approximately the same area as the case studies. All groundwater response units and case studies were assigned values for recharge, evaporation and extraction determined with remote sensing. The response units were allocated to one of the five case studies by comparing the response units with the case studies using the characteristic recharge, evaporation and extraction values and selecting the most similar location. Subsequently, the areas of the response units were summed for every case study and multiplied by the fluxes to get total representative fluxes for the study area.

Assumptions and parameter choice influence in methodology

The response units were assumed to be representative of the type of terrain. They were assumed to be extrapolatable to the whole study area because no unreasonable fluxes were found. Furthermore, because the case studies were given different magnitudes by the response units no type of terrain got undeserved too great of an importance.

Spatial CHIRPS precipitation data in combination with NVDI data was assumed to be representative of recharge. The CHIRPS precipitation data was not reliable as was discussed earlier because of the lack of calibration. However, the internal differences in CHIRPS precipitation are likely correct. Only the internal differences were important because the response units were normalized. Therefore, the CHIRPS precipitation data could be used to characterize precipitation per response unit. NVDI is positively correlated with infiltration rate but is not the only influencing factor for infiltration. For instance, the porosity of the soil, the macrostructure of the soil and the depth of the groundwater are crucial as well. However, these values were not quantifiable per response unit due to the limited subsurface information in the study area. The NVDI was therefore assumed to solely give representative estimates for infiltration.

The population was assumed to be correlated with extraction. In areas with a larger population, more domestic extractions were expected. However, more population does likely not lead to more extraction for irrigation because more population in an area means less room for farming lands. Therefore, for irrigation extraction likely a smaller population would increase the chance for significant irrigation amounts as was seen at location five. The exact population versus extraction curve is thus not known. However, by assuming the case studies had a representative extraction per population, the extractions of the case studies were still estimated as best as possible with the limited data.

Discussion on findings

The extrapolated fluxes showed a stable value for recharge. The recharge positively contributed 88% of the storage change. This was a stable value because in the scenarios the recharge contribution was a maximum of 6% different. Clearly, recharge is an important flux. When in the future climate change alters the precipitation intensity, runoff could become significant. Ultimately, this would decrease recharge and put the groundwater resources under pressure.

Extractions were 62% of the decreased volume in the whole study area. However, 40% of the extraction volume returned back to the subsurface. This was partly attributed to the minimal evaporation during irrigation at both locations by the low solar radiation during irrigation hours. The net extraction contributed 21% of the storage loss in the total study area which was a relatively stable value in the scenarios. The net extraction fluctuated with 2% in the scenarios or was insignificant compared to the other fluxes.

Lateral recharge via the Babbar zone North of the study area is considered one of the main groundwater

recharge factors. Quantifying exact values for lateral flow was not possible in this approach. However, it is visible that individual locations get recharged by the lateral flow if limited extractions are present in the case study. Mostly locations four and six got heavily recharged by subsurface flow even though there were median extractions and the neighbouring areas were similar. This suggests the subsurface flow is recharging the study area which is visible unless local heavy extractions compromise the results. This occurred in case study three where the irrigation well was often used just outside the case study border causing heavy outward subsurface flows. Ultimately, the subsurface flow does replenish the groundwater table. However, as seen in the results, the combined net subsurface flow and percolation flux in the upper aquifer flows net outward of the study area. Because subsurface flow was positively net contributing, the net percolation could be substantially transporting water to a deeper layer. This research focused on shallow unconfined aquifers. However, around 36% of the inhabitants have deeper wells (Section 2.3). This deep extraction might lead to decreasing pressure in lower aquifers over time. Eventually, this would increase the percolation from the shallow subsurface to the deeper aquifer. Transpiration accounted for 165% of the groundwater storage loss. This number stayed relatively constant with different scenarios and was therefore a stable number. Thus the transpiration flux was approximately 8 times bigger than the groundwater resource loss by net extraction. Additionally, evaporation occurred in the time frame as precipitation and irrigation evaporation. Together this shows how insignificant the net extraction is compared to the contribution of evaporation in the study area.

6.3. Groundwater resources depletion

To estimate groundwater resource depletion, the effective precipitation in the region was compared to the groundwater table recovery and level after the seasons. Relations between the two would suggest potential depletion.

Reflection on methodology

For the monsoon and the dry season, the effective precipitation was compared to the corresponding groundwater table recovery. Extractions played an insignificant role in the dry season if there was a relation between groundwater decrease and effective precipitation. Groundwater resources were not recovered in the monsoon season if effective precipitation differences between the two years led to different recoveries. Additionally, the groundwater level at the end of the seasons was compared to the effective precipitation. For the dry season, this was used to potentially verify the insignificant role of extractions. For the monsoon season, it was used to check whether the groundwater resources were not replenished at a deeper depth. Lastly, the precipitation of the last 10 years was estimated via CHIRPS data to check whether the last two years were not out of the ordinary.

Assumptions and parameter choice influence in methodology

CHIRPS data was assumed to be representative. This is a fair assumption because the precipitation relative between locations is important and not the exact value. However, when an exact value is wanted it would be best to measure precipitation using weather stations and compare the effective precipitation and groundwater recovery in the same matter as was done in this research. Thus, the precipitation threshold of 600 millimetres is not reliable but the drawn conclusion using this threshold can be relied on.

Due to the hydrological determination of the seasons and the limited frequency of groundwater table measurements, the groundwater table could not have been at its lowest or highest point at the transition between the next season. This caused some uncertainties and outliers but the general picture of the relation and thus conclusions still remains clear.

Discussion on findings

There is no clear relation between effective precipitation and groundwater level increase in the dry season. This suggested that flux contributions are not only dominated by precipitation and evaporation. Extraction and subsurface flow also contribute to the local groundwater table fluctuation in the dry season. However, the regional role of extraction was relatively insignificant as was concluded in

the previous paragraph. Furthermore, the effective precipitation and groundwater level table decrease were similar for both seasons. This means that there was not a sudden significant general increase in subsurface flow or extraction between the two years.

The sum of effective precipitation was 675 millimetres in the monsoon season in 2021 using CHIRPS. The effective precipitation was 907 millimetres during the monsoon season in 2022. The latter is significantly more. However, the groundwater increase was approximately the same between the seasons. Locations that received around 600 millimetres or more of effective precipitation had a similar groundwater level increase over the two years. This same applies to the groundwater levels at the end of the monsoon period. Conclusively, the upper aquifers are replenished if the effective precipitation in a year is around 600 millimetres or more and the groundwater table where resources are potentially replenished does not deepen over the years. In the last ten years, effective precipitation was once below this threshold, in 2015. Nonetheless, the average effective precipitation over the last ten years was 799 millimetres. Therefore, nothing suggests that groundwater resources in the upper aquifers are currently depleting.

6.4. Limitations and recommendations

The case studies were assumed to be representative even though there were only six and they were not spatially distributed. This was for a number of reasons. First of all, there was limited time to install and revisit sites. The travel time would drastically increase by spreading the case studies more, especially considering the accessibility of most rural areas in the Banke district and the state of the roads. Secondly, limited resources made only six groundwater time series possible. Lastly, completely abandoned wells where the surroundings matched the different types of terrain were difficult to find in an unknown region. There is a possibility that the six case studies had similar fluxes which were not representative of the whole region. This potentially gave a distorted picture of the groundwater flux distribution. Therefore, to strengthen the reliability of the results it would be beneficial to increase the number and spatial distribution of the case studies.

This research focused on the upper aquifer. However, because of the intense deep extractions, there could also be a building depletion in deeper layers. This depletion would result in increased percolation and eventually deplete the upper aquifer as well. Percolation could be substantial as observed in this research, but we did not isolate the percolation flux therefore exactly quantifying this flux is impossible. CIMMYT is already observing five deep wells in the study area. Unlike the shallow wells, no full groundwater recovery can be distinguished after the monsoon season for the deep wells (Figure 6.1). Therefore, we recommend expanding the number of monitored deep wells and performing local research in deep well extractions to see if these limited numbers of wells are representative.

Three weathering stations measured precipitation close to the study area. Furthermore, two weather stations measured the required parameters for potential evapotranspiration. Therefore, spatial interpolation of precipitation and evaporation data was required. This decreased the reliability of the data. Additionally, both precipitation and evaporation data contained multiple missing days. This unmistakably decreased the reliability of the recharge flux using effective precipitation. The reliability of the flux could be strengthened if there was more spatial data. For instance, there were 4 unused meteorological institutions close to the area which could also measure data. Additionally, the documentation of data by the meteorological stations could be updated to miss fewer days of data.

The recharge determined via the CMB method did not coincide with the results via the meteorological stations. It would be interesting to see the results of longer-term chloride observations with a bigger spatial distribution in future research. However, there is a great possibility that the results will again be unsatisfactory due to the number of unjustified assumptions.

We also used precipitation and actual evaporation data from satellite products. These satellite products have limited resolutions. For instance, VIIRS ET SSEBop data has a spatial resolution of 1000 meters and CHIRPS data even has a resolution of 4800 meters. The resolution surface is respectively 125 and 2900 times bigger than the size of the areas of the case studies. Likely, field location six was assigned a higher crop factor than expected due to this resolution issue. The issue could be solved by larger response units in future research. However, this would also increase the necessary local resources. Irrigation occurred at beneficial times during the measurement time frame. The farmers at locations four and five both irrigated in the evening, night or early morning. During these times the potential

evaporation was at its lowest. It is likely that not all farmers irrigate during these times. Therefore, the real evaporation during irrigation in the total region is potentially larger. The irrigation moment could be a question in the next questionnaire by CIMMYT. This way it can be researched if all farmers have the same timing as the farmers at locations four and five. Otherwise, awareness about irrigating outside of high radiation hours could be increased in the region.

Another limitation of the study was the amount of farming during the measurement period. In the measurement time frame, the majority of farmers did not farm crops anymore due to the heat. They recently harvested their maize and waited for the monsoon to farm rice. Therefore, the extraction due to irrigation could have been underestimated. Performing the same research at another time frame in the dry season would be interesting for future studies.

The potential depletion of groundwater resources was investigated by looking at the sum of effective precipitation in the monsoon seasons. However, the distribution of the effective precipitation was not examined. A precipitation event with high intensity leads in general to less infiltration because more water runs off to rivers. Although the general trend was so clear, this could potentially have an effect. The monsoon season in 2023 could be included in the analysis to strengthen reliability. This can be done as soon as measurements of precipitation, evaporation and the groundwater table of the monsoon season 2023 are ready. The hypothesis of non-depleting groundwater resources is strengthened with an extra sample year.

This study accurately estimated potential depletion and the contribution of fluxes to the groundwater table decrease in the dry seasons. However, a general regional groundwater flow trend was not distinguishable. Whether upstream groundwater resources are heavily recharged by lateral flow and whether this decreases downstream was not determined. A lateral subsurface flow flux from the Banke district to India in the South was thus not quantifiable either. When these regional subsurface flow patterns are desired, we recommend building a groundwater model regardless of the uncertainties accompanying it.

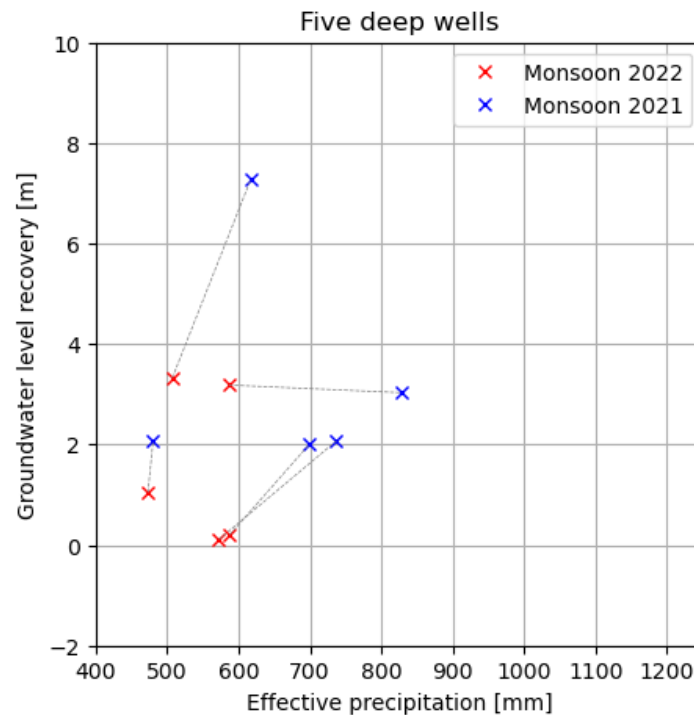


Figure 6.1: The monsoon groundwater recovery at the end of the monsoon season against the effective precipitation for the five deep wells monitored by CIMMYT

Summary and conclusions

Groundwater extraction increased significantly in the last decade. Together with climate change this potentially puts groundwater resources at risk. The Banke district in the Terai is one of the most critical areas in Nepal regarding socioeconomic indicators and is therefore vulnerable to depletion. This study assessed the current availability of groundwater resources in this area. Specifically, we researched the impact of extraction on the potential depletion during the most critical dry season. This was done by investigating the different fluxes that influence the groundwater table and observing groundwater trends. The research question to answer was formulated as follows:

“Are the groundwater resources in the agricultural and urban development areas of the Banke district depleting due to the intensification of extractions from the groundwater?”

This research question consists of two parts.

- “How can the fluxes in the area be quantified and what is the proportional contribution of extractions during the dry season?”
- “How well are groundwater resources replenished after the monsoon seasons?”

Field research at six case studies was performed to obtain insight into local fluxes influencing the groundwater table. Extraction volumes were estimated by interviewing the local residents of these field locations. Furthermore, recharge and evaporation were estimated using data from meteorological measuring stations and satellite products. Potential irrigation patterns and their corresponding net extractions were inquired from local farmers. The groundwater storage changes between the 24th of March and 4th of June were determined using a time series of the groundwater table. Water pressure devices measured the hourly groundwater tables of six representative locations. A specific yield was extracted from the time series to calculate the groundwater volume of the decreased groundwater table. Finally, subsurface flow and percolation were merged as a combined lateral and vertical groundwater flow flux and considered to be closing the groundwater balance. Subsequently, the fluxes were extrapolated using groundwater response units. The response units were delineated using population data and actual evaporation and precipitation were extracted from satellite products. By giving similarity scores the response units were assigned to case studies. The groundwater response units were treated the same as their most similar case study. In the end, transpiration was the most dominant driver for groundwater table decrease during the dry season. However, surface evaporation fluxes during irrigation and precipitation were not significant. High percentages of precipitation and irrigated water therefore reached the groundwater table as recharge and irrigation return flow respectively. The net surface flow and percolation flux varied over the study area but led to a small net loss in the whole area. Ultimately, the net extraction in the area contributed to 21 % of the total groundwater depletion

during the dry season.

Twenty-two shallow wells in the area were monitored approximately every month for over two years by CIMMYT. Thereby, they measured the groundwater levels of two monsoon and dry seasons. The groundwater increase and groundwater levels were compared to the effective precipitation in both seasons to get an insight into the effect of seasonal precipitation. No relation was found between effective precipitation and groundwater recovery in the dry season. This suggests that fluxes like extraction could locally play significant roles. No heavily enhanced extraction or subsurface flow can be found between the years either. In the monsoon season, no difference was seen between the years regarding groundwater recovery. Even though, the effective precipitation between the years was significantly different. This suggested that there is a certain current threshold of effective precipitation where the groundwater resources are replenished again. The average precipitation of the last ten years was significantly above this threshold. Ultimately, this means that the groundwater resources are replenished during the monsoon seasons.

Conclusively, groundwater resources in the agricultural and urban development areas of the Banke district do not seem to be depleting due to the intensification of extractions from the groundwater. Specifically, other fluxes than extraction play a more significant role in the groundwater balance during the dry season. Furthermore, currently, the monsoon season is ample possible to replenish the decreased volume during the dry season.

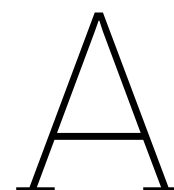
References

- [1] M Ali and S Mubarak. "Approaches and methods of quantifying natural groundwater recharge—a review". In: *Asian Journal of Environment & Ecology* 5.1 (2017), pp. 1–27.
- [2] Richard G Allen et al. "Crop evapotranspiration-Guidelines for computing crop water requirements-FAO Irrigation and drainage paper 56". In: *Fao, Rome* 300.9 (1998), p. D05109.
- [3] Mark Bakker and Vincent Post. *Groundwater Modeling*. CRC Press, Jan. 2022.
- [4] Christopher Bowden, Timothy Foster, and Ben Parkes. "Identifying links between monsoon variability and rice production in India through machine learning". In: *Scientific Reports* 13.1 (Feb. 2023). DOI: 10.1038/s41598-023-27752-8. URL: <https://www.nature.com/articles/s41598-023-27752-8.pdf>.
- [5] Il-Moon Chung et al. "Estimating groundwater recharge in the humid and semi-arid African regions: review". In: *Geosciences Journal* 20.5 (Sept. 2016), pp. 731–744. DOI: 10.1007/s12303-016-0001-5.
- [6] Ian D. Clark and Peter Fritz. *Environmental Isotopes in Hydrogeology*. CRC Press, July 1997.
- [7] Intergovernmental Panel on Climate Change. *Climate Change 2022*. Tech. rep. ISBN 978-92-9169-161-6. 2022. URL: <https://www.ipcc.ch/report/ar6/wg2/>.
- [8] Raoul A Collenteur et al. "Estimation of groundwater recharge from groundwater levels using nonlinear transfer function noise models and comparison to lysimeter data". In: *Hydrology and Earth System Sciences* 25.5 (2021), pp. 2931–2949.
- [9] Lassâad Dassi. "Use of chloride mass balance and tritium data for estimation of groundwater recharge and renewal rate in an unconfined aquifer from North Africa: a case study from Tunisia". In: *Environmental Earth Sciences* 60.4 (July 2009), pp. 861–871. DOI: 10.1007/s12665-009-0223-1. URL: <https://doi.org/10.1007/s12665-009-0223-1>.
- [10] Frank De Olde. *EC-tabel schetst zouttolerantie - Boeren Meten Water*. Mar. 2022. URL: <https://boerenmetenwater.nl/ec-tabel-schetst-zouttolerantie/>.
- [11] Kauê de Sousa et al. "chirps: API Client for the CHIRPS Precipitation Data in R". In: *The Journal of Open Source Software* 5.51 (2020), p. 2419. DOI: 10.21105/joss.02419. URL: <https://doi.org/10.21105/joss.02419>.
- [12] Jacobus J. De Vries and Ian Simmers. "Groundwater recharge: an overview of processes and challenges". In: *Hydrogeology Journal* 10.1 (Jan. 2002), pp. 5–17. DOI: 10.1007/s10040-001-0171-7.
- [13] K Devito et al. "A framework for broad-scale classification of hydrologic response units on the Boreal Plain: Is topography the last thing to consider?" In: *Hydrological Processes: An International Journal* 19.8 (2005), pp. 1705–1714.

- [14] Praval Devkota et al. "Land use land cover changes in the major cities of Nepal from 1990 to 2020". In: *Environmental and sustainability indicators* 17 (Feb. 2023), p. 100227. DOI: 10.1016/j.indic.2023.100227. URL: <https://doi.org/10.1016/j.indic.2023.100227>.
- [15] DHM. URL: <https://www.dhm.gov.np/climate-services/monsoon-onset-and-withdrawal>.
- [16] Petra Döll and Stefan Siebert. "Global modeling of irrigation water requirements". In: *Water resources research* 38.4 (2002), pp. 8–1.
- [17] Facebook Connectivity Lab and Center for International Earth Science Information Network - CIESIN - Columbia University. 2016. URL: <https://data.humdata.org/dataset/nepal-high-resolution-population-density-maps-demographic-estimates>.
- [18] Costantino Faillace. "Simple and low-cost technology for irrigation from shallow aquifers in the Western Terai, Nepal". In: *International Symposium on Engineering Geology, Hydrogeology, and Natural Disasters with Emphasis on Asia: 28-30 September 1999, Kathmandu, Nepal*. Vol. 22. Nepal Geological Society. 2000, pp. 327–334.
- [19] *Flora of Nepal - Country Information - Land and Climate - Seven zones*. URL: <http://www.floraofnepal.org/countryinformation/landandclimate/sevenzones>.
- [20] Luke Flores and Ryan T. Bailey. "Review: Revisiting the Theis solution derivation to enhance understanding and application". In: *Hydrogeology Journal* (Aug. 2018). DOI: 10.1007/s10040-018-1843-x. URL: <https://doi.org/10.1007/s10040-018-1843-x>.
- [21] Wolfgang-Albert Flügel. "Combining GIS with regional hydrological modelling using hydrological response units (HRUs): An application from Germany". In: *Mathematics and Computers in Simulation* 43.3-6 (1997), pp. 297–304.
- [22] GISGeography. "What is NDVI (Normalized Difference Vegetation Index)?" In: *GIS Geography* (July 2023). URL: <https://gisgeography.com/ndvi-normalized-difference-vegetation-index/>.
- [23] SO Grinevskii and SP Pozdnyakov. "Principles of regional estimation of infiltration groundwater recharge based on geohydrological models". In: *Water resources* 37 (2010), pp. 638–652.
- [24] Richard W Healy. *Estimating groundwater recharge*. Cambridge university press, 2010.
- [25] Richard W Healy et al. *Water budgets: foundations for effective water-resources and environmental management*. Vol. 1308. US Geological Survey Reston, Virginia, 2007.
- [26] Richard W. Healy and Peter G. Cook. "Using groundwater levels to estimate recharge". In: *Hydrogeology Journal* 10.1 (Jan. 2002), pp. 91–109. DOI: 10.1007/s10040-001-0178-0. URL: <https://doi.org/10.1007/s10040-001-0178-0>.
- [27] Industrybuying.com. *Kirloskar 6 HP Borewell Submersible Pump Set 100HHN-0606*. URL: <https://www.industrybuying.com/borewell-submersible-pumps-kirloskar-PU.AG.B0.289194/>.
- [28] *Inequities in household water consumption in Kathmandu, Nepal*. Dec. 2017. URL: <https://www.globalwaterforum.org/2017/12/04/inequities-in-household-water-consumption-in-kathmandu-nepal/>.
- [29] G. P. Kruseman and N. A. De Ridder. *Analysis and evaluation of pumping test data*. Jan. 1990.

- [30] Sanjeet Kumar and Ashok Mishra. "Critical erosion area identification based on hydrological response unit level for effective sedimentation control in a river basin". In: *Water Resources Management* 29 (2015), pp. 1749–1765.
- [31] *Land use Geo-Portal*. URL: <http://nlupgeoportal.gov.np/>.
- [32] Gunther Liebhard et al. "Estimation of evaporation and transpiration rates under varying water availability for improving crop management of soybeans using oxygen isotope ratios of pore water". In: *International Agrophysics* 36.3 (July 2022), pp. 181–195. DOI: 10.31545/intagr/150811. URL: <https://doi.org/10.31545/intagr/150811>.
- [33] André Geraldo de Lima Moraes et al. "Steady infiltration rate spatial modeling from remote sensing data and terrain attributes in southeast Brazil". In: *Geoderma Regional* 20 (2020), e00242.
- [34] Mike Listman. *Scientist urges upgrades to monitor groundwater use for agriculture in low-income countries*. Sept. 2022. URL: <https://www.cimmyt.org/news/scientist-urges-upgrades-to-monitor-groundwater-use-for-agriculture-in-low-income-countries/>.
- [35] Murilo Cesar Lucas et al. "Evaluation of remotely sensed data for estimating recharge to an outcrop zone of the Guarani Aquifer System (South America)". In: *Hydrogeology Journal* 23.5 (Mar. 2015), pp. 961–969. DOI: 10.1007/s10040-015-1246-1.
- [36] Jean-Christophe Maréchal et al. "Combined estimation of specific yield and natural recharge in a semi-arid groundwater basin with irrigated agriculture". In: *Journal of Hydrology* 329.1-2 (Sept. 2006), pp. 281–293. DOI: 10.1016/j.jhydrol.2006.02.022. URL: <https://doi.org/10.1016/j.jhydrol.2006.02.022>.
- [37] Andrew M. McCallum et al. "River-aquifer interactions in a semi-arid environment stressed by groundwater abstraction". In: *Hydrological Processes* 27.7 (Apr. 2012), pp. 1072–1085. DOI: 10.1002/hyp.9229. URL: <https://doi.org/10.1002/hyp.9229>.
- [38] Abhijit Mukherjee. *Groundwater of South Asia*. Springer, June 2018.
- [39] *Nepal - Countries and Regions - IEA*. URL: <https://www.iea.org/countries/nepal>.
- [40] Roger Parsons and Johan Wentzel. *Groundwater resource directed measures manual*. Water Research Commission (WRC), 2007.
- [41] Suraj Kumar Singh and A. K. Pandey. "Geomorphology and the controls of geohydrology on waterlogging in Gangetic Plains, North Bihar, India". In: *Environmental Earth Sciences* 71.4 (Feb. 2014), pp. 1561–1579. DOI: 10.1007/s12665-013-2562-1. URL: <https://doi.org/10.1007/s12665-013-2562-1>.
- [42] Prajwol Babu Subedi et al. "Mapping of major land use Land cover dynamics and its driving factors: A case study of Nepalgunj Sub-Metropolitan City, Banke, Nepal". In: *Indonesian Journal of Social and Environmental Issues* 3.1 (Apr. 2022), pp. 67–80. DOI: 10.47540/ijsei.v3i1.468. URL: <https://doi.org/10.47540/ijsei.v3i1.468>.
- [43] C Sudhakar Reddy et al. "Quantifying nationwide land cover and historical changes in forests of Nepal (1930–2014): Implications on forest fragmentation". In: *Biodiversity and Conservation* 27 (2018), pp. 91–107.
- [44] *The Soils of Nepal*. Springer Nature (Netherlands), Jan. 2021. DOI: 10.1007/978-3-030-80999-7. URL: <https://doi.org/10.1007/978-3-030-80999-7>.

- [45] C.V. Theis. "The relation between the lowering of the Piezometric surface and the rate and duration of discharge of a well using ground-water storage". In: *Transactions* 16.2 (Jan. 1935), p. 519. DOI: 10.1029/tr016i002p00519. URL: <https://doi.org/10.1029/tr016i002p00519>.
- [46] R. M. Tuladhar. *Shallow Ground Water Resources of the Terai Banke District Mid Western Development Region Nepal*. Tech. rep. NEP/86/025. Mar. 1992.
- [47] Marcelo Varni et al. "Application of the water table fluctuation method to characterize groundwater recharge in the Pampa plain, Argentina". In: *Hydrological Sciences Journal-journal Des Sciences Hydrologiques* 58.7 (Oct. 2013), pp. 1445–1455. DOI: 10.1080/02626667.2013.833663. URL: <https://doi.org/10.1080/02626667.2013.833663>.
- [48] Yoshihide Wada. "Modeling groundwater depletion at regional and global scales: Present state and future prospects". In: *Surveys in Geophysics* 37.2 (2016), pp. 419–451.
- [49] Yoshihide Wada and Marc FP Bierkens. "Sustainability of global water use: past reconstruction and future projections". In: *Environmental Research Letters* 9.10 (2014), p. 104003.
- [50] Yoshihide Wada et al. "Global depletion of groundwater resources". In: *Geophysical research letters* 37.20 (2010).
- [51] Department of Water Resources and Irrigation. *Irrigation Master Plan 2019*. Tech. rep. 2019. URL: <https://dwri.gov.np/files/document/20210222080845.pdf>.
- [52] William W. Woessner. *3.6 Specific yield and specific retention*. Aug. 2020. URL: <https://books.gw-project.org/hydrogeologic-properties-of-earth-materials-and-principles-of-groundwater-flow/chapter/specific-yield-and-specific-retention/>.
- [53] Willem J Zaadnoordijk et al. "Automated time series Modeling for piezometers in the National Database of The Netherlands". In: *Groundwater* 57.6 (2019), pp. 834–843.
- [54] Xi Zhang et al. "Study on groundwater recharge based on chloride mass balance and hydrochemistry in the irrigated agricultural area, North China Plain". In: *Environmental Earth Sciences* 82.3 (Jan. 2023). DOI: 10.1007/s12665-022-10682-5. URL: <https://doi.org/10.1007/s12665-022-10682-5>.



Appendix A: Additional information

A.1. CIMMYT

CIMMYT is an international organisation that focuses its efforts on aiding developing countries. Their attention centres on farming, mainly wheat and maize. Their primary focus in Nepal is to a great extent on the specified study area. This research is at their request.

Data by CIMMYT

CIMMYT has been monitoring multiple wells in the study area at an approximate one-month interval. In the study region, 22 shallow wells (Figure B.10) have been monitored for over two years. Additionally, 5 deep wells have been monitored. The median of well depths by participants of CIMMYTs questionnaire was approximately 20 metres (Figure A.1).

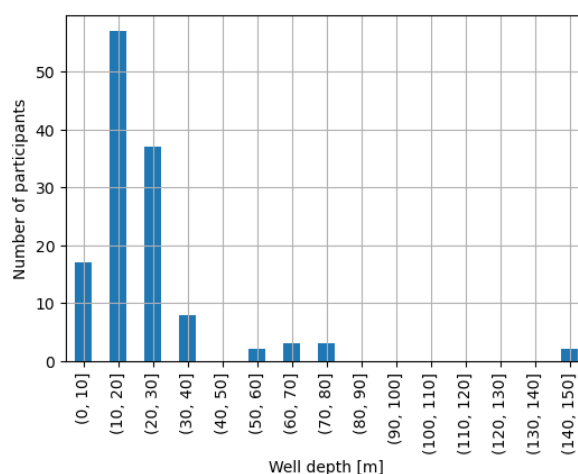


Figure A.1: Well depths occurrences by the questionnaire from CIMMYT

A.2. Meteorological station data

Changes made to precipitation data

- Precipitation was given in UTC and therefore had an offset of 5:45 hours. It was assumed the offset was 6 hours.
- Single missing values in a sequence of zero precipitation were assumed 0.
- All values from the meteorological station Khajura Khurda were missing between 13/04/2023 at 05:00 and 16/04/2023 at 14:00. The values were adopted from Nepalgunj Airport because that was the closest station.
- Between 28/04/2023 at 06:00 and 02/05/2023 at 10:00 all values were missing for all stations. Station Khajura copied values from CHIRPS data. During those days it precipitated for 11 millimetres according to CHIRPS data. This was most likely between the 30th between 05:00 and 08:00 according to the time series at Khajura Khurda (case study one). Therefore, the daily CHIRPS precipitation was uniformly distributed over these four hours. Based on CHIRPS data, at Nepalgunj Airport and Shyano Chepang it precipitated 10.5 millimetres and 14.5 millimetres respectively. The timing was copied from Khajura Khurda because no time series were measured so close to a weather station as Khajura Khurda which makes the timing at Khajura the most reliable.
- Values from 21/04/2023 between 07:00 and 25/04/2023 at 00:00 were missing for Nepalgunj Airport and were taken from Khajura Khurda because that is the closest station.
- Values from 21/04/2023 at 07:00 till 27/04/2023 00:00 were missing for Shyano Chepang and were adopted from Khajura Khurda.

Precipitation data selection per location

- The data of Khajura Khurda was entirely used for location one due to its proximity within a kilometre of the station.
- Location two lies directly in between the Airport station and Shyano station. The data for location two was therefore a combination of those two stations in quadratic inverse proportion to the distance which was 12 and 16 km respectively. Station Khajura Khurda was not used for this data.
- The Nepalgunj Airport weather station was most relevant for locations three and four. The other stations were in approximately the same direction and farther than the Nepalgunj Airport station and were thus neglected.
- Data at location five was determined by weathering stations Shyano Chepang and Khajura Khurda because case study five lays directly between those two stations. This was calculated quadratically inversely proportional to the distances which were 9 and 19 km respectively. The airport weather station was ignored for this location.
- The data for location six was approximated by a combination of the stations Airport and Shyano and have distances of 13 and 16 km respectively.

Changes made to evaporation data

- Daily sunshine hour data was received as hourly data and resampled to daily for Nepalgunj Airport.
- Relative humidity by measuring station Khajura Khurda was given at 3 AM and 12 AM, which was assumed to be the highest and lowest of the day.
- Relative humidity was measured four times per day by measuring station Nepalgunj Airport, namely 3, 6, 9 and 12 AM. The minimum and maximum of every day was calculated regardless of the exact time.

- Maximum air temperature was measured daily at 12 AM and minimum air temperature at 3 AM by the weathering stations of Nepalgunj Airport and Khajura.
- Solar radiation is in UTC and therefore has an offset of 5:45 hours. It is assumed the offset was 6 hours.
- Solar radiation data from Khajura Khurda was missing between the 13th of April at 1 PM until the 16th of April at 1 PM. The data from Nepalgunj Airport was copied during those days.
- Solar radiation data from Khajura Khurda and Nepalgunj Airport was missing between the 28th of April and 2nd of May. The radiation on the 27th of April was copied for all those dates.
- Missing solar radiation values in the night were assumed to be zero.
- Single missing hours were filled in by linearly interpolating.

Evaporation data selection per location

- The data of Khajura Khurda was fully used for location one.
- Location two is 14 kilometres from Khajura Khurda and 12 kilometres from Airport. The quadratic inverse distance was used to calculate the weight of each station.
- Locations three and four were one-on-one copied from Nepalgunj Airport.
- Location five is 19 kilometres from both stations and was assumed to be the average of the two data sets.
- Location six is 15 kilometres from Khajura Khurda and 13 kilometres from Nepalgunj Airport. The quadratic inverse distance was used to calculate the proportion of each station.

A.3. Pastas Python package

Pastas is a Python package which simulates a time series based on an evaporation data set, optional irrigation data set, precipitation data set and measurements [8]. Precipitation and evaporation data sets are simulated as gamma functions and extractions as the Hantush function. The parameters required for these functions are fitted using least squares to the observed data. The fitted model parameters A , n and a are used to fit the gamma function, the parameter f is the crop factor, the trend parameters are to fit the trend, α and β represent parameters to fit the noise model and parameter d is the constant base level of the simulation. The specific yield is a parameter that is not reported but can be extracted from the simulated data set.

The Pastas package does not make a distinction between transpiration or evaporation during irrigation and recharge. It uses the crop factor with the potential evapotranspiration over the whole time series. Even though, the evaporation during precipitation and irrigation is higher, namely the full potential evapotranspiration. The precipitation and irrigation depth were therefore adjusted with the inverse of the crop factor times the potential evapotranspiration. Subsequently, the correct evaporation was used when the Pastas package fits the crop factor with the potential evaporation to the time series.

A linear trend was added to the fit to represent the additional groundwater table decrease by domestic extraction, net subsurface flow and percolation during the dry season. The fit does not perfectly capture the observed data because hourly fluxes of for instance extractions and subsurface flow were unknown. Fortunately, it is only important that recharge events are fitted well. Specific yield is not one of the fitted parameters but can be determined with the WTF-method using the simulated recharge contribution. The differences between the lowest and highest points were extracted at every location. This sometimes included extrapolation when the low point was not reached yet. The difference was only calculated if the high point was at a local high and not increasing.

A.4. Percentile modelling choice

Uncompensated and compensated occurrences of data were visualized without the 1st percentile and 99th percentile. This is because the lowest and highest bins had significantly more data points than the other bins. Therefore, the distribution of the middle part would not have been visible. Note, this is

also why the count on the y-axis varies per category. Before, normalized population occurrences were skewed on the low side between 0 and 0.1 (Figure A.2). The occurrences are more uniformly spread by removing the 2.5% percentiles. Secondly, normalized recharge was highly concentrated around 0.7 (Figure A.3). Recharge is more uniformly spread by removing the percentiles. Lastly, Evaporation occurrences were mostly located around 0.5 and are much more uniform by removing the percentiles (Figure A.4). It is important to make the data more uniform because the similarity score calculates an absolute distance. Uniform-like distributions are beneficial to prevent one parameter from dominating.

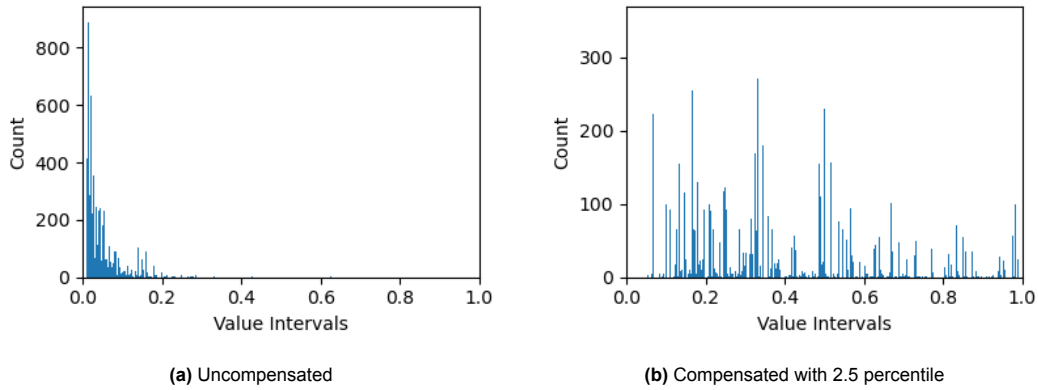


Figure A.2: Normalized population occurrences in response units

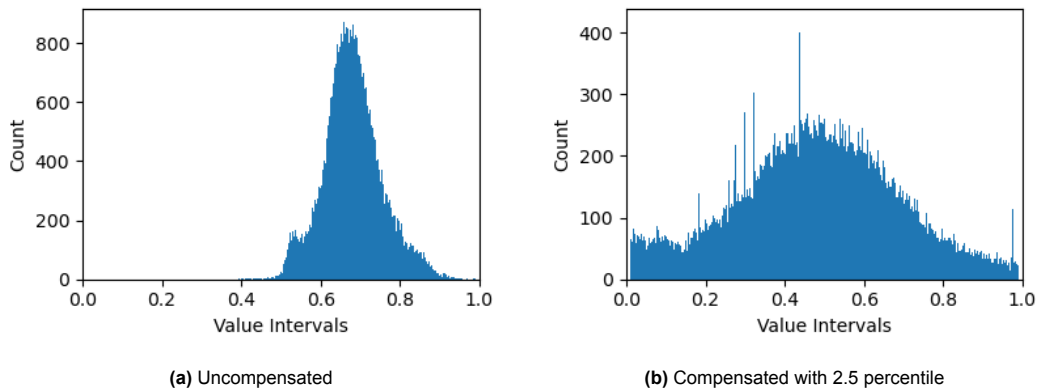


Figure A.3: Normalized recharge occurrences in response units

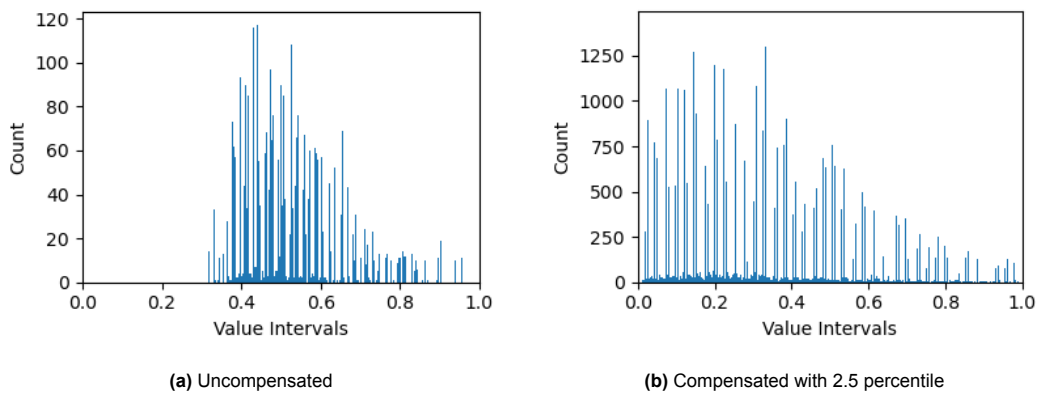


Figure A.4: Normalized evaporation occurrences in response units

A.5. Case study coordinates

Coordinates pressure device	Latitude (N)	Longitude (E)
1	28.11907	81.59702
2	28.21098	81.68452
3	28.04282	81.71287
4	28.07743	81.70812
5	28.27472	81.66850
6	28.21077	81.71328
Barometer	28.16053	81.67240

Table A.1: The coordinates of the six case studies in WGS decimal degrees N and E

A.6. Irrigation times correction

The farmer at location five was instructed to keep a record of when and for how long he irrigated and thus removed the water pressure device from his well. The farmer removed the water pressure device for the first time at the first big drop in the hourly time series (Figure A.5). He irrigated for two days in a row and looking at the data he left the pressure device out overnight. After converting Nepali dates into European dates, he recorded irrigation on the nights of the 25th/26th and 26th/27th of April. The time series showed however that that should have been the nights of the 19th/20th and the 20th/21st. The hours he wrote down were assumed to be correct (Table 4.7). The night of the 11th/12th of May was not mentioned by the farmer. However, there was an extraction by the recovering time series after the removal. It was assumed that he or someone else irrigated nonetheless from his groundwater well with the same discharge. At 7 PM the first measurement outside the well was taken and at 5 AM the last measurement outside the well was done, which is a 10-hour difference (Table 4.7). The last two discharge events were on the nights of the 18th/19th and 19th/20th of May according to the data, which was two days later than the dates the farmer wrote down. Regardless the corresponding irrigation timings were adopted one-by-one (Table 4.7). The farmer did not record the last removal of the water pressure device and no drawback is visible. Therefore, it was assumed that accidentally someone pulled it out for a couple of hours without removing any water.

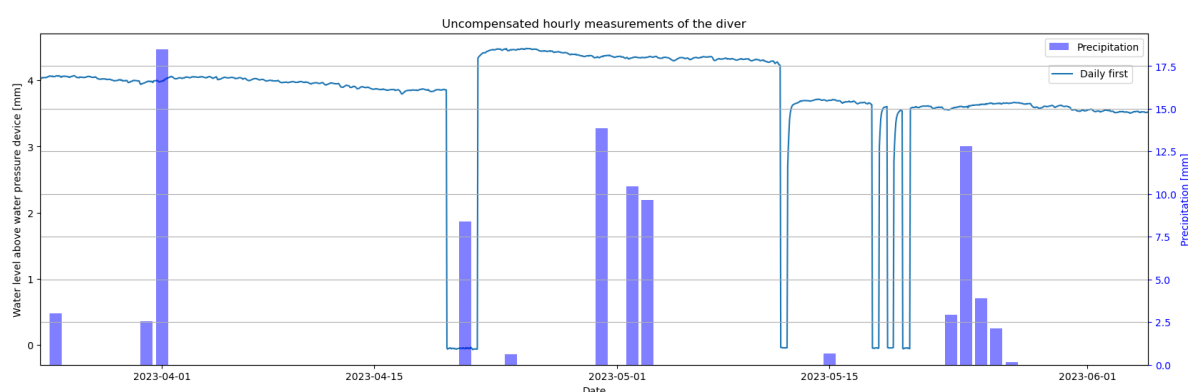


Figure A.5: Uncompensated time series of groundwater levels at case study five

The data was also corrected for the incorrect way that the pressure device was returned inside the well on the 21st of April. Eight hours after the device was put back the groundwater level stabilized for 6 hours. All measurements after that were compensated by taking the difference between the last measurement before the pressure device was removed and this temporary equilibrium. Later on the 11th of May, the device was correctly put back as it initially hung in the well before the 21st of April.

The data after the 11th of May was therefore not compensated. This was assumed because the pressure device was thoroughly attached to the lid on the well. When the lid was put back the pressure device would automatically be in the same location. It is unclear how this went wrong on the 21st of April.

A.7. Transpiration results

The actual evaporation at every location was obtained from VIIRS with the SSEBop method. By subtracting the evaporation during irrigation and precipitation from the actual evaporation, the transpiration was calculated (Table A.2).

Field location	$\sum V_{ET_a}$ [m ³]	$\sum V_{ET_{Rch}}$ [m ³]	$\sum V_{ET_{Irri}}$ [m ³]	$ \sum V_{Trans} $ [m ³]
1	1073	25	-	-1048
3	950	25	-	-925
4	1876	25	1	-1850
5	1376	40	5	-1331
6	1794	37	-	-1757

Table A.2: Transpiration calculation via the evaporation sum

A.8. Net subsurface flow and percolation results

The net sub-surface flow/percolation flux (Table 5.16) was estimated to close the water balance and thus calculated by reversing the water balance (Formula 3.17).

Field location	$\sum V_{Rch}$ [m ³]	$\sum V_{Extr}$ [m ³]	$\sum V_{Ret-Flw}$ [m ³]	$\sum V_{GWT-Evap}$ [m ³]	$\Delta V_{Storage}$ [m ³]	$\sum V_{SSF-Perc}$ [m ³]
1	584	-153	-	-1048	-593	23
3	549	-251	-	-925	-1360	-733
4	549	-269	56	-1850	-849	666
5	664	-2538	2533	-1331	-698	-26
6	597	-146	-	-1757	-1038	268

Table A.3: Net sub-surface flow/percolation calculation via the reversed water balance

A.9. Intermediate calculation flux contributions

All fluxes per case study were multiplied by the assigned area (Table A.4).

Field location	$\sum V_{Rch}$ [m ³]	$\sum V_{Extr}$ [m ³]	$\sum V_{Ret-Flw}$ [m ³]	$\sum V_{Ext-Net}$ [m ³]	$\sum V_{GWT-Evap}$ [m ³]	$\sum V_{SSF-Perc}$ [m ³]	$\Delta V_{Storage}$ [m ³]
1	2.771E7	-7.26E6	0	-7.26E6	-4.980E7	1.11E6	-2.820E7
3	2.03E6	-9.3E5	0	-9.3E5	-3.41E6	-2.71E6	-5.01E6
4	5.0E5	-2.4E5	5E4	-1.9E5	-1.66E6	6.0E5	-7.7E5
5	4.34E6	-1.656E7	1.654E7	-4E4	-8.70E6	-1.7E5	-4.57E6
6	1.52E6	-3.7E5	0	-3.7E5	-4.47E6	6.8E5	-2.64E6
Total	3.62E7	-2.54E7	1.66E7	-8.8E6	-6.81E7	-5E5	-4.12E7

Field loca- tion	$\sum V_{Rch}$ [m ³]	$\sum V_{Extr}$ [m ³]	$\sum V_{Ret-Flw}$ [m ³]	$\sum V_{Ext-Net}$ [m ³]	$\sum V_{GWT-Evap}$ [m ³]	$\sum V_{SSF-Perc}$ [m ³]	$\Delta V_{Storage}$ [m ³]
Total propor- tion	88%	-62%	40%	-21%	-165%	-1%	-

Table A.4: Assigned contribution volumes in m³ and percentage for all relevant case studies

B

Appendix B: Additional figures

B.1. Chapter 2

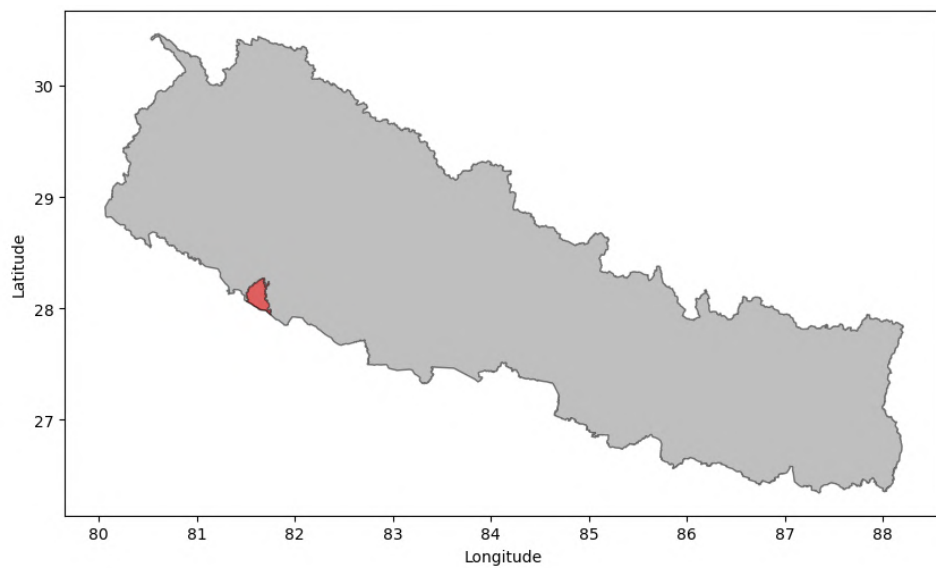


Figure B.1: Location of study area within Nepal

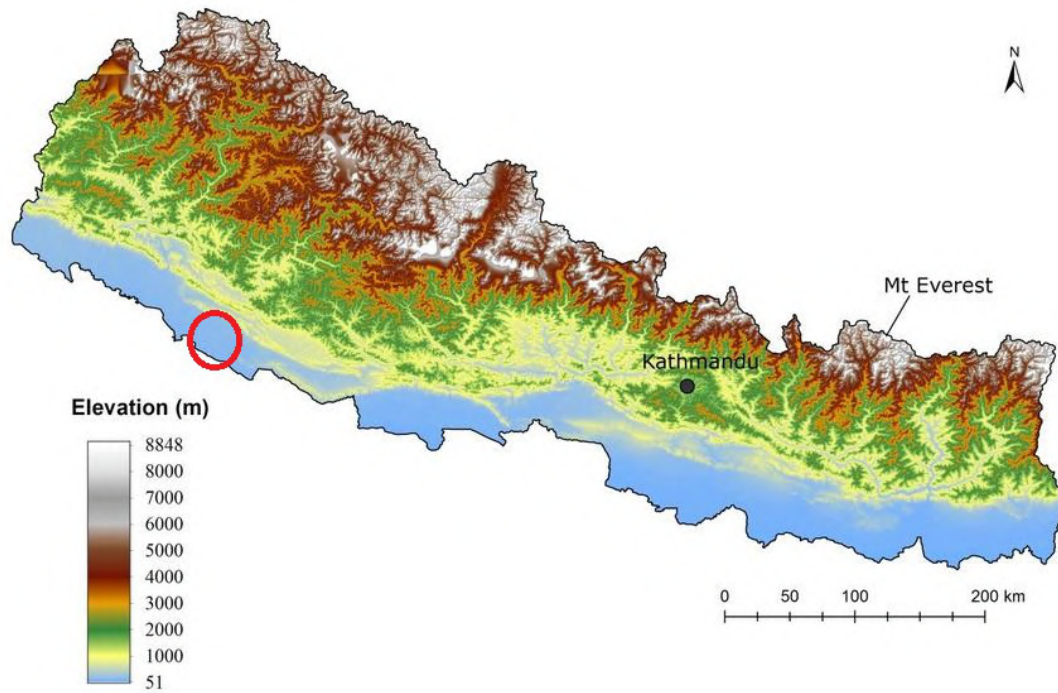


Figure B.2: Elevation map of Nepal where the red circle marks the approximate location of the study area [43]

B.2. Chapter 3

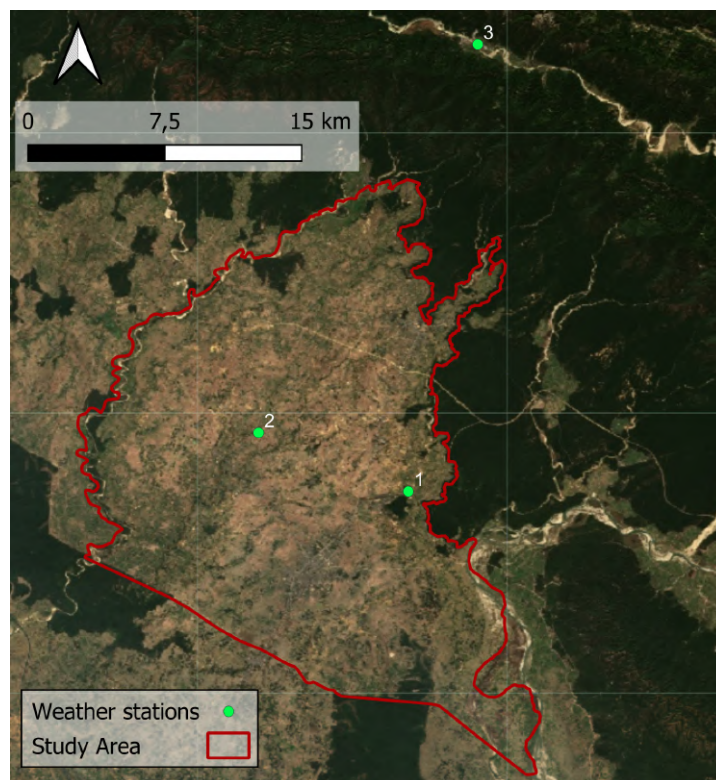


Figure B.3: Three precipitation stations denoted by green markers. Station one is Nepalgunj Airport, station two is Khajura Khurda and station three is Shyano Chepang

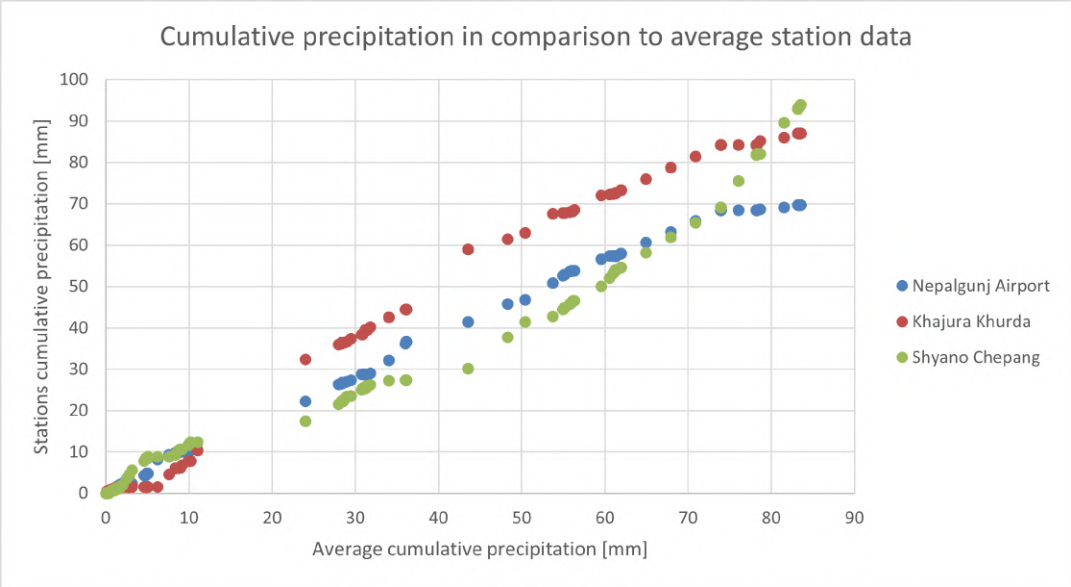


Figure B.4: Double mass curve of measurements of one station against the average cumulative measurement of all stations

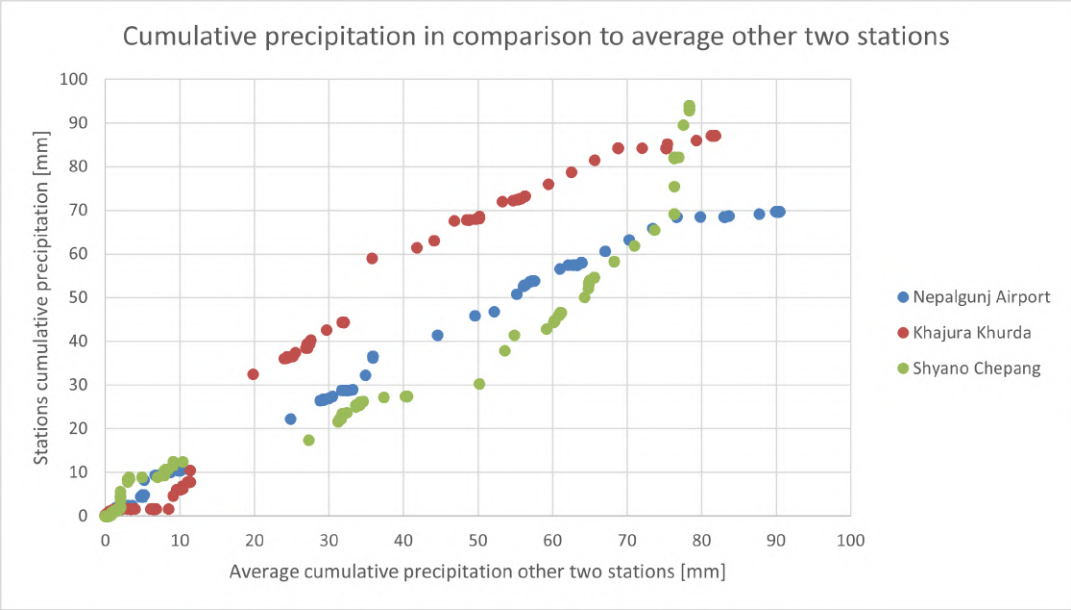


Figure B.5: Double mass curve of measurements of one station against the average cumulative measurement of all other stations

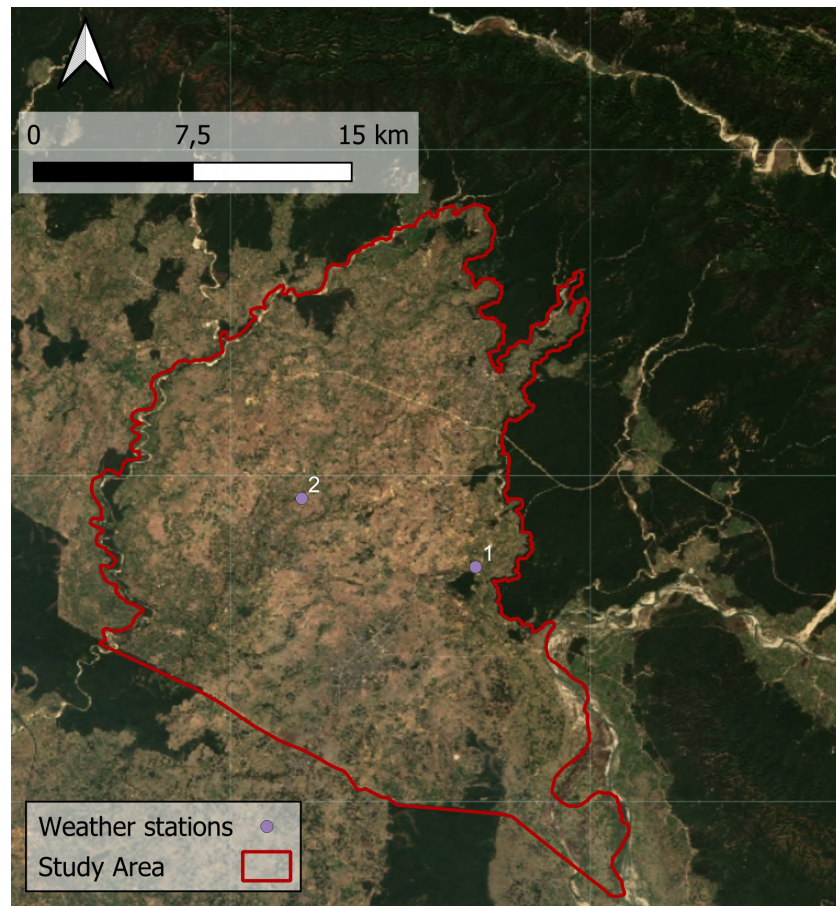


Figure B.6: Two stations denoted by purple markers measuring the required parameters to estimate potential evapotranspiration. Station one is Nepalgunj Airport and station two is Khajura Khurda

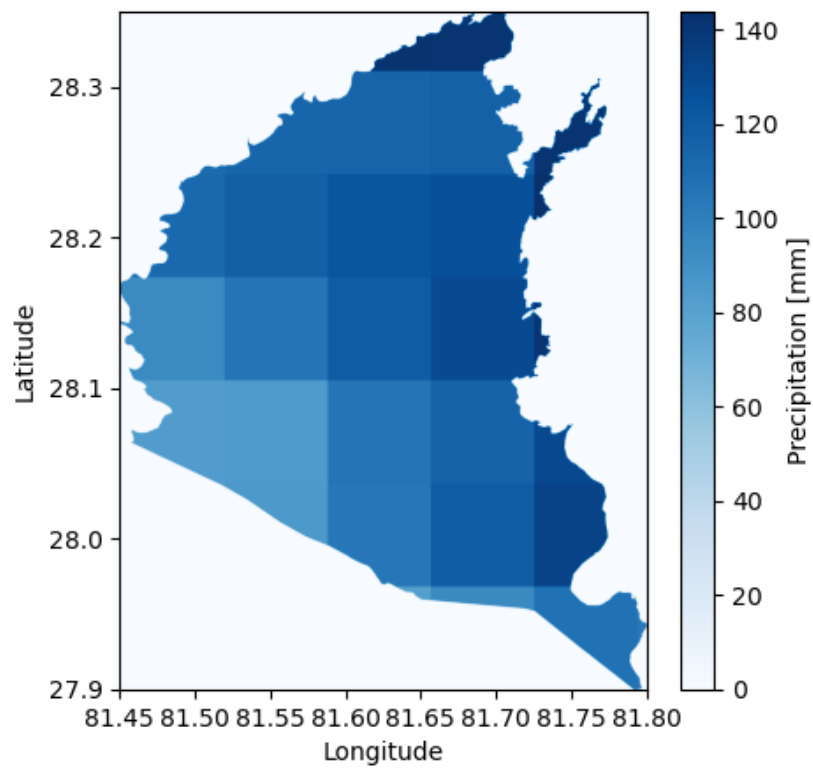


Figure B.7: Precipitation sum of the study area over the relevant time frame using CHIRPS

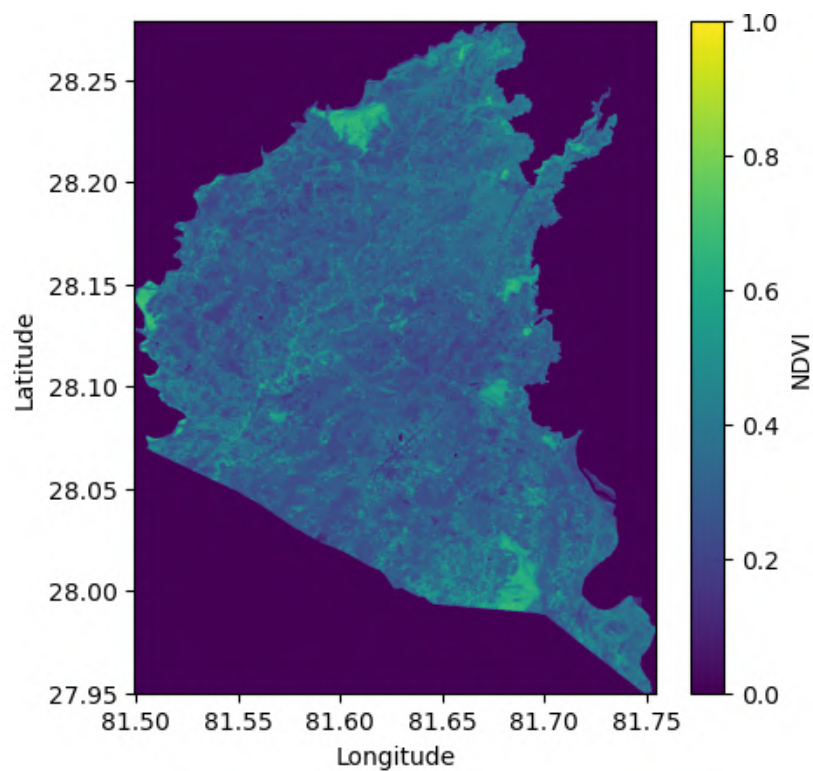


Figure B.8: Average NDVI of the study area over the relevant time frame using Landsat 5, 7, 8 and 9

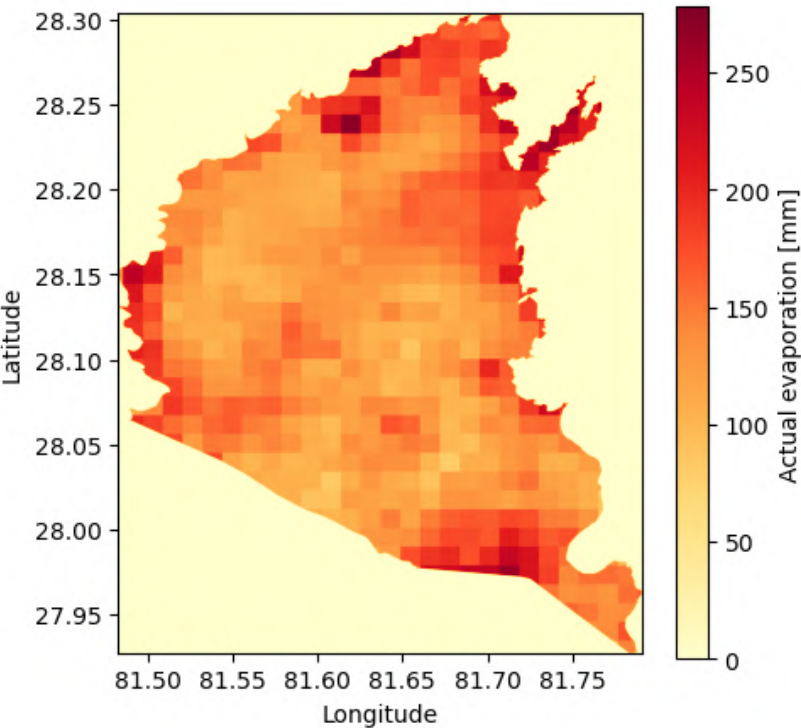


Figure B.9: Actual evaporation sum of the study area over the relevant time frame using Visible Infrared Imaging Radiometer Suite

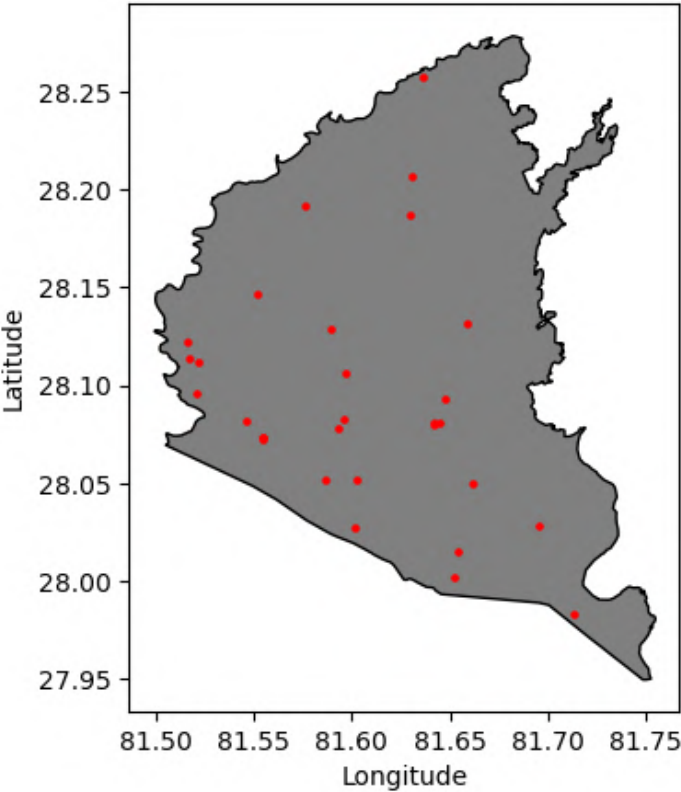


Figure B.10: Locations of 22 relevant monitoring wells of CIMMYT

B.3. Chapter 4

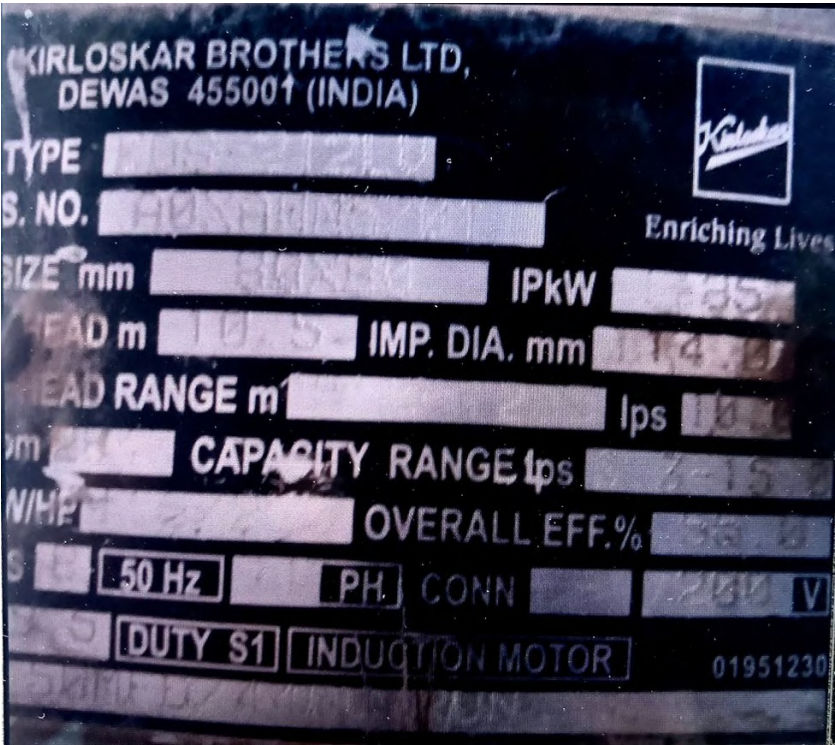


Figure B.11: Photo of pump characteristics of the farmer at case study five

B.4. Chapter 5

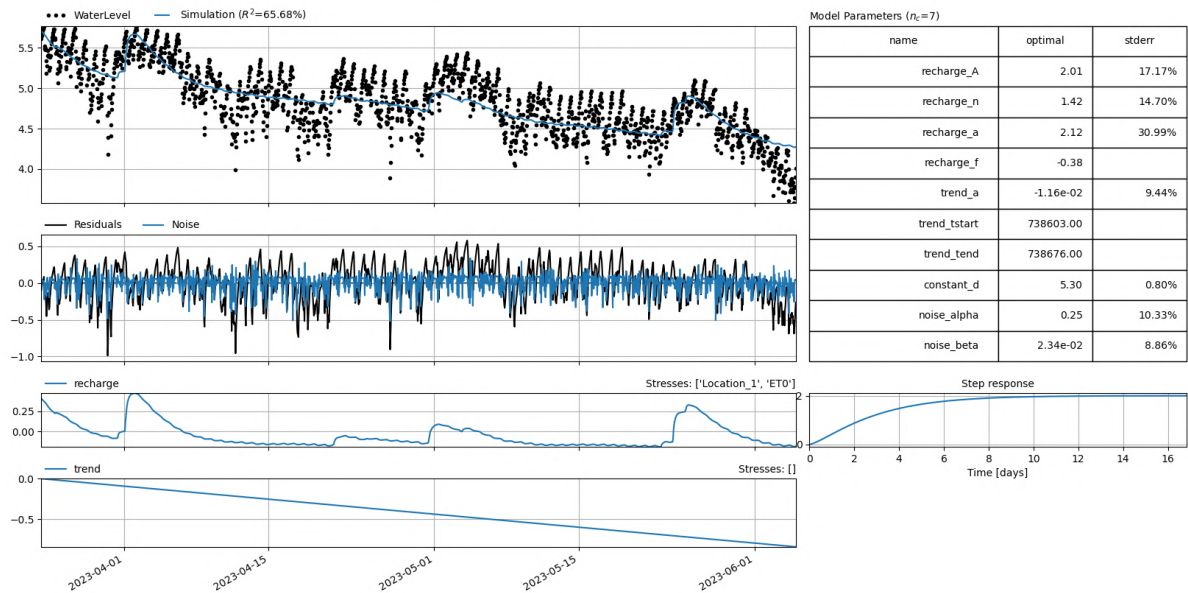


Figure B.12: Fitted Pastas time series of case study one with residuals, recharge and transpiration contribution, trend and step response all in meters accompanied by the fitted model parameters. The fitted model parameters A, n and a are used to fit the gamma function, the parameter f is the crop factor, the trend parameters are to fit the trend, alpha and beta represent parameters to fit the noise model and parameter d is the constant base level of the simulation

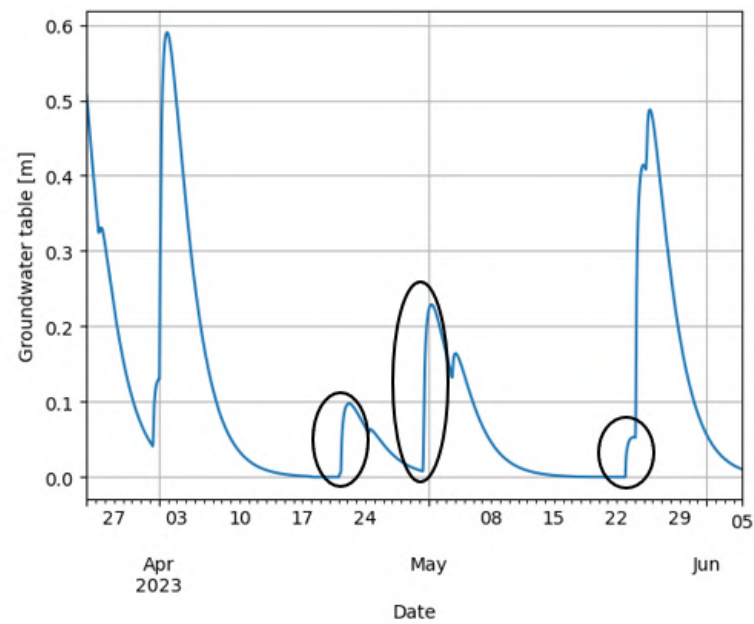


Figure B.13: Observed peaks of recharge contribution to the groundwater table of case study one

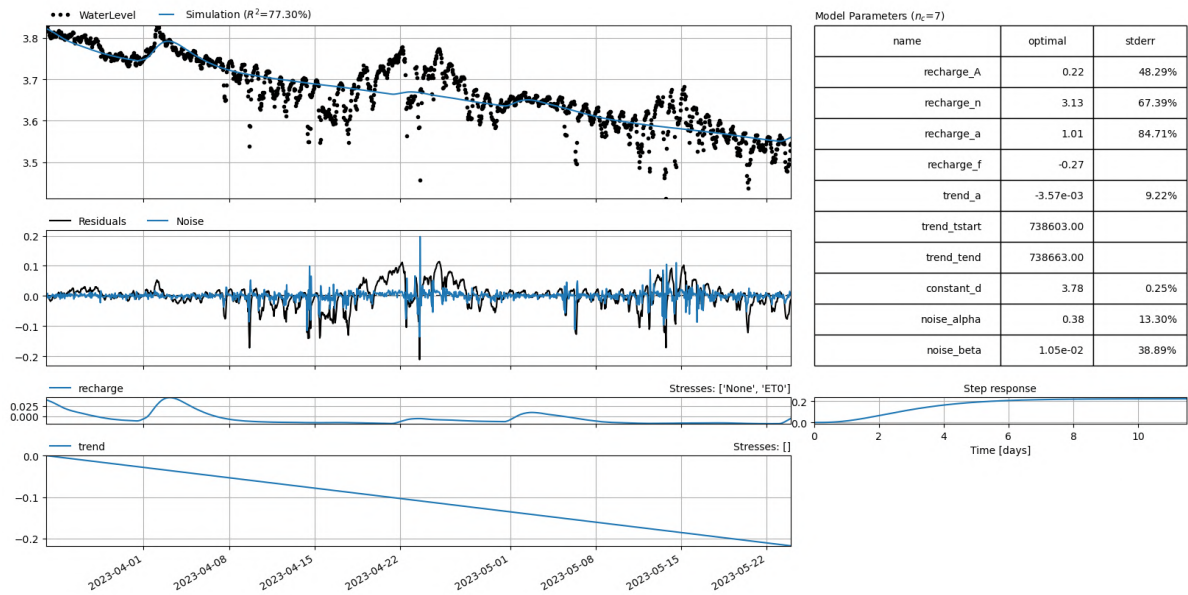


Figure B.14: Fitted Pastas time series of case study three with residuals, recharge and transpiration contribution, trend and step response all in meters

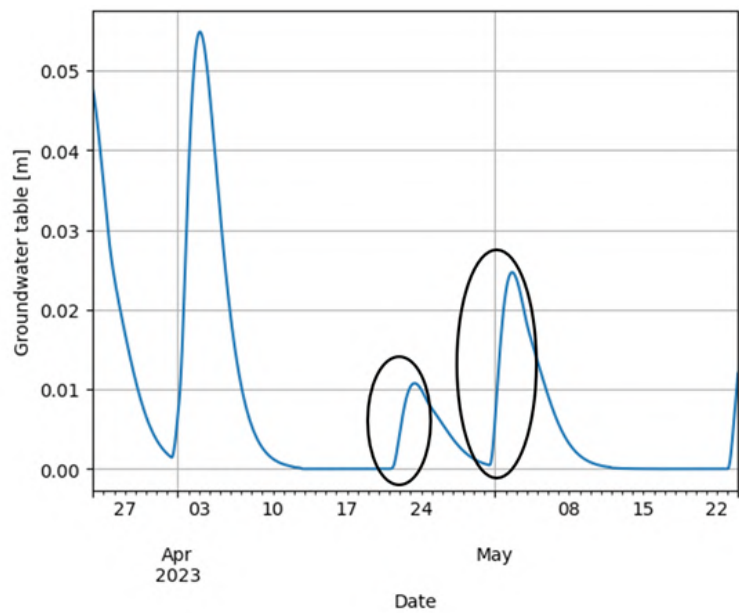


Figure B.15: Observed peaks of recharge contribution to the groundwater table of case study three

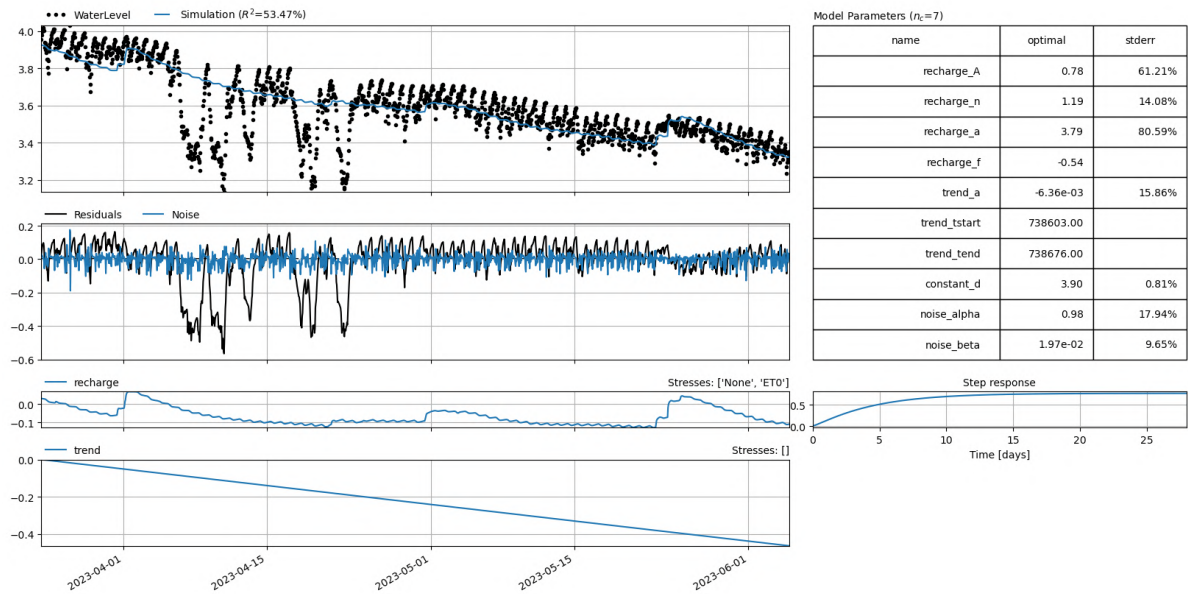


Figure B.16: Fitted Pastas time series of case study four with residuals, recharge and transpiration contribution, trend and step response all in meters accompanied by the fitted model parameters

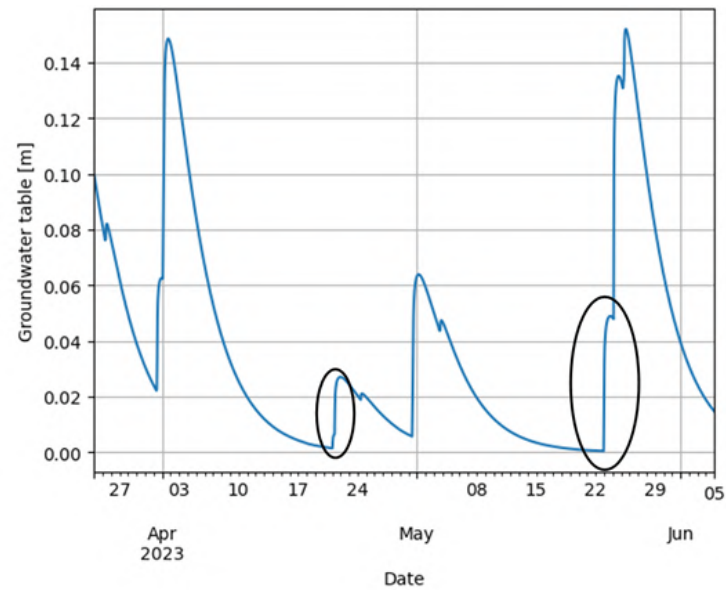


Figure B.17: Observed peaks of recharge contribution to the groundwater table of case study four

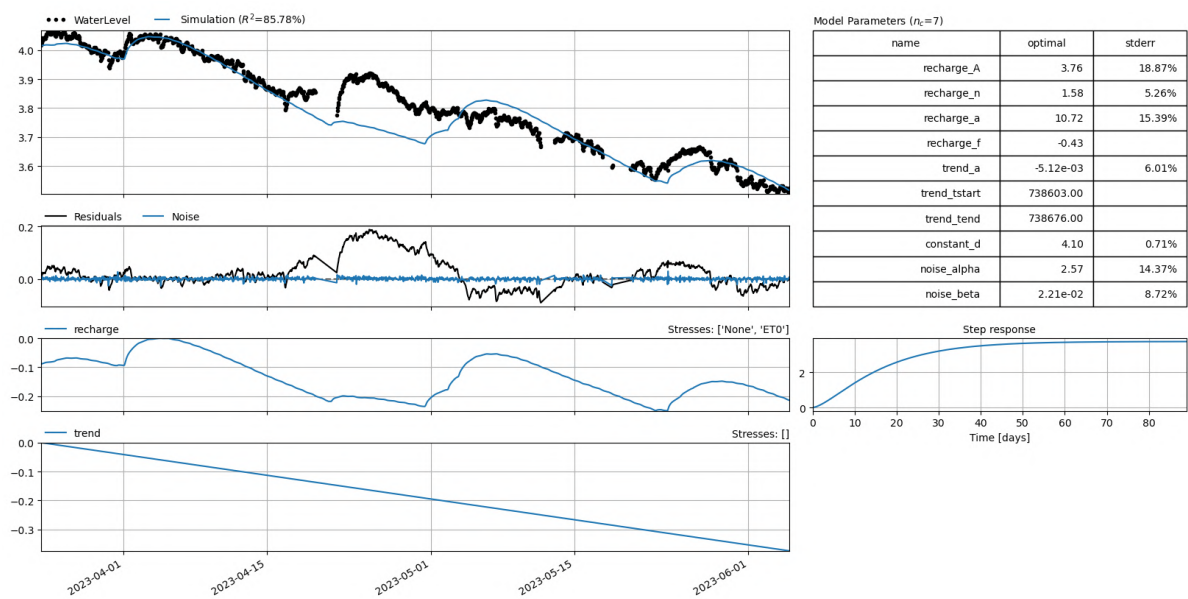


Figure B.18: Fitted Pastas time series of case study five with residuals, recharge and transpiration contribution, trend and step response all in meters accompanied by the fitted model parameters

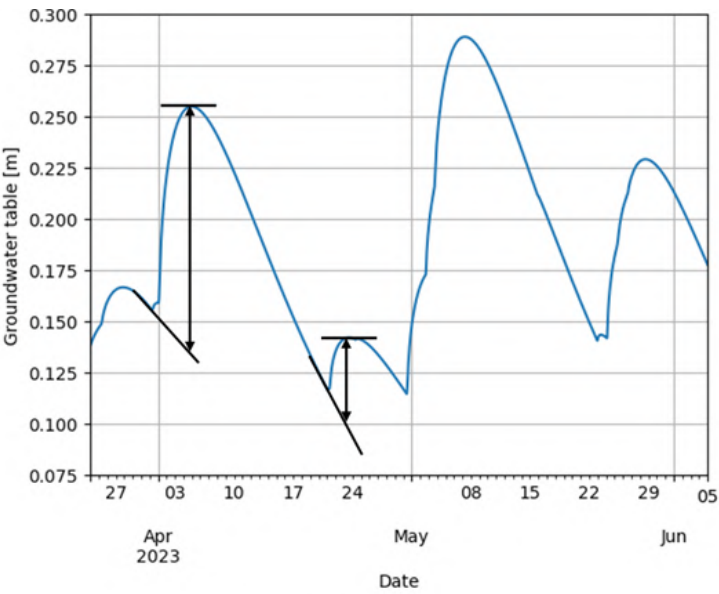


Figure B.19: Observed peaks of recharge contribution to the groundwater table of case study five

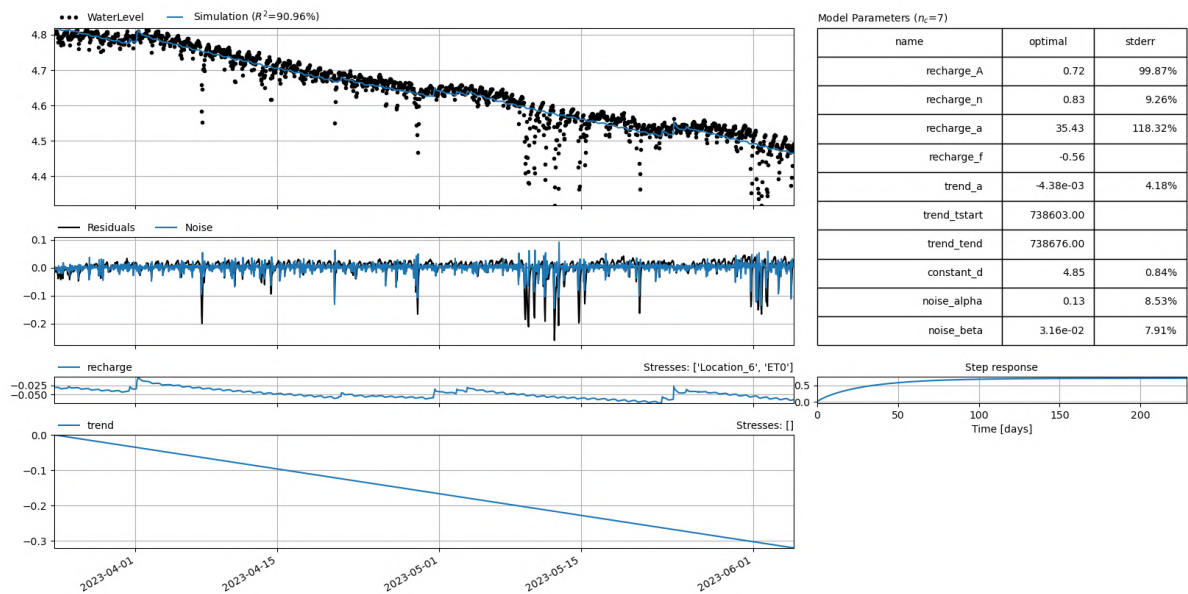


Figure B.20: Fitted Pastas time series of case study six with residuals, recharge and transpiration contribution, trend and step response all in meters accompanied by the fitted model parameters

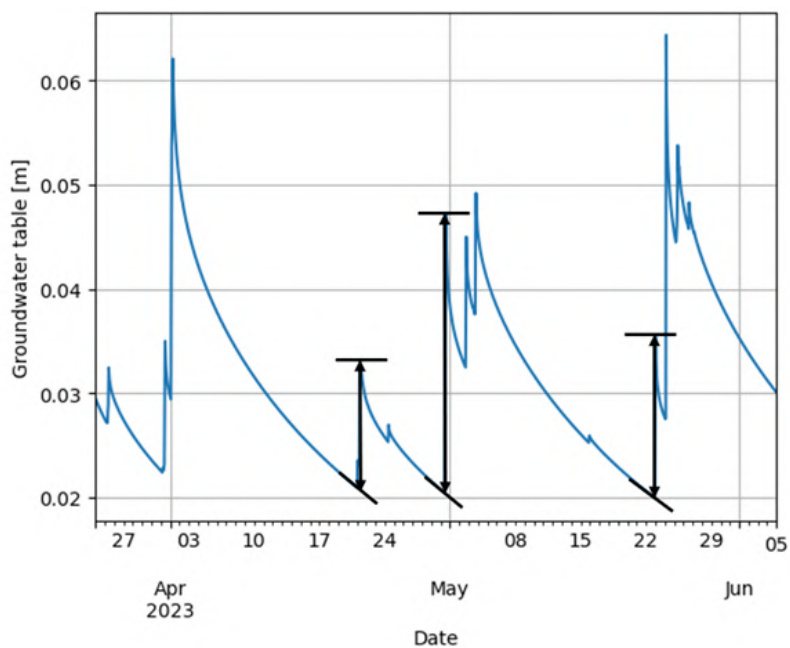


Figure B.21: Observed peaks of recharge contribution to the groundwater table of case study six

Measurements of Specific Yield for Some Common Earth Materials (Percent)		
Material	Number of Samples	Range of Specific Yield %
Unconsolidated Sediments		
Clay	27	1 – 18
Silt	299	1 – 40
Loess	5	14 – 22
Eolian sand	14	32 – 47
Sand (fine)	287	1 – 46
Sand (medium)	297	16 – 46
Sand (coarse)	143	18 – 43
Gravel (fine)	33	13 – 40
Gravel (medium)	13	17 – 44
Gravel (coarse)	9	13 – 25

Figure B.22: Typical specific yield values according to the online books published by The Groundwater Project [52]

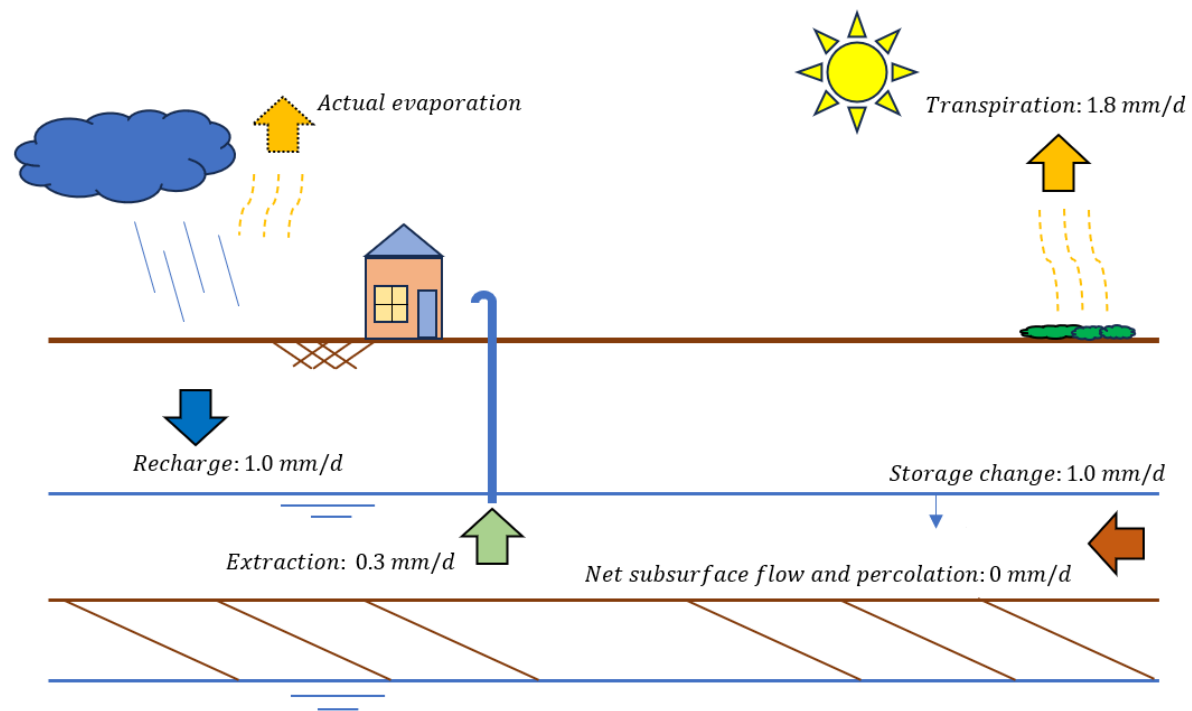


Figure B.23: Schematic drawing with estimated one-dimensional vertical average fluxes at case study one

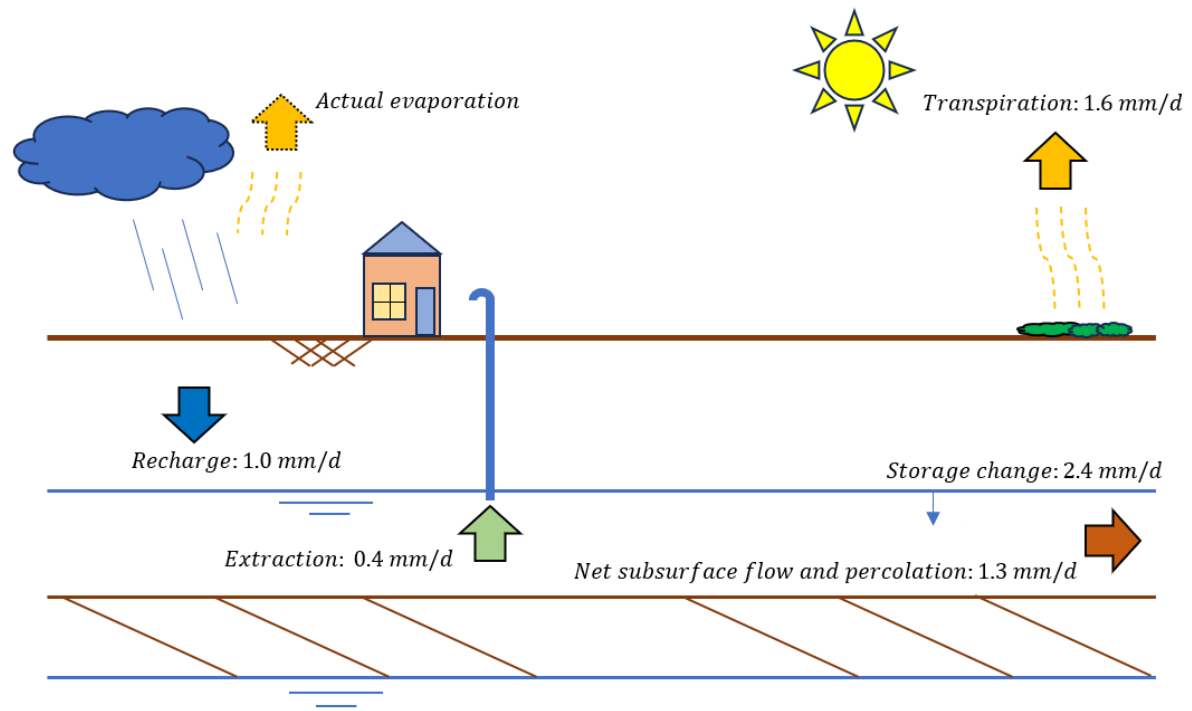


Figure B.24: Schematic drawing with estimated one-dimensional vertical average fluxes at case study three

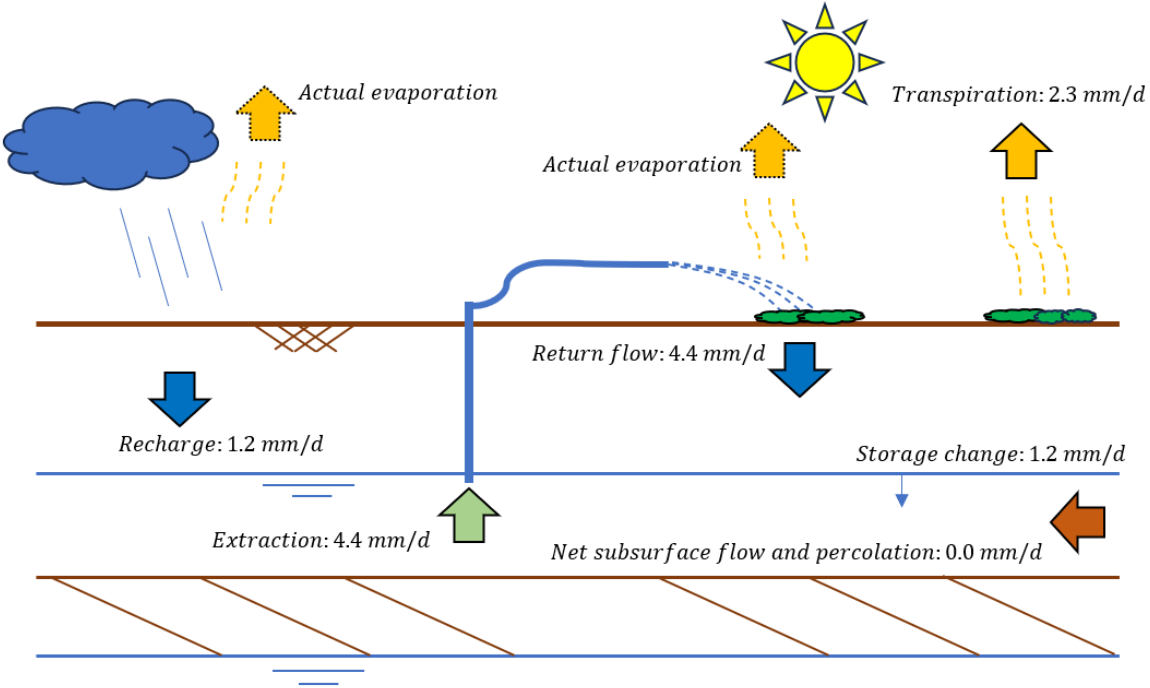


Figure B.25: Schematic drawing with estimated one-dimensional vertical average fluxes at case study five

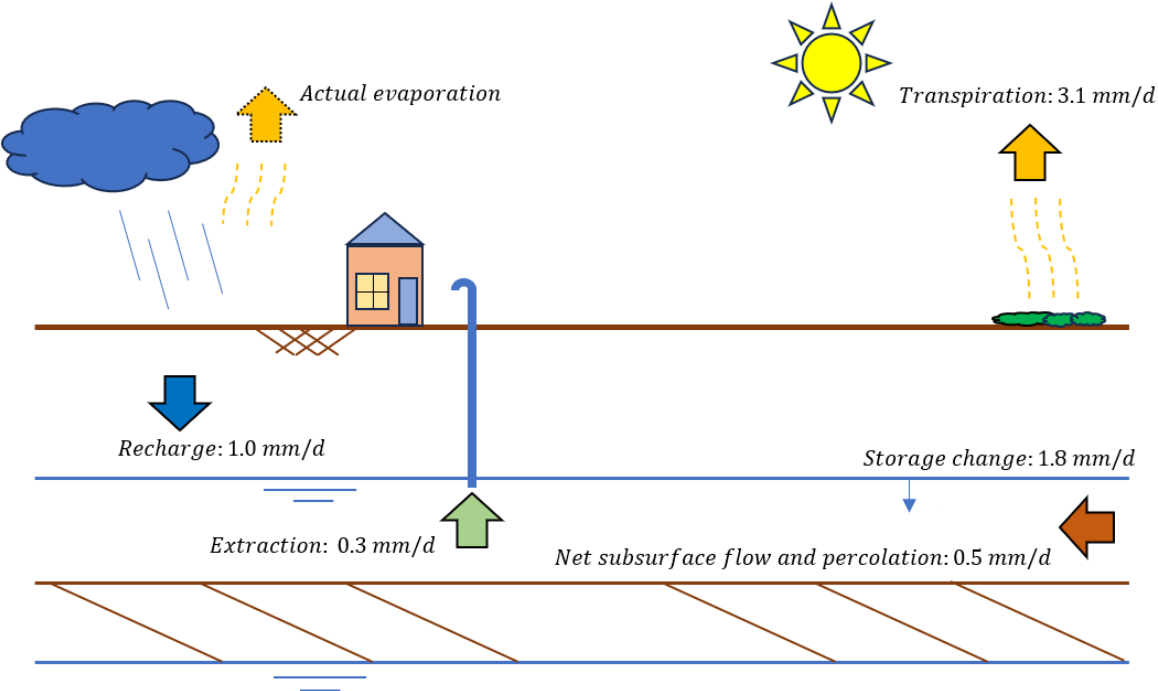


Figure B.26: Schematic drawing with estimated one-dimensional vertical average fluxes at case study six

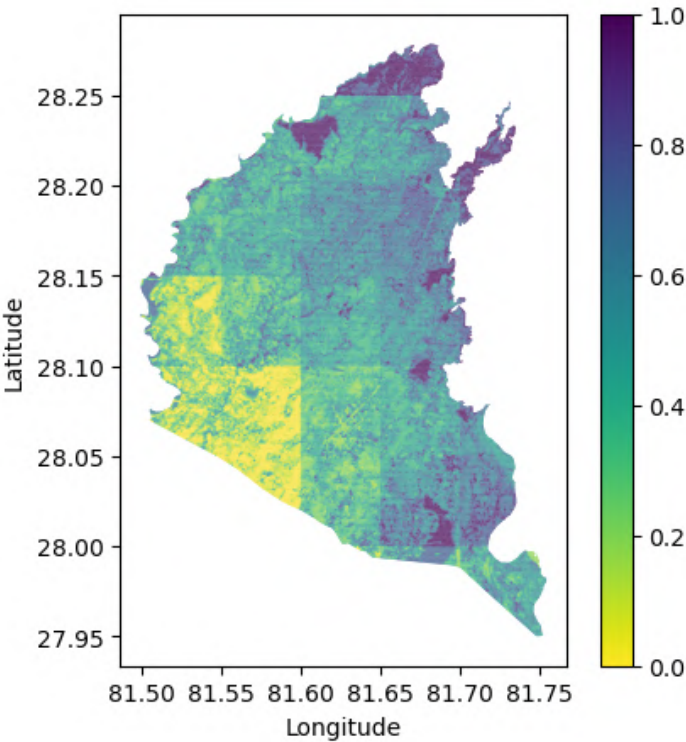


Figure B.27: Groundwater response units with normalized recharge

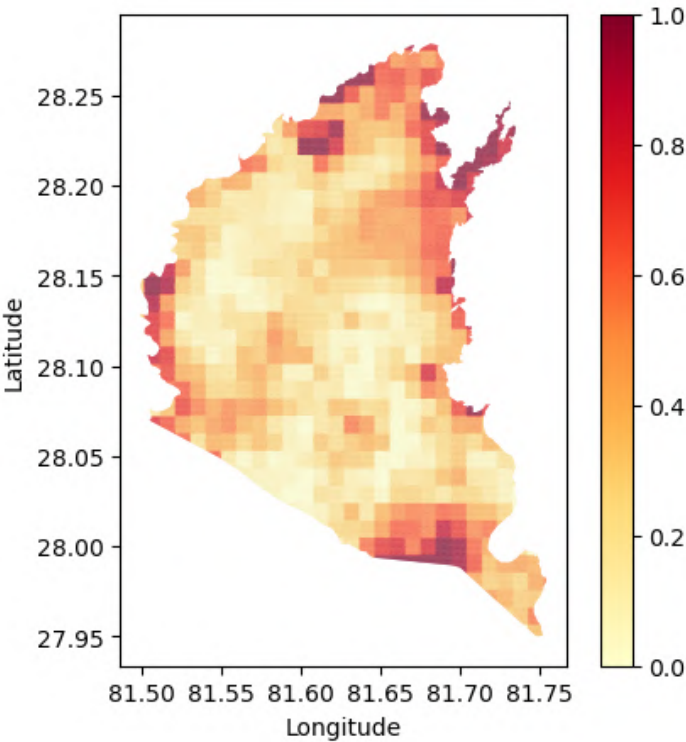


Figure B.28: Groundwater response units with normalized evaporation

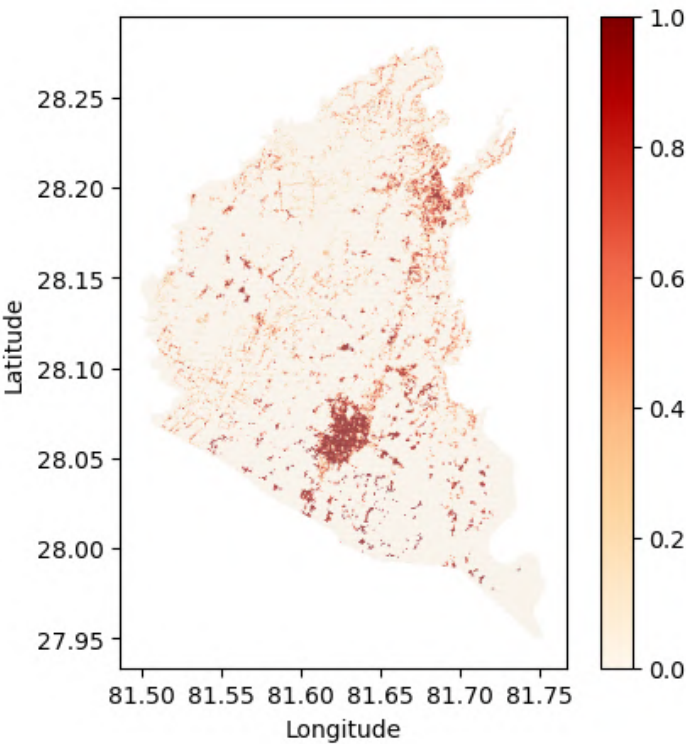


Figure B.29: Groundwater response units with normalized population density

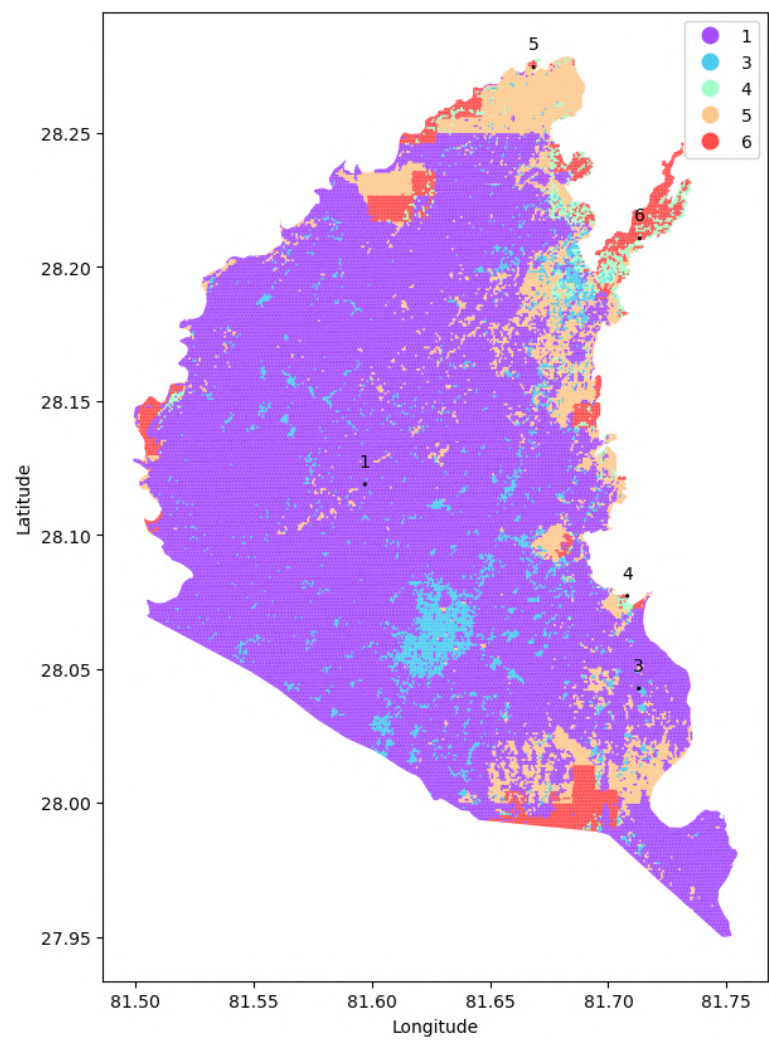


Figure B.30: Groundwater response units with an assigned location

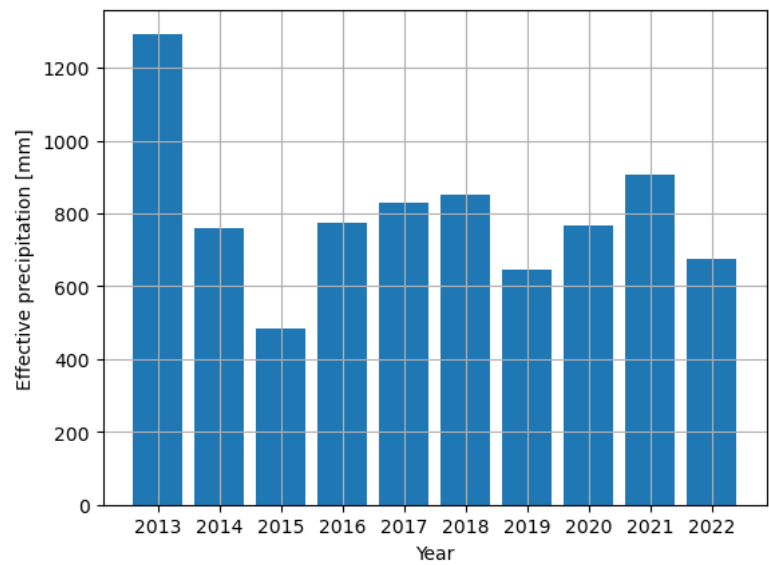


Figure B.31: Average yearly CHIRPS precipitation minus VIIRS actual evaporation in the study area

C

Appendix C: Additional documents

The Environment Research Laboratory in Kathmandu measured the chloride and electrical conductivities of the sampled water. The codes G stands for 'Groundwater', the R for 'River' water and the P for 'Precipitation'. The first number after the letter stands for the measurement location and the second number behind the point denotes the sample number during that specific fieldwork.

During the first batch of samples, the electrical conductivity was measured wrongly. All these values were structurally far too high [10]. The electrical conductivity of the first batch was judged to be not reliable enough to be used for any calculation in this report. The second batch indicates that the water is not brackish, but the EC measurements were not used any further. Eventually, the median of groundwater chloride samples for every case study of the groundwater was used.



NEPAL ACADEMY OF SCIENCE & TECHNOLOGY

CENTRAL OFFICE

NAST

Environment Research Laboratory

Water Analysis Report

Date: 2023-04-17

Date Received: 2023-04-11

Received From: Mr. P.A. van Sabben

Source: Groundwater/Precipitation/River

Location: Terai - Banke District

S.N.	Sample	Conductivity ($\mu\text{S/cm}$)	Chloride (mg/L)
1.	G2.2	2415	42.60
2.	G4.3	1924	14.20
3.	G6.2	2203	8.52
4.	G6.1	2216	8.52
5.	R3.1	1235	11.36
6.	R4.2	1208	8.52
7.	G5.1	2067	9.94
8.	R5.2	1946	7.10
9.	G1.1	2980	7.10
10.	G4.1	1914	7.10
11.	G2.1	2388	42.60
12.	G4.2	1910	7.10
13.	G3.2	1946	11.36
14.	R5.3	1926	7.10
15.	R6.3	1475	5.68
16.	G5.2	2063	8.52
17.	R3.2	1586	12.78
18.	R4.3	1155	7.10
19.	G3.1	1982	15.62
20.	R6.2	1459	5.68
21.	G3.3	1977	12.78
22.	G1.2	2957	7.10
23.	R4.1	1311	5.68
24.	P1.1	1308	25.56
25.	R6.1	1464	2.84
26.	R5.1	1936	4.26
27.	P2.1	76.2	2.84
28.	P6.1	147.5	4.26
29.	P5.1	139.2	2.84
30.	P2.2	449.7	2.84

Approved by

Tista


Dr. Tista Prasai Joshi, Senior Scientific Officer

Notes:

- The result refers only to the parameters tested for the sample received in the laboratory for analysis.
- The reproduction of this report wholly or partially cannot be used as evidence in the court of law and should not be used in any advertising media without the written approval of the laboratory

Address : Khumaltar, Lalitpur, Nepal, GPO Box 3323 Kathmandu, E-mail: Info@nast.gov.np
Telephone: 977-1-5547715, 5547720, 5547721, 5553132 Fax: +977-1-5547713

Figure C.1: Water analysis report 1



NEPAL ACADEMY OF SCIENCE & TECHNOLOGY

CENTRAL OFFICE

Environment Research Laboratory

Water Analysis Report

Date: 2023-06-11


Date Received: 2023-06-09
 Received From: Pepijn van Sabben
 Source: Groundwater/Precipitation/River water
 Location: Nepalgunj Banke

S.N	Sample Code	Conductivity ($\mu\text{S/cm}$) *NDWQS 2022 (1500 $\mu\text{S/cm}$)	Chloride (mg/L) *NDWQS 2022 (250 mg/L)
1	R3.1	447	14.2
2	R3.2	468	17.04
3	R3.3	391	15.62
4	R4.1	355	7.1
5	R4.2	380	7.1
6	R4.3	399	8.52
7	R5.1	587	7.1
8	R5.2	516	7.1
9	R5.3	524	5.68
10	R6.1	418	5.68
11	R6.2	442	8.52
12	R6.3	454	9.94
13	G1.1	934	80.94
14	G1.2	927	5.68
15	G1.3	922	5.68
16	G1.4	920	9.94
17	G1.6	917	26.98
18	G1.8	917	7.1
19	G2.1	791	58.22
20	G2.2	794	46.86
21	G2.3	803	44.02
22	G2.4	630	45.44
23	G2.6	459	38.34
24	G2.8	553	45.44
25	G3.1	607	14.2
26	G3.2	606	14.2
27	G3.3	610	12.78
28	G3.4	604	15.62
29	G3.6	340	17.04
30	G3.8	585	15.62
31	G4.1	578	5.68
32	G4.2	585	5.68

Tista

Address : Khumaltar, Lalitpur, Nepal, GPO Box 3323 Kathmandu, E-mail: Info@nast.gov.np
 Telephone: 977-1-5547715, 5547720, 5547721, 5553132 Fax: +977-1-5547713

Figure C.2: Water analysis report 2 page 1




NEPAL ACADEMY OF SCIENCE & TECHNOLOGY

CENTRAL OFFICE

NAST			
33	G4.3	592	7.1
34	G4.6	441	5.68
35	G4.7	397	35.5
36	G4.8	560	9.94
37	G5.1	643	12.78
38	G5.2	626	12.78
39	G5.3	620	8.52
40	G5.4	344	8.52
41	G5.6	598	9.94
42	G5.8	631	163.3
43	G6.1	674	12.78
44	G6.2	674	11.36
45	G6.3	676	8.52
46	G6.4	564	5.68
47	G6.6	387	5.68
48	G6.8	526	7.1
49	P1.3	106	5.68
50	P1.4	170	8.52
51	P1.6	472	21.3
52	P2.4	102	5.68
53	P2.8	73	5.68
54	P3.4	97	4.26
55	P3.8	1644↑	5.68
56	P4.4	64	25.56
57	P4.5	62	214.42
58	P4.8	45	11.36
59	P5.4	162	5.68
60	P5.6	183	4.26
61	P5.8	281	4.26
62	P6.4	312	7.1
63	P6.6	666	11.36
64	P6.8	1277	8.52

• NDWQS - National Drinking Water Quality Standards, 2022

Approved by

 Dr. Tista Prasai Joshi
 Senior Scientific Officer

Notes:

The result refers only to the parameters tested for the sample received in the laboratory for analysis.

- The reproduction of this report wholly or partially cannot be used as evidence in the court of law and should not be used in any advertising media without the written approval of the laboratory

Address : Khumaltar, Lalitpur, Nepal, GPO Box 3323 Kathmandu, E-mail: Info@nast.gov.np
 Telephone: 977-1-5547715, 5547720, 5547721, 5553132 Fax: +977-1-5547713

Figure C.3: Water analysis report 2 page 2

A4 Landscape

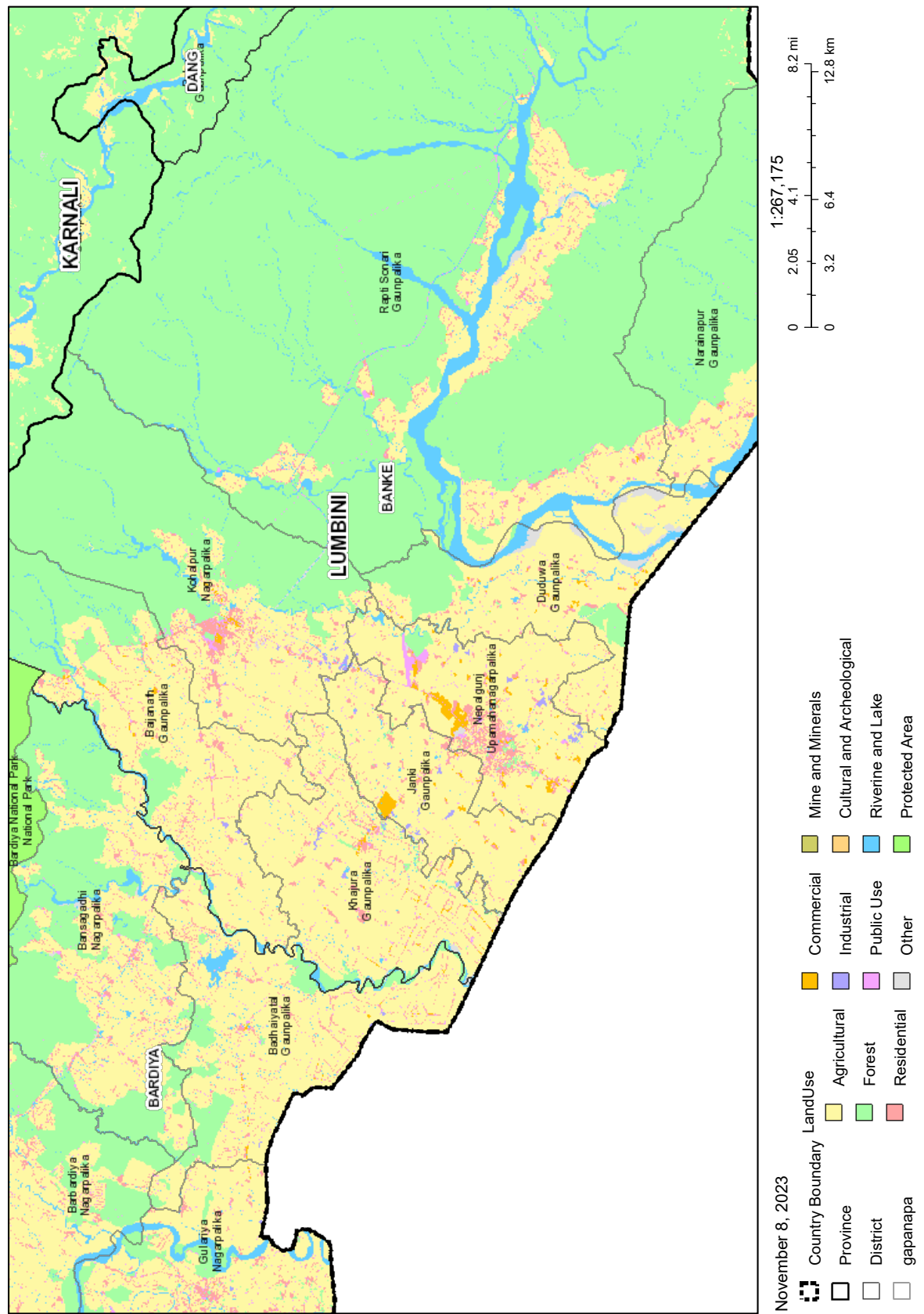


Figure C.4: Full size land use map of the Banke district [31]

D

Appendix D: Pictures field locations



Figure D.1: Photos taken at case study one



Figure D.2: Photos taken at case study two



Figure D.3: Photos taken at case study three



Figure D.4: Photos taken at case study four



Figure D.5: Photos taken at case study five



Figure D.6: Photos taken at case study six